The Journey of Science, Medicine, and Life

Get Out of Your Own Way!

Hardeep Phull MD, MS

Oncologist, Scientist, Educator, Pilot, Yachtsman, Girl Dad, BRAVO/UBRP Alum '03

Lesson #1: Get Going and Start Somewhere

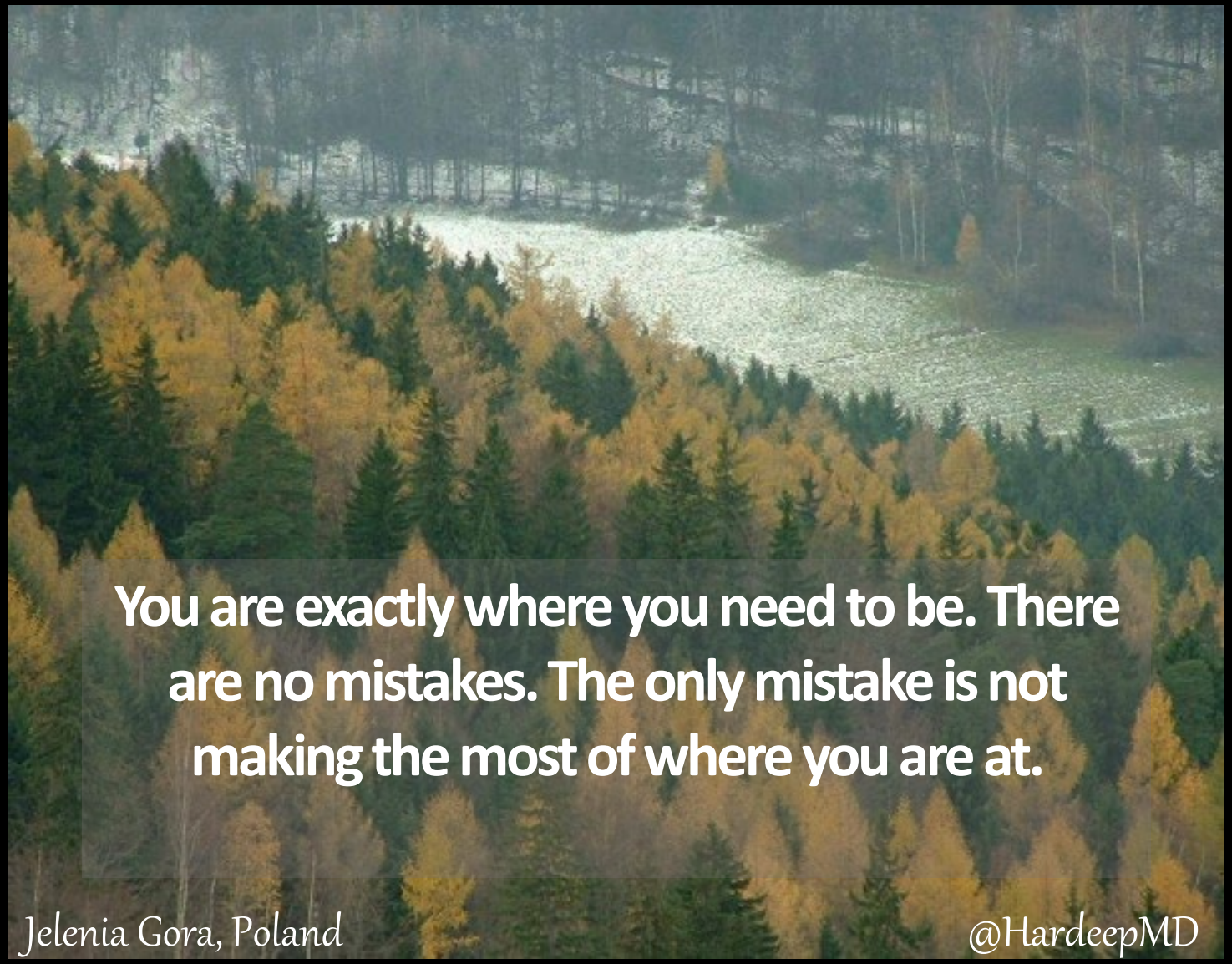

DNA Microarrays on Glass Slides

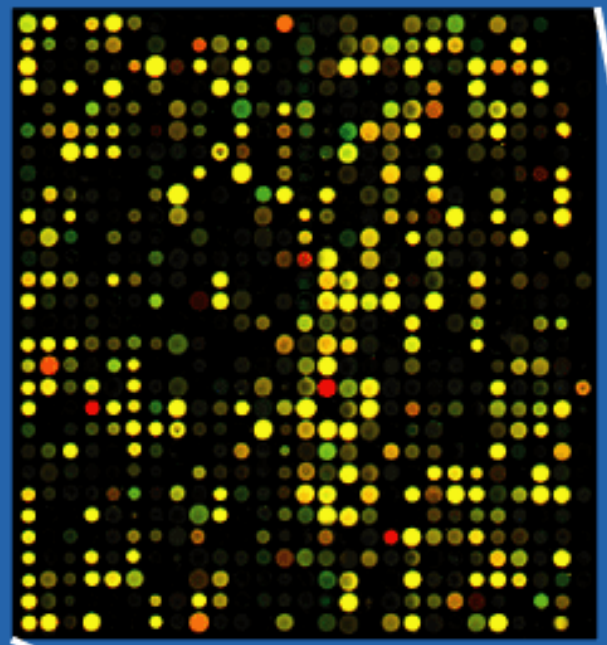

- Array of single-stranded cDNA probes on coated glass slides
- Printed robotically via automation
- Each spot represents a particular gene
- High-density grid (29x29x12x4 = 40,368!)

David Galbraith

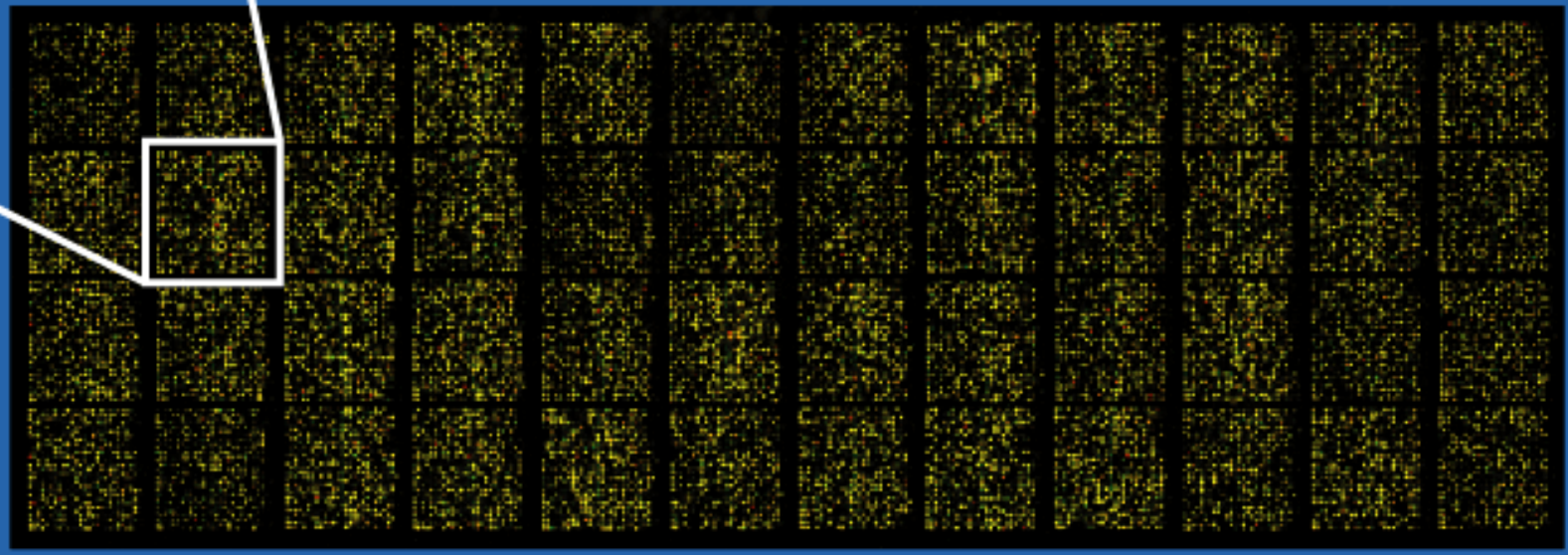

DNA Microarray Applications

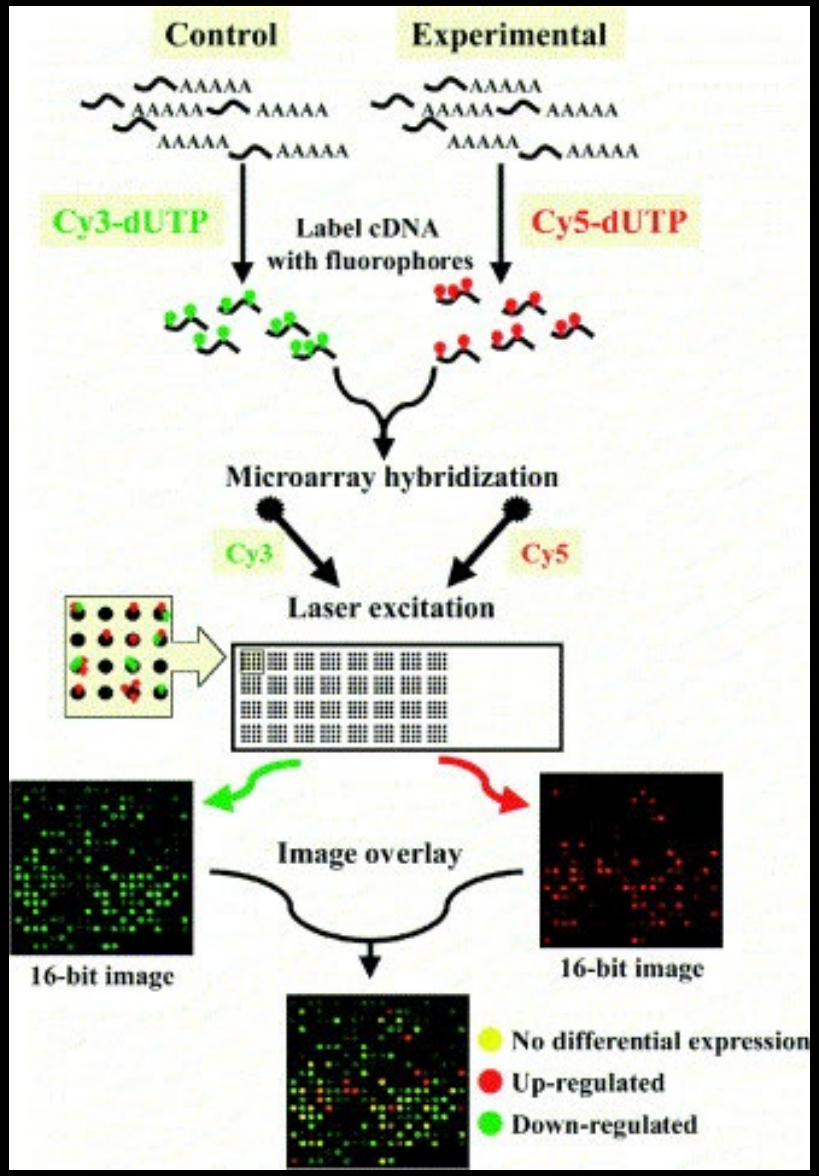

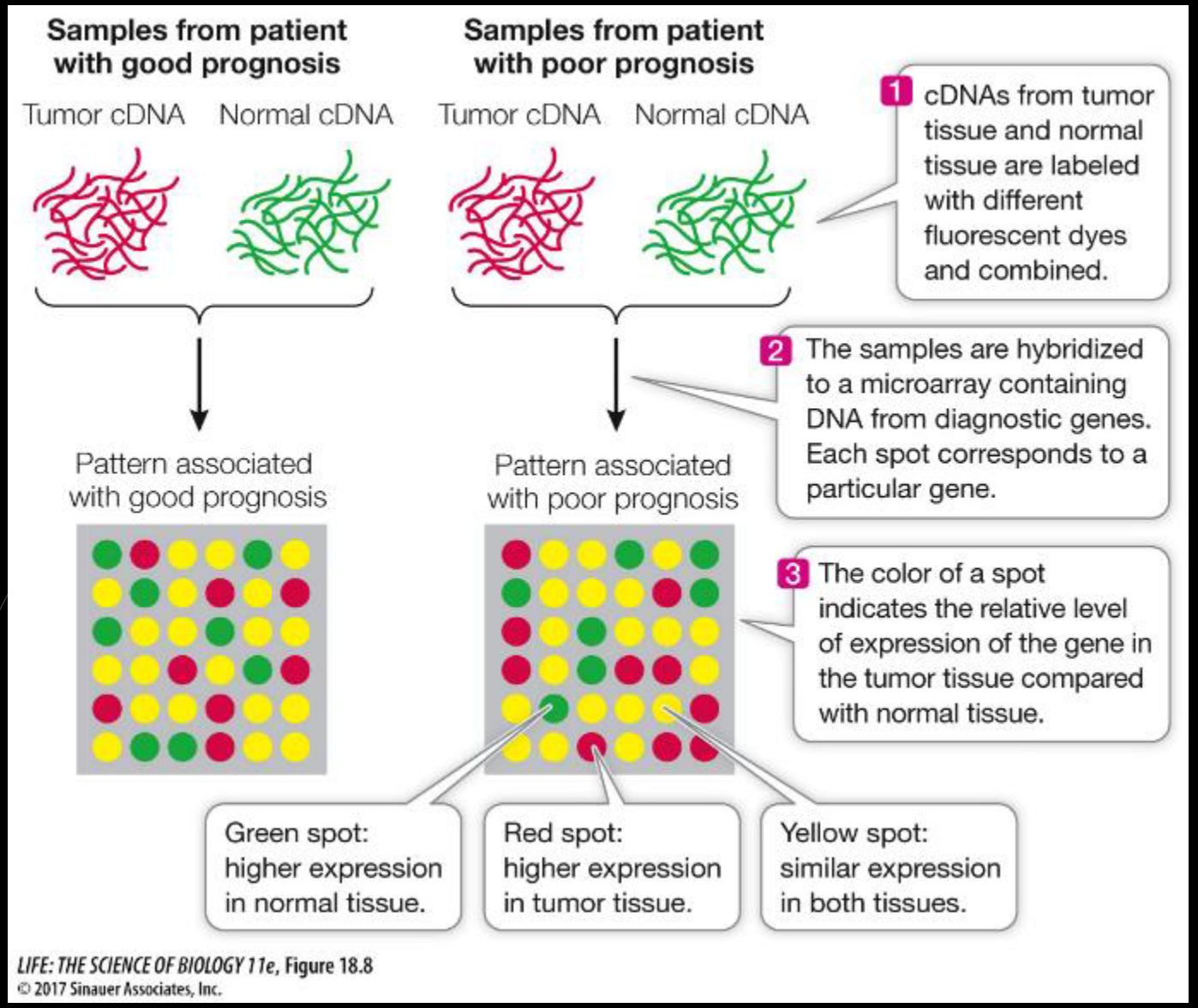

LIFE: THE SCIENCE OF BIOLOGY 11e, Figure 18.8

DNA Microarray Printer

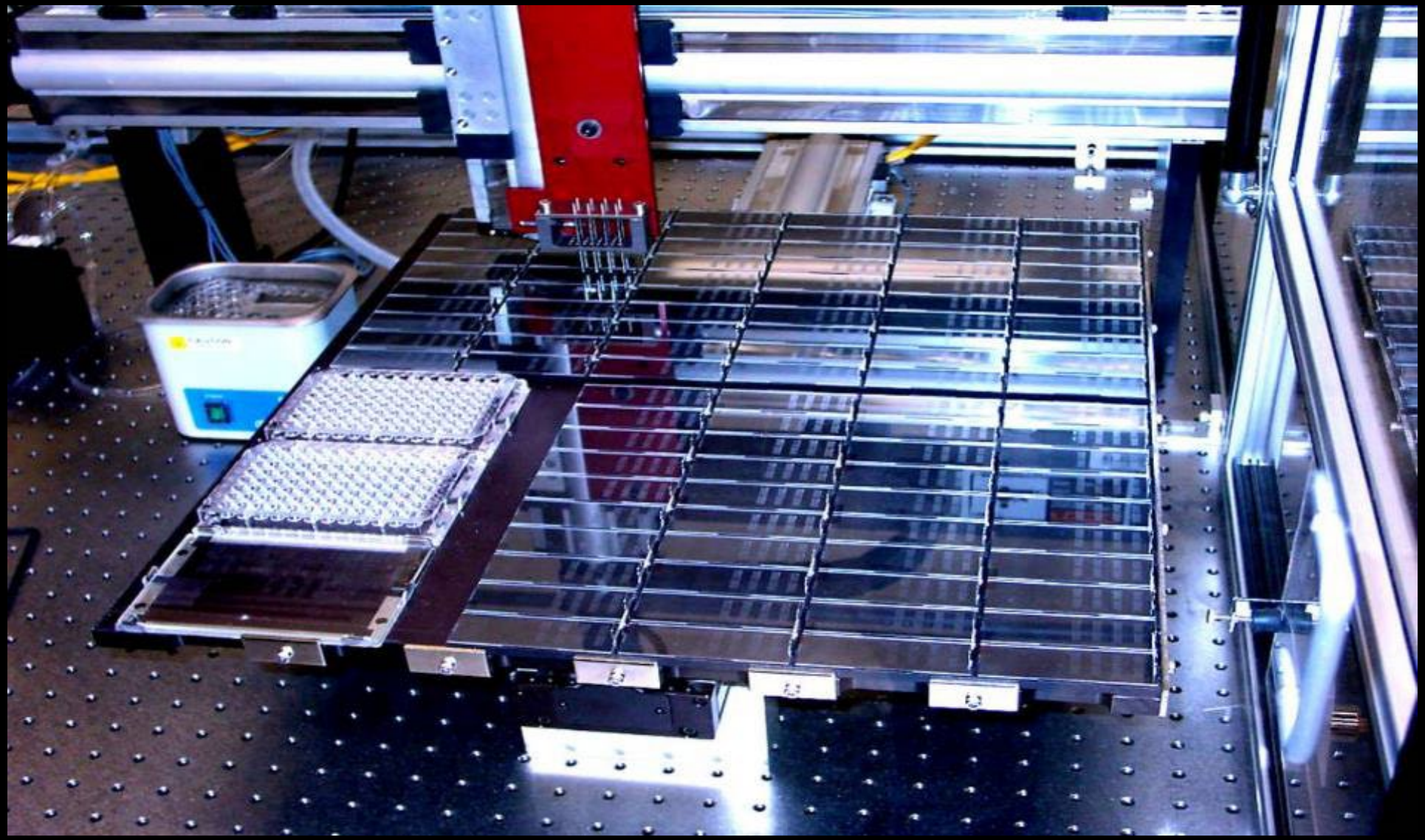

My Oligonucleotide DNA Microarray Project

Buffer Combinations for Oligo Probes (20-80 µM)

Combination	[SSC]	[Betaine]	[Herring Sperm]
1	3x	1.5 M	0.2 µg/µL
2	2x	1.5 M	0.2 µg/µL
3	1x	1.5 M	0.2 µg/µL
4	3x	1.5 M	0.1 µg/µL
5	3x	1.5 M	0 µg/µL
6	3x	0 M	0.2 µg/µL
7	0x	1.5 M	0.2 µg/µL
8	0x	0 M	0.2 µg/µL

Data Analysis

1° Score	$[(N_1\text{-}B_1) + (N_2\text{–}B_2) + (N_3\text{-}B_3)\ /3)]\ \div$ % Covariance
2° Score	# of times (0-4) the primary score is of the top 5 in a given buffer combination
3° Score	(2° score / average % covariance) x average signal intensity

My Oligonucleotide DNA Microarray Project

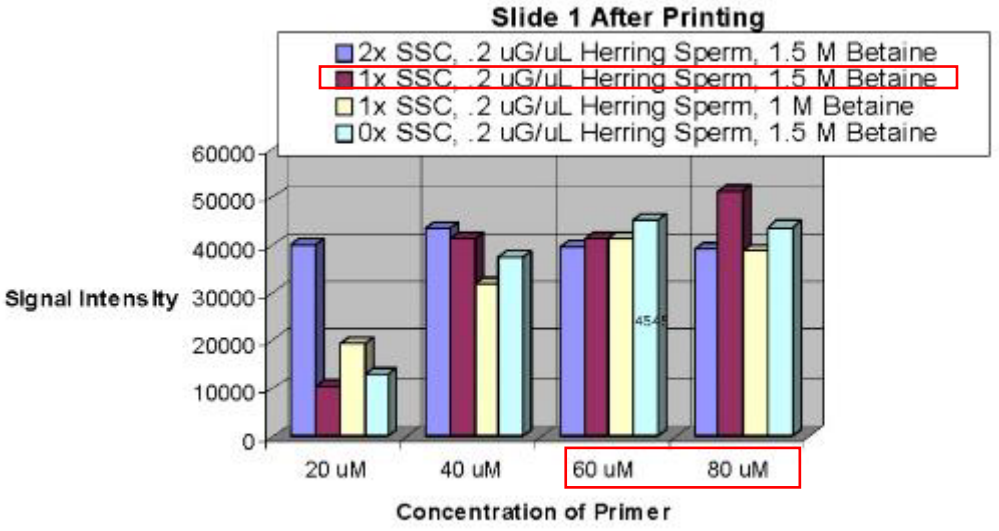

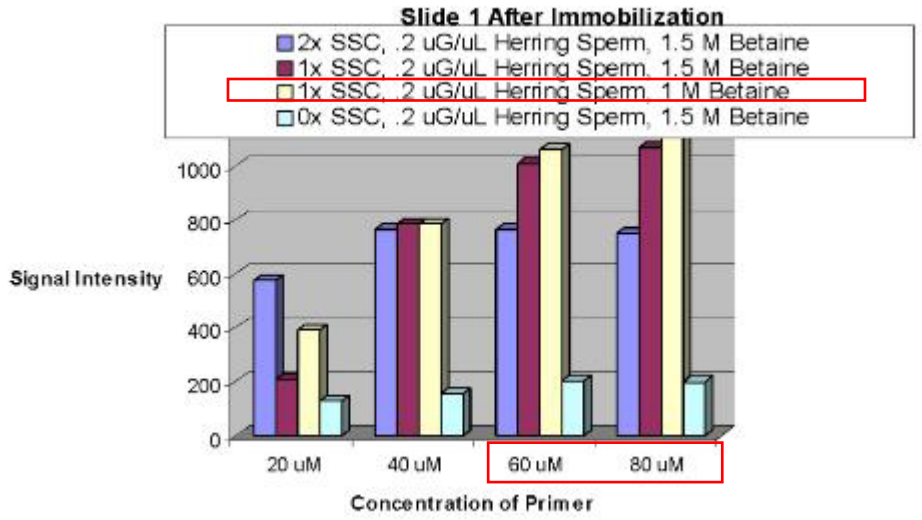

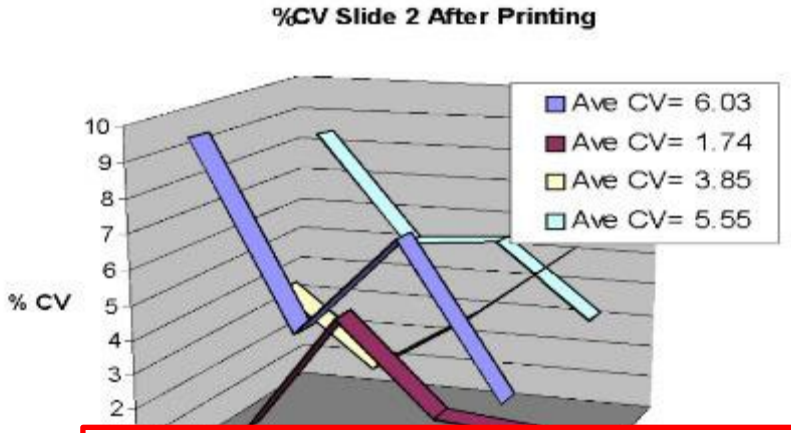

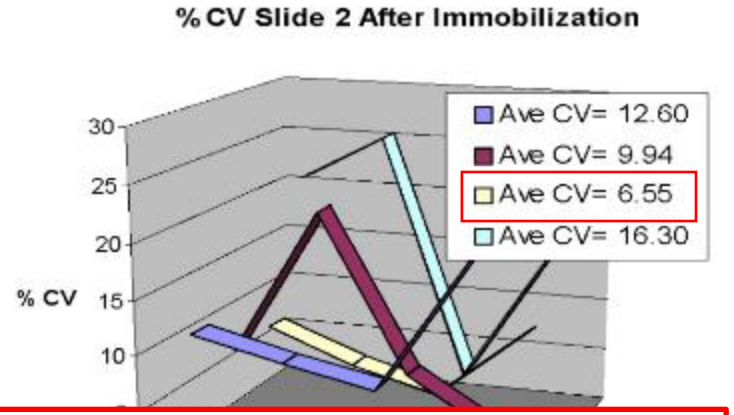

143. **Phull HS**, Galbraith DW. Unmodified oligonucleotides as microarray probes. *Poster Presentation* by H. Phull at the 13th Annual Undergraduate Biology Research Conference at the University of Arizona: Tucson, AZ, February 16, 2002.

Finding Oneself: Taking Risks/Being Someone Else's Risk

Being a Lab Ambassador

Lesson #1: Get Going and Start Somewhere

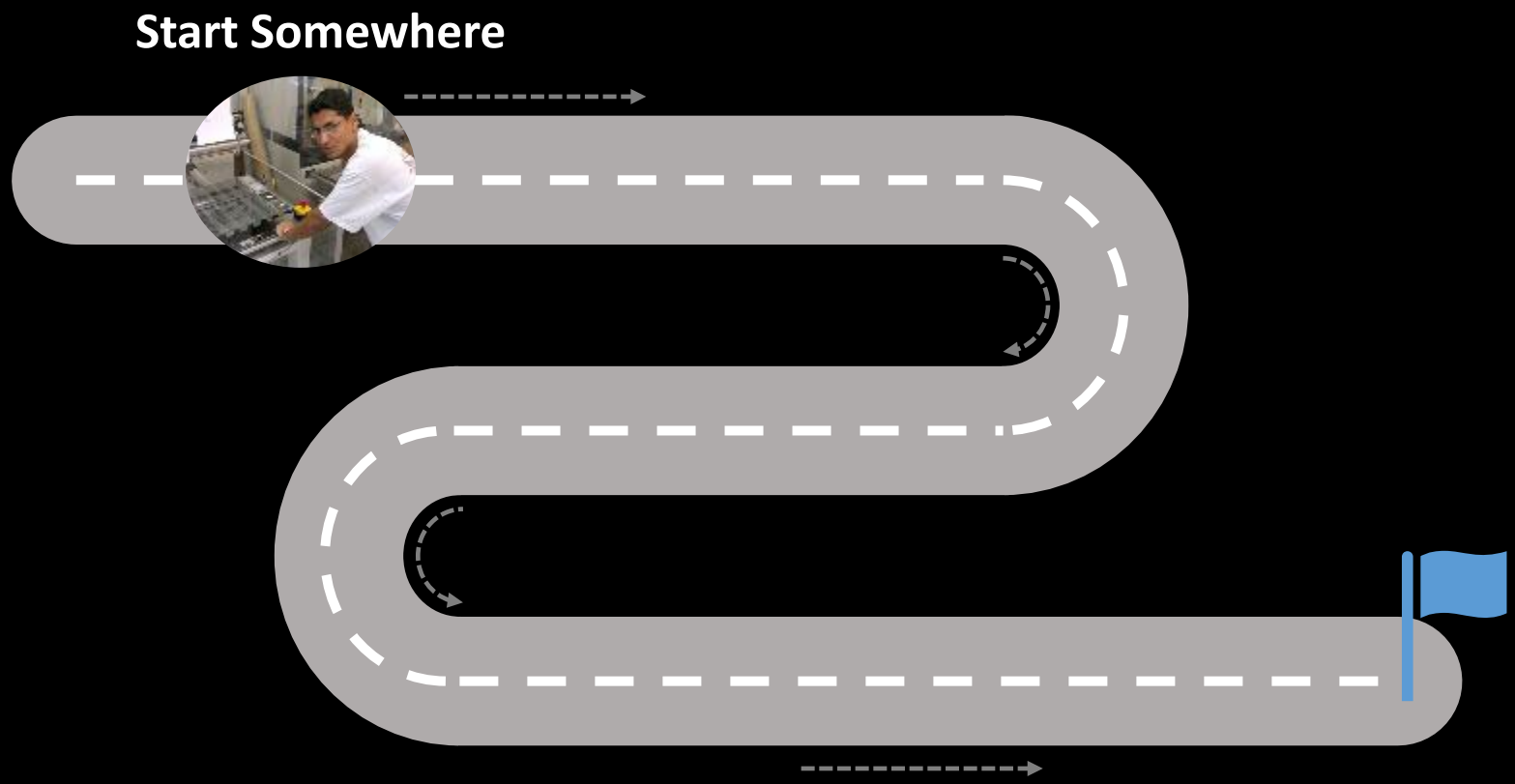

Lesson #2: Speak the World's Universal Language

Bydgoszcz, Poland

Beta vulgaris

Elwira Sliwinska

Iwona Jedrezjczyk

Sugar Beet Microarrays

Hardeep Phull

Sugar Beet Phenotypes

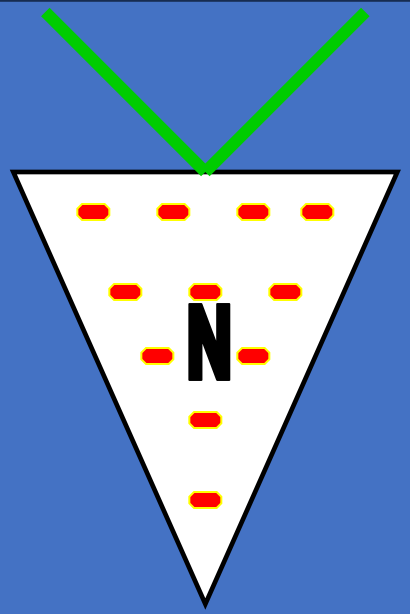

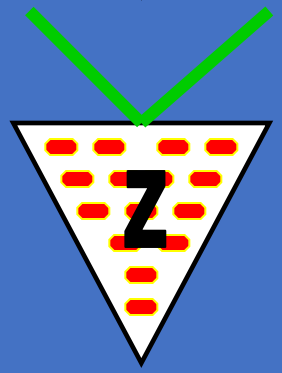

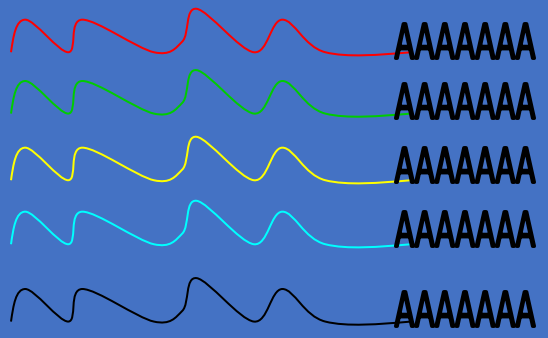

Inversely Proportional in Sugar Content and Yield

Transcribing various genes at different frequencies

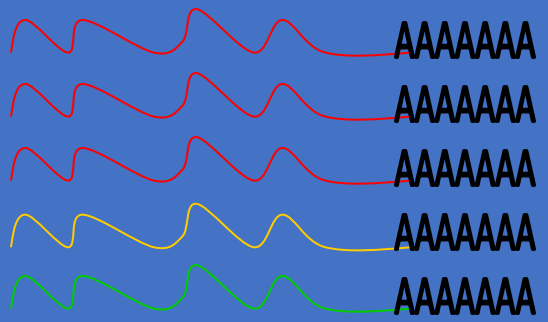

Creating a cDNA Library

Step 1: Isolate mRNA from both plant phenotypes.

Step 2: Produce cDNA and propagate in a vector

Step 3: Sequence clones and print microarrays

Step 4: Hybridize total RNA and analyze data

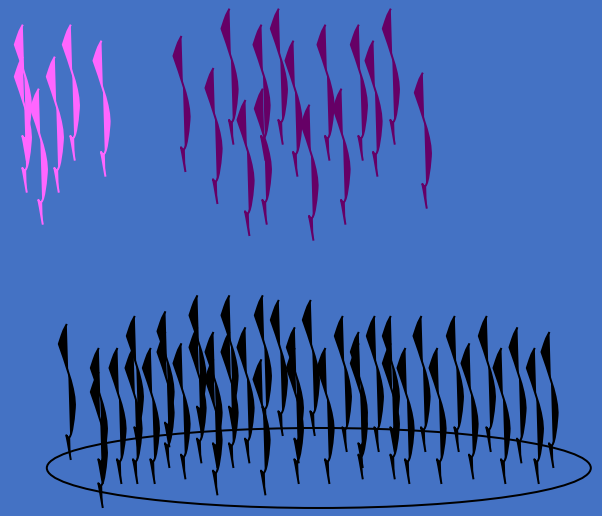

Science Does the Translation

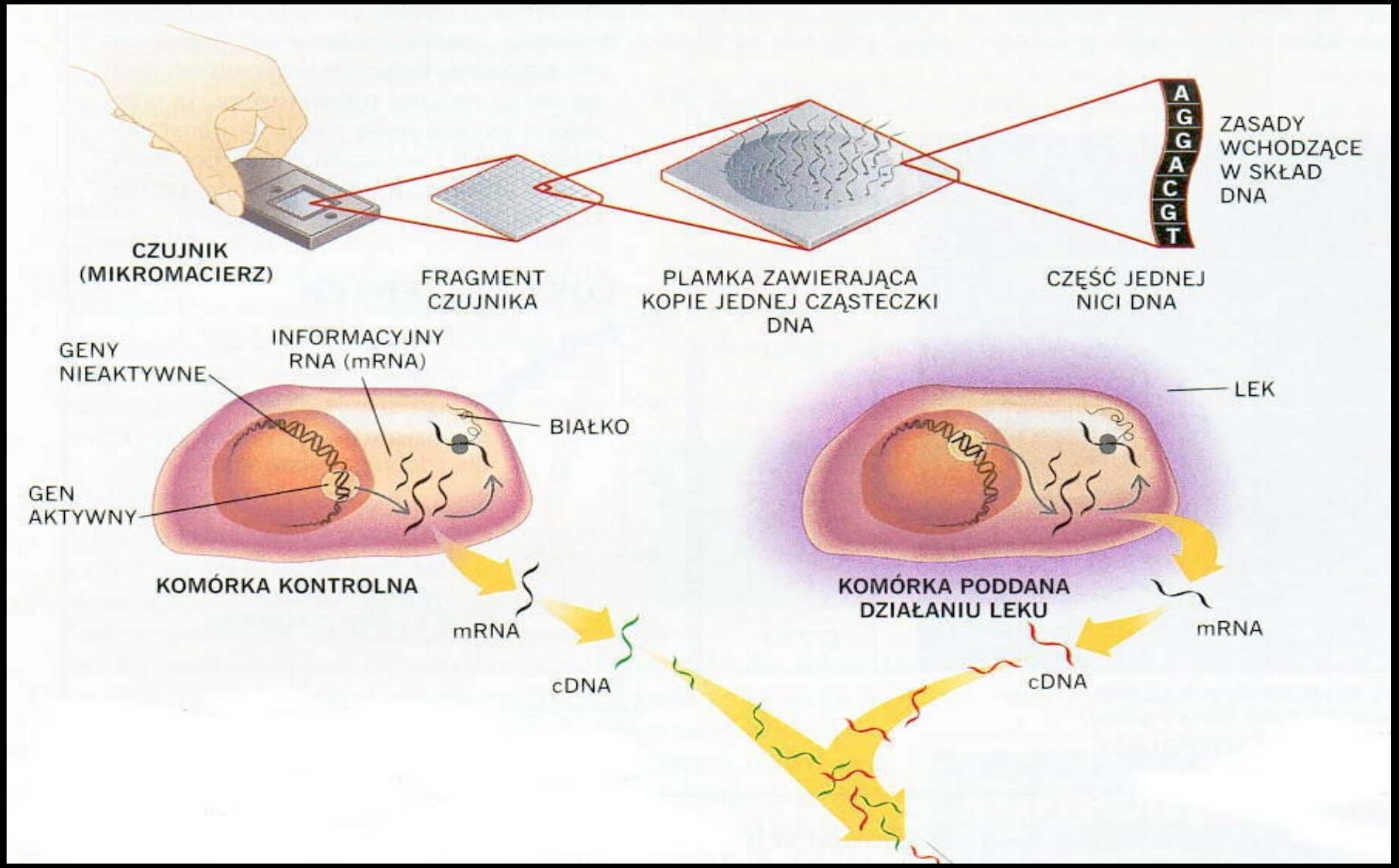

Science Does the Translation

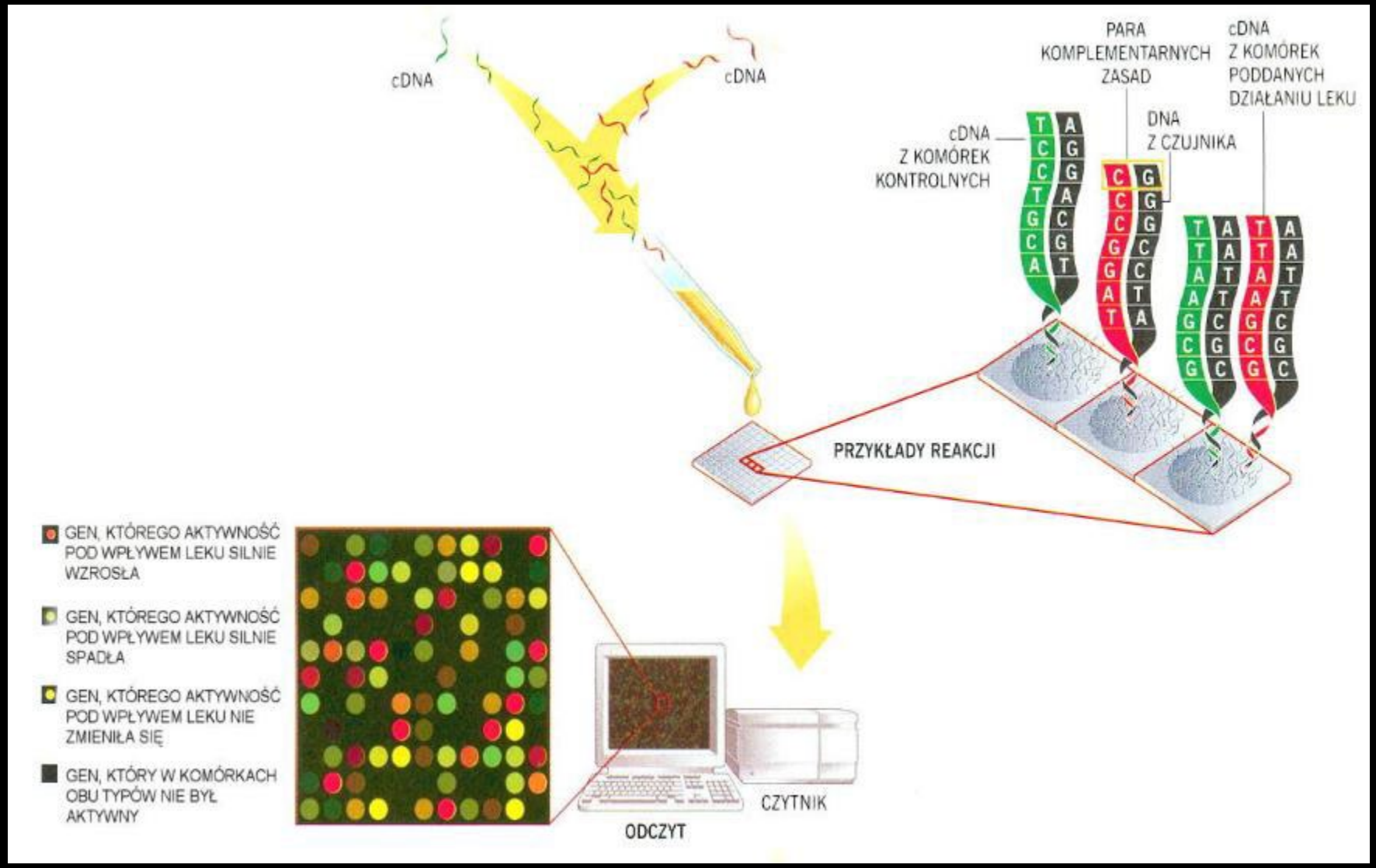

Lecturing at Akademia Techniczno Rolnicza

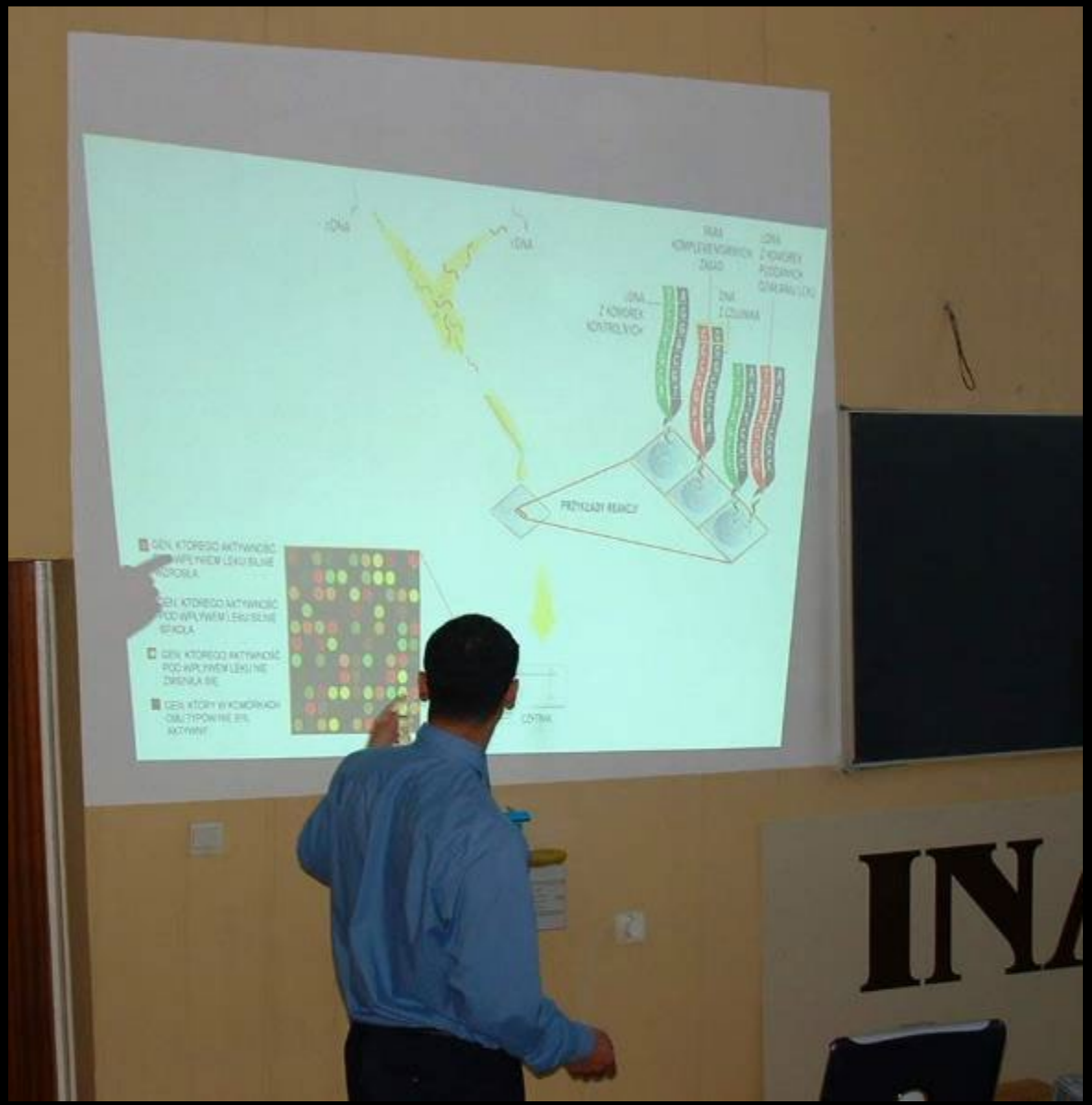

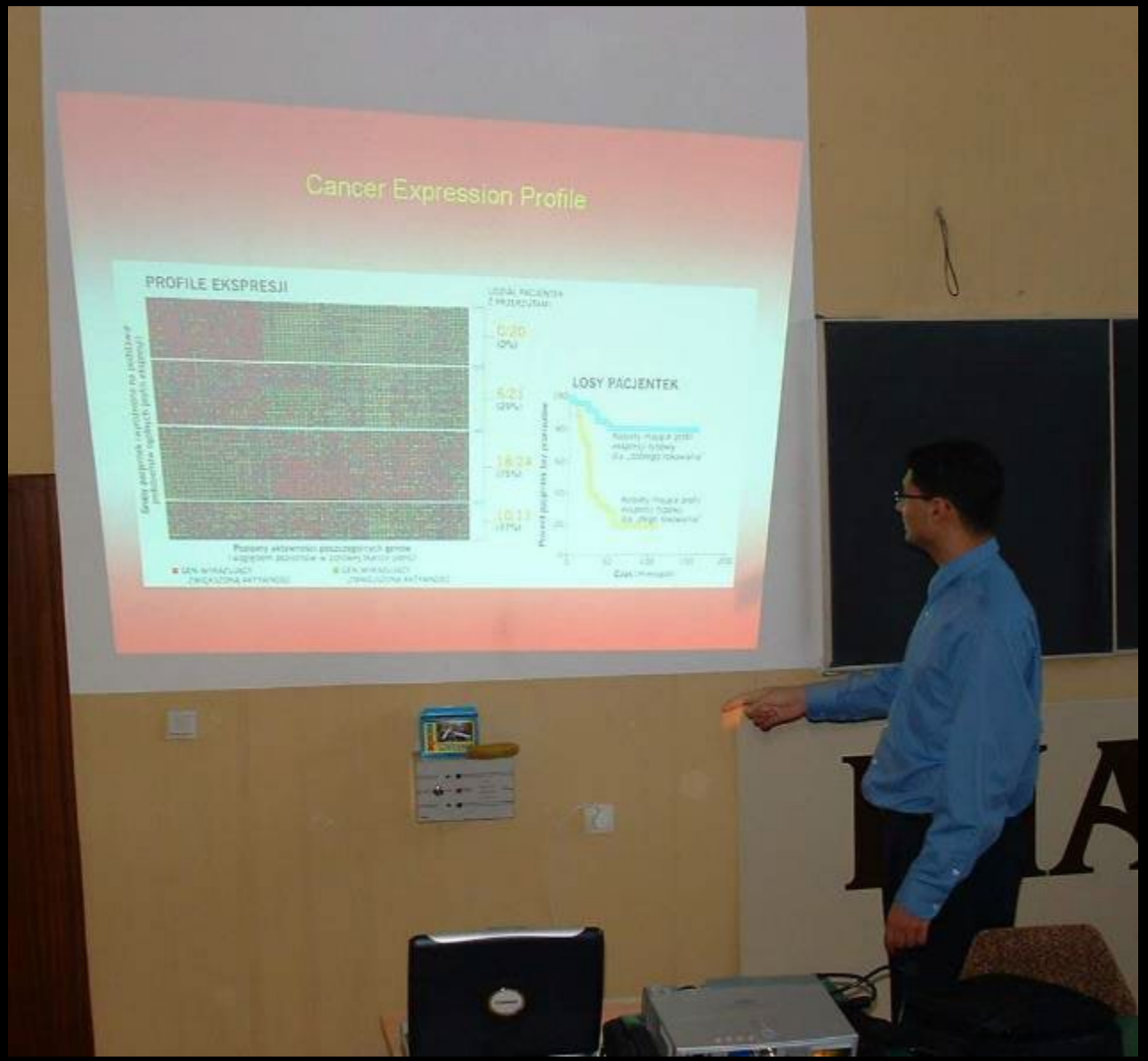

Hunkering Down for Winter's Precipitation

Getting stuck with Molecular Precipitation

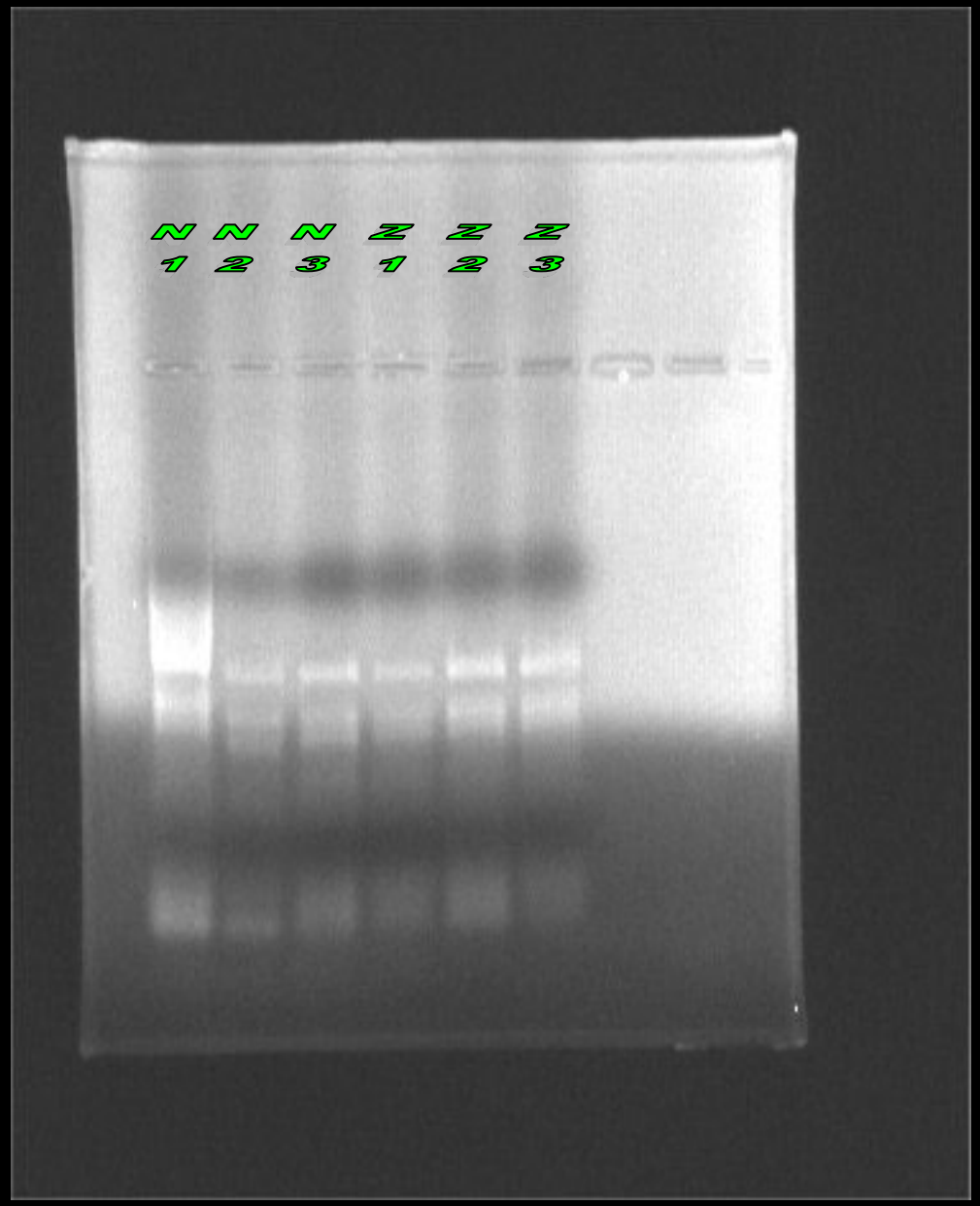

Jaroslaw Burczyk

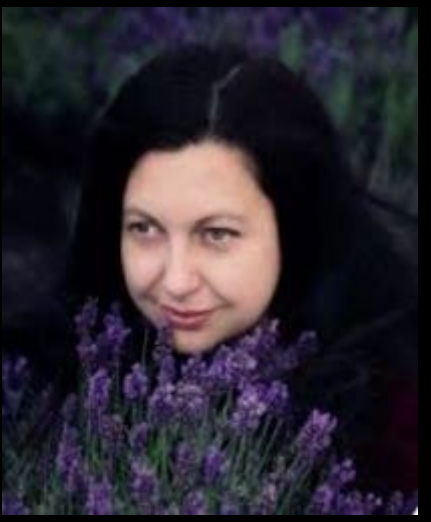

Magdalena Trojankiewicz

Wielki University

The Joy of Friendship and Collaboration

Polish Flag on Top of Copernicus' Home

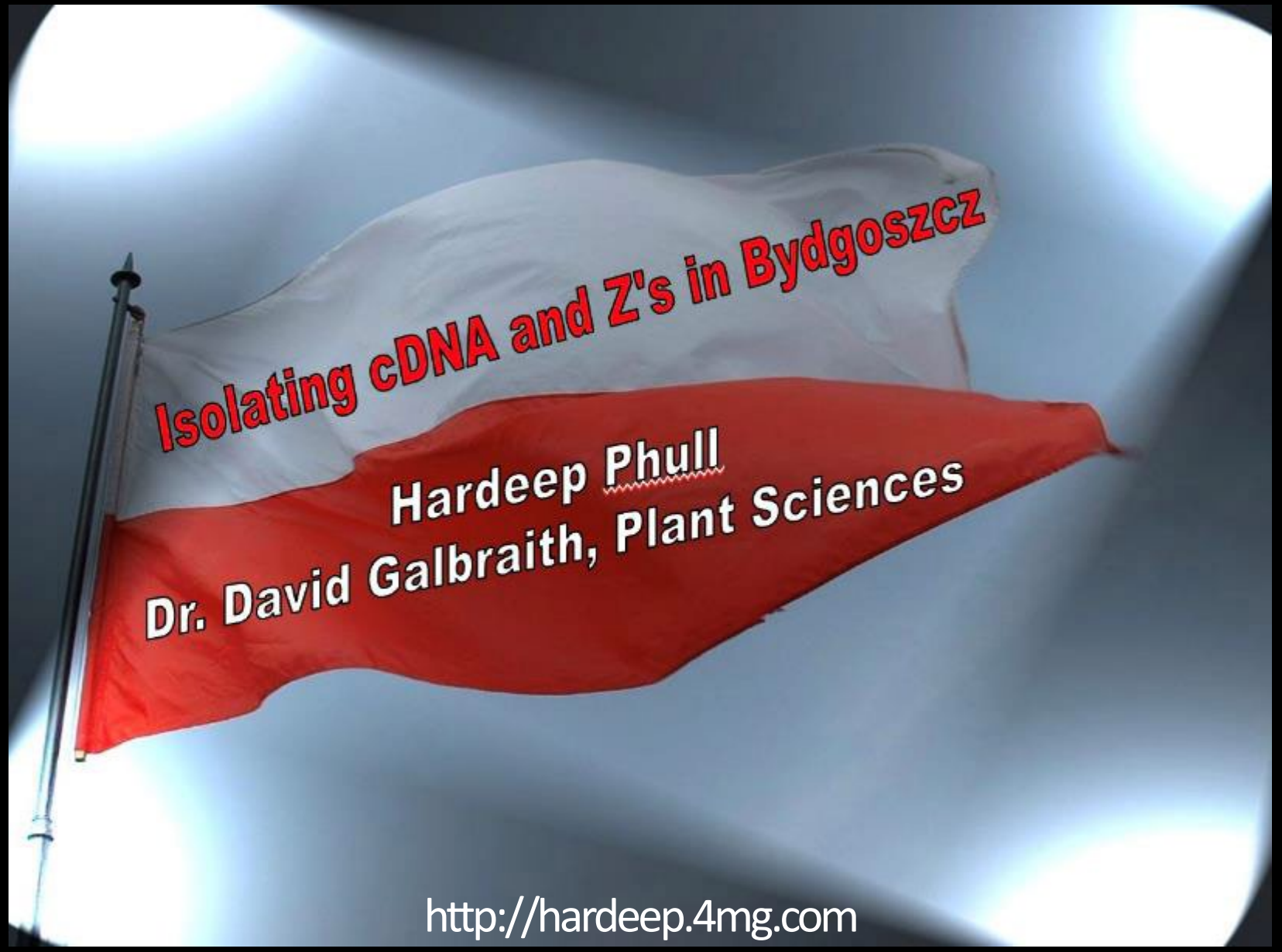

Break Through "Copernicus Moment": The World Does Not Revolve Around Us

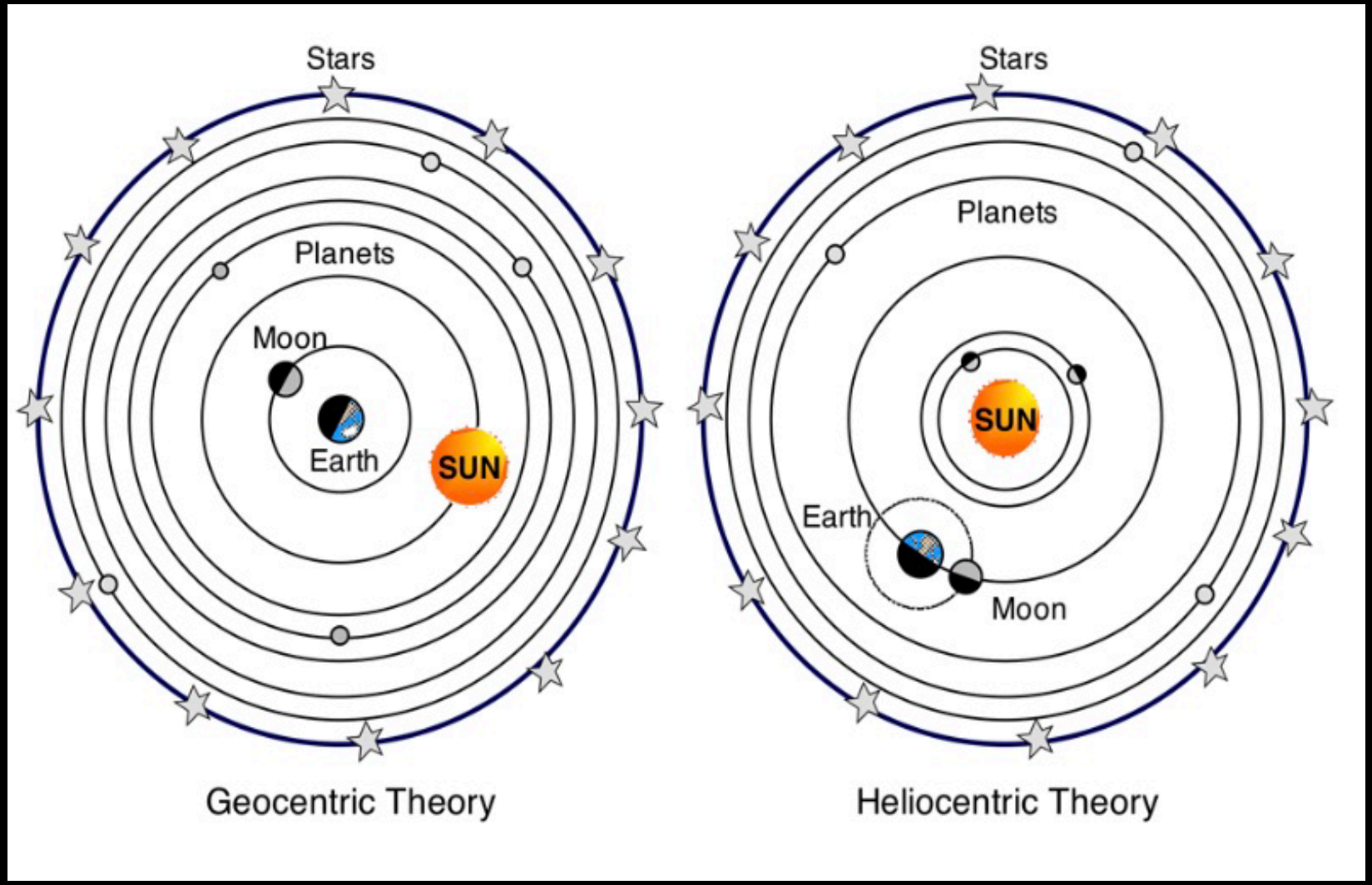

Poland's Cultural History and Beauty

Powerful Impact of Auschwitz

"We see the shell of what remains. We haven't lived here. We haven't died here."

Recognizing What Matters Most

Going Viral…


Google
bravo ubrp
All
Images
Saved
University of Arizona
University of Arizona | BRAVO! Student
UBRP - The University of Arizona
Undergraduate Biology Research ...
UBRP - The University of Arizona
Biology Research Abroad: Vist...
UBRP - The University of Arizona
Biology Research Abroad: Vist...
UBRP - The Universit...
Undergraduate Biol...
Dr. Katalin Gothard
Jeaho Lim
UBRP - The University of Arizona
Undergraduate Biology Research Progr...
YouTube
2023 UBRP Conference Keynote Talk ...
YouTube
ubrpbravo - YouTube

Hiding in Plain Sight…

Lesson #2: Speak the World's Universal Language

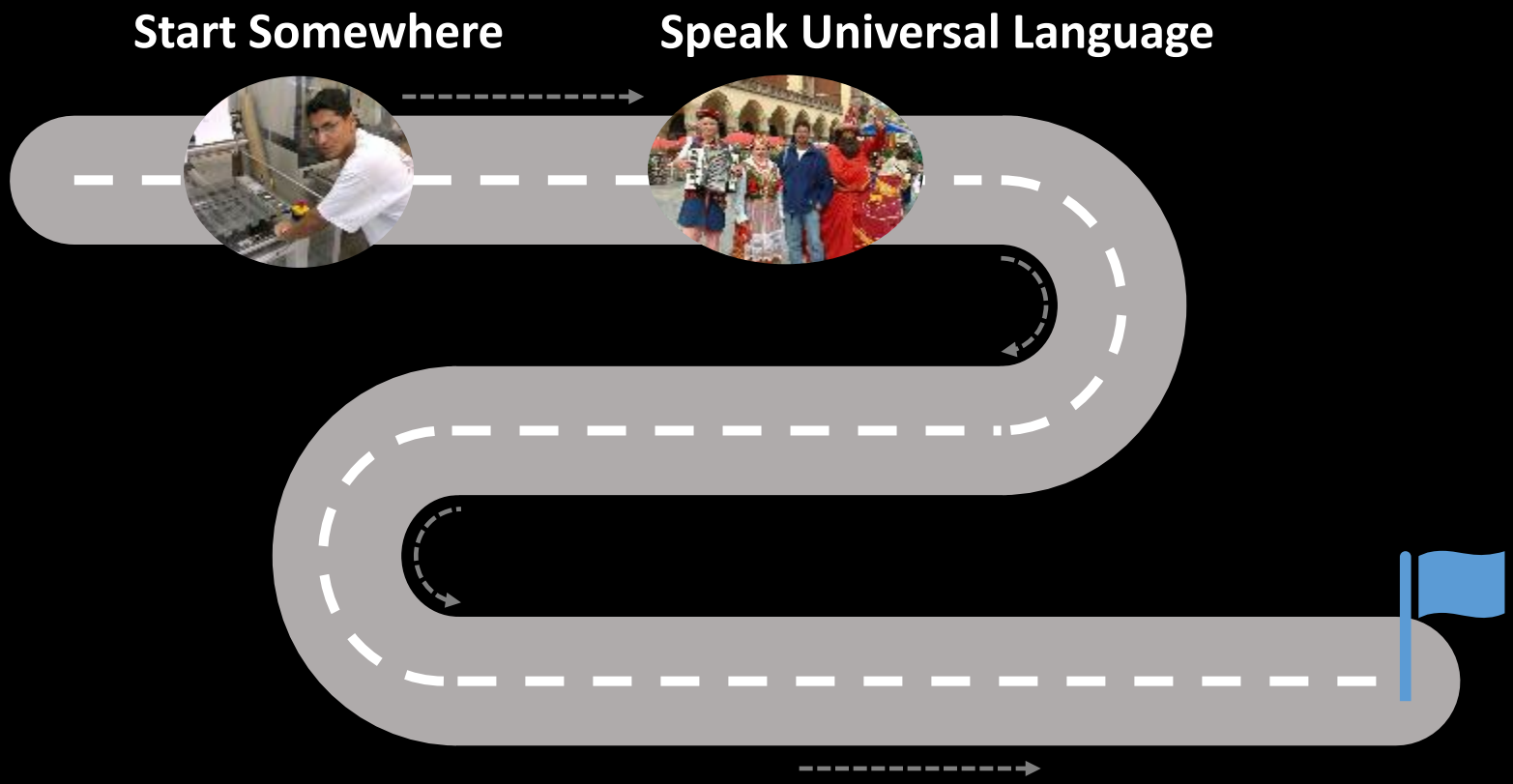

Lesson #3: Transcend Artificial Boundaries

Importance of Preparation and Checklists


U of A Campus


University Medical Center

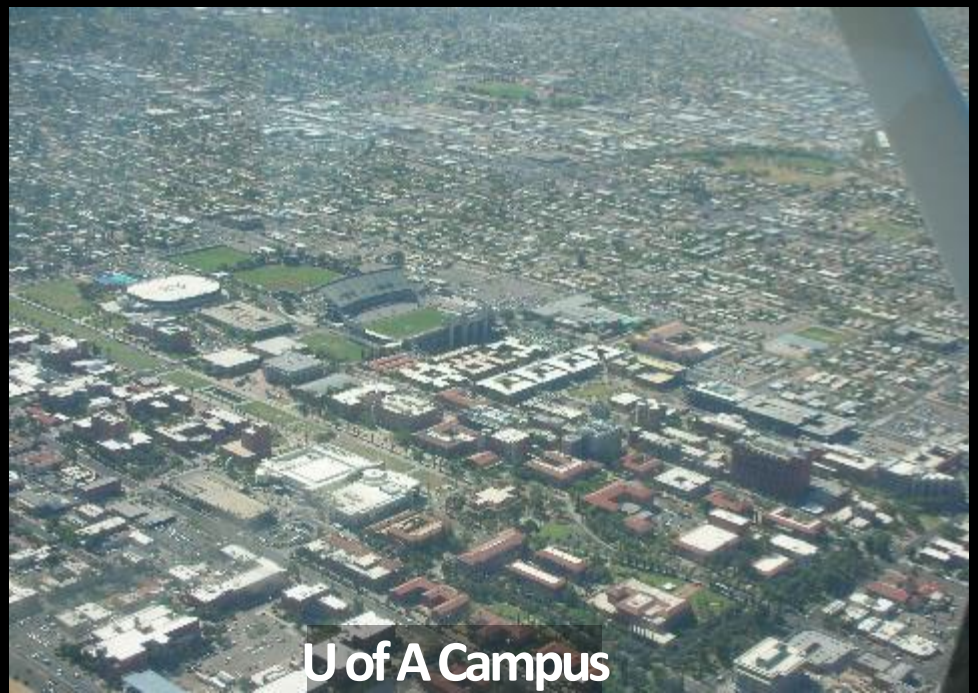
U of A Campus


“A” Mountain


Mt. Lemmon


Kitt Peak


Mt. Wrightson


Mt. Lemmon (Winter)

Burke Lakefront Airport

Lake Erie Islands

Sandusky, Ohio

Downtown Cleveland

Being an Aviation Ambassador

Flying into Med School

AAMC

AMCAS APPLICATION REPORT - 2006 ENTERING CLASS

Applicant Copy

REPORT DATE: 09/08/2005 06:08 PM **SUBMISSION DATE:** 06/26/2005 06:42 PM **PROCESSED DATE:** 06/30/2005 03:32 PM

Applicant's Legal Name: Mr. Hardeep Singh Phull **Page:** 10

EXPERIENCE

Experience Type: Extracurricular/Hobbies/Avocations

Experience Name: Private Pilot (FAA Rating: Single Engine Land) **Dates:** 08/2003 - Until Present **Hours/Week:** 3

Contact Name & Title: Sean Grace, Flight Instructor/Pilot, Delta Airlines

Organization Name: Federal Aviation Administration

City, State, Country: Tucson, AZ, United States

Experience Description: Pilots and doctors are held down by the same force of gravity, but both find ways to soar above it: the former relies on thrust and lift, while the latter is propelled by sincere compassion and selfless service. They each perform tasks with precise dexterity. The pilot maneuvers in three axes, making highly coordinated movements of the arms and legs on the ailerons, elevators, and rudders. Meanwhile, the doctor's hands are equally capable of executing an intricate laparoscopic surgery, gently cradling a baby's head during birth, or providing a comforting touch to a patient in need of reassurance. They are both creatures of meticulous observation. A pilot's vigilance is divided between the surge of data from flight instruments, intermittent relays from air traffic controllers, and the expanse of sky surrounding the aircraft. Likewise, a doctor is thoroughly attentive to a patient's total health needs: sincerely listening to their emotional fears and frustrations; appreciating and encouraging their cultural and spiritual beliefs; and scrutinizing the tools of modern medicine to address their physical ailments. Indeed, pilots and doctors are headed in the same direction, rising above obstacles and transcending artificial boundaries on their ongoing journey towards the horizon.

If you focus on being authentic and interesting, you are no longer interviewed. Every interaction becomes an opportunity.

Challenges of Laparoscopic Partial Nephrectomy

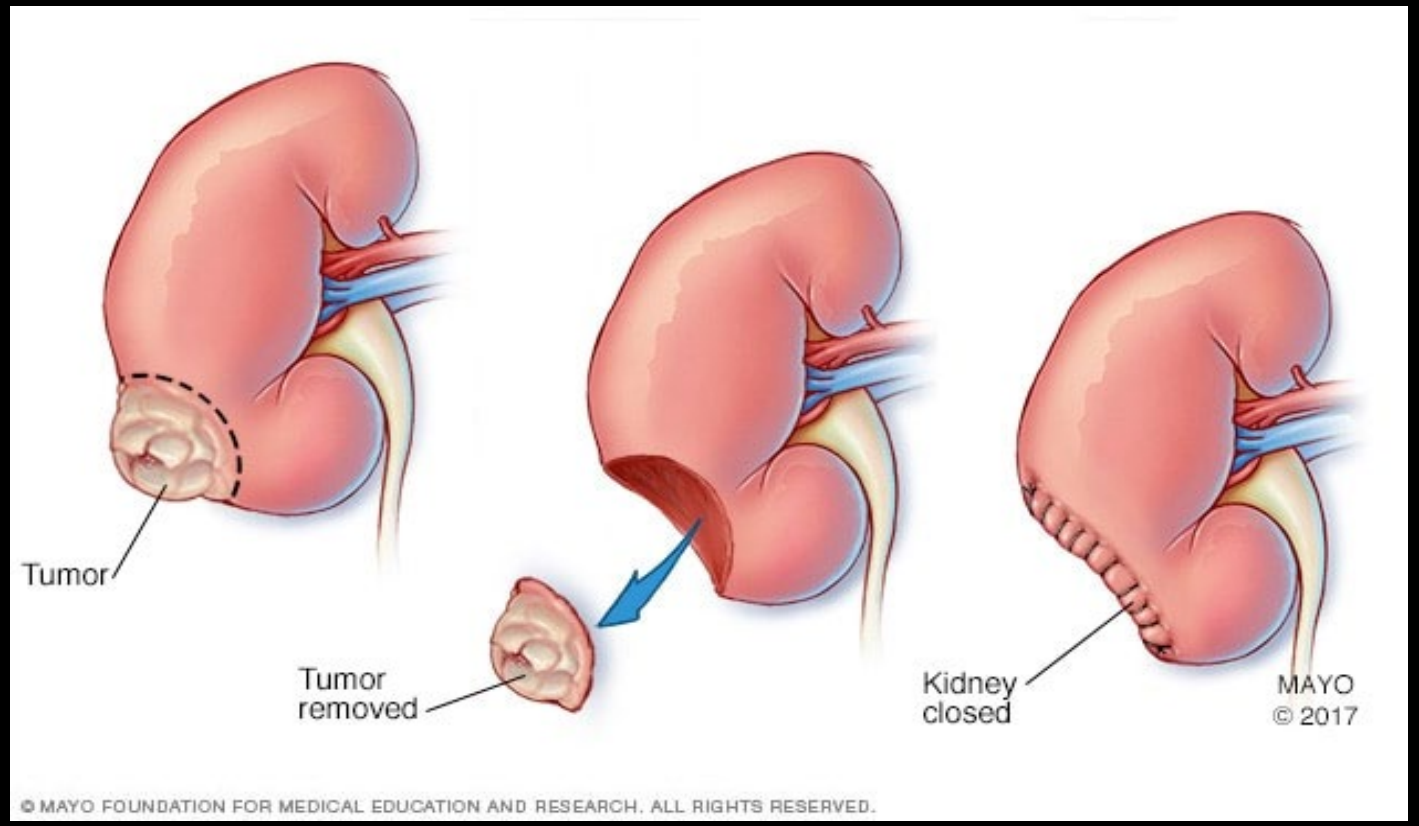

Sanjay Ramakumar

Craig Comiter

- Technically challenging
- Time-intensive task (i.e. steep learning curve)
- Closure of the collecting system
- Hemostasis
- Prolonged warm ischemia

Challenges of Hemostasis

- Gold standard: sutures over bolsters
- Biodegradable tissue sealants
  - Synthetic polyethylene glycol-lactide
  - FDA approved as lung sealant
  - Tailored resorption and physical properties

Ischemia/Reperfusion (IR) Injury Mechanism

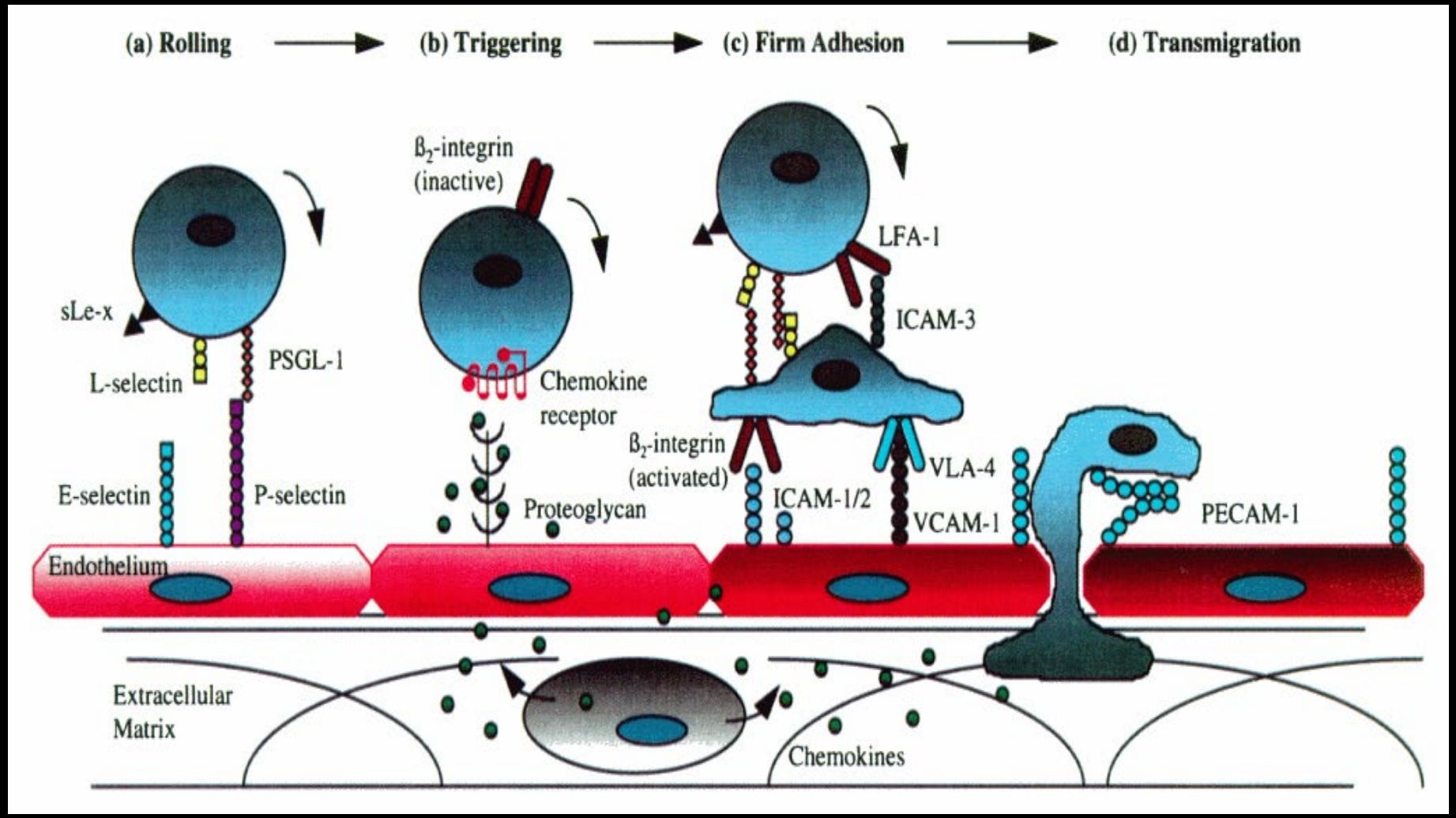

ICAM-1 is up-regulated, resulting in leukocyte adhesion & tissue damage

Blocking IR Injury Via ICAM-1 Antisense Oligonucleotides

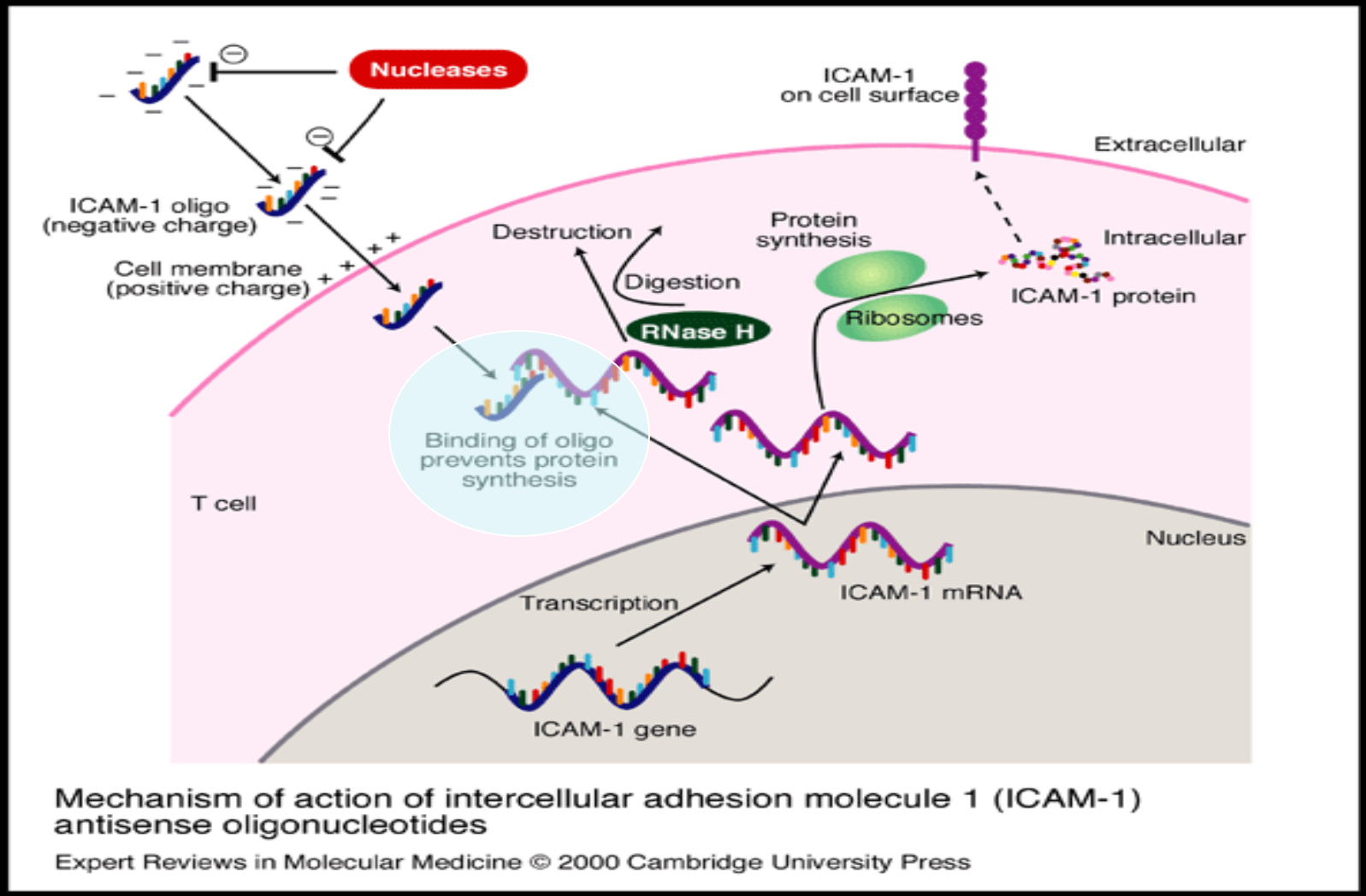

Mechanism of action of intercellular adhesion molecule 1 (ICAM-1) antisense oligonucleotides

Antisense Oligonucleotides against ICAM-1

Delivering Labeled Oligonucleotides via a Hydrogel in a Mouse Model

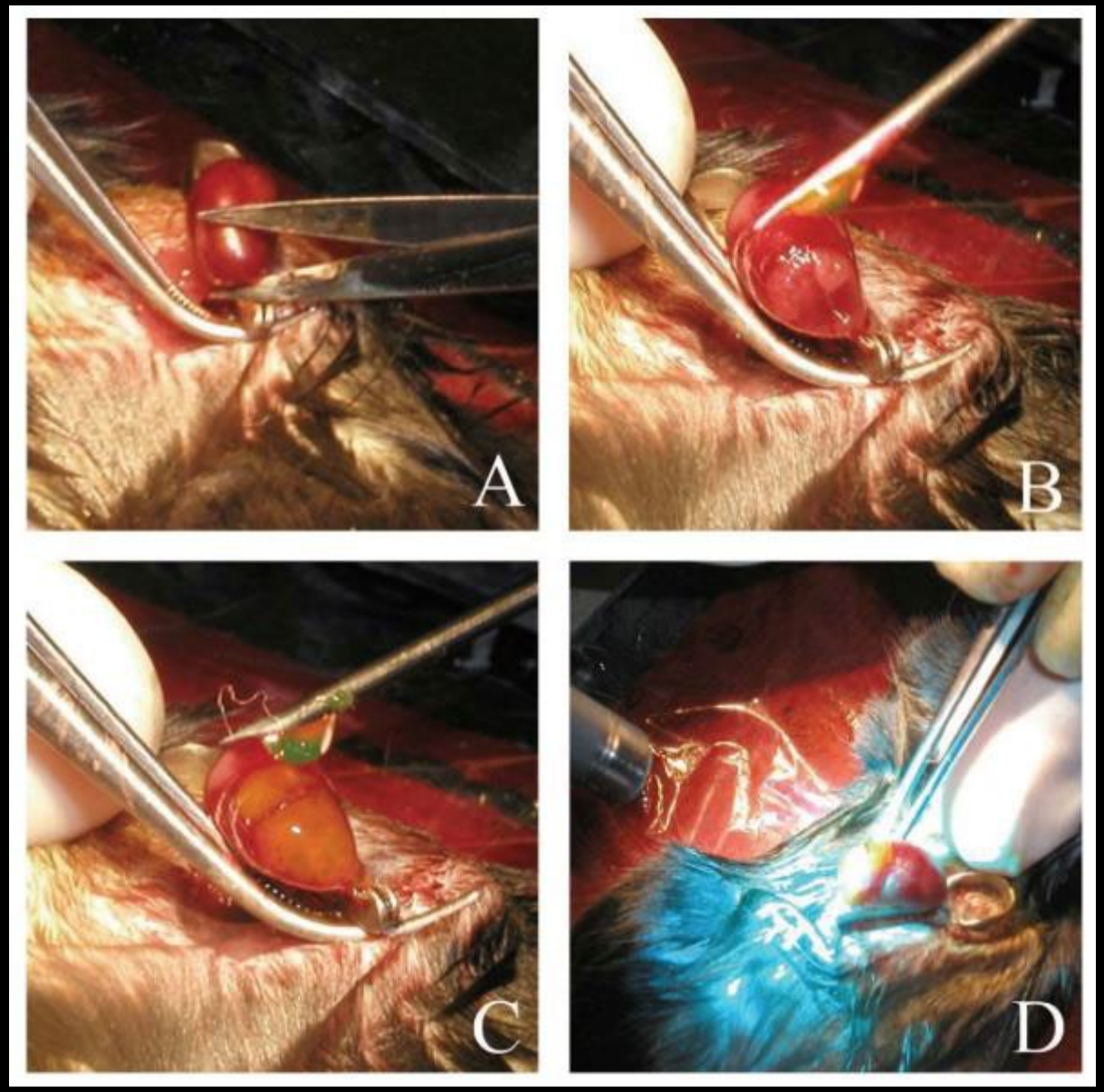

Using a Microarray Confocal Scanner for Quantification

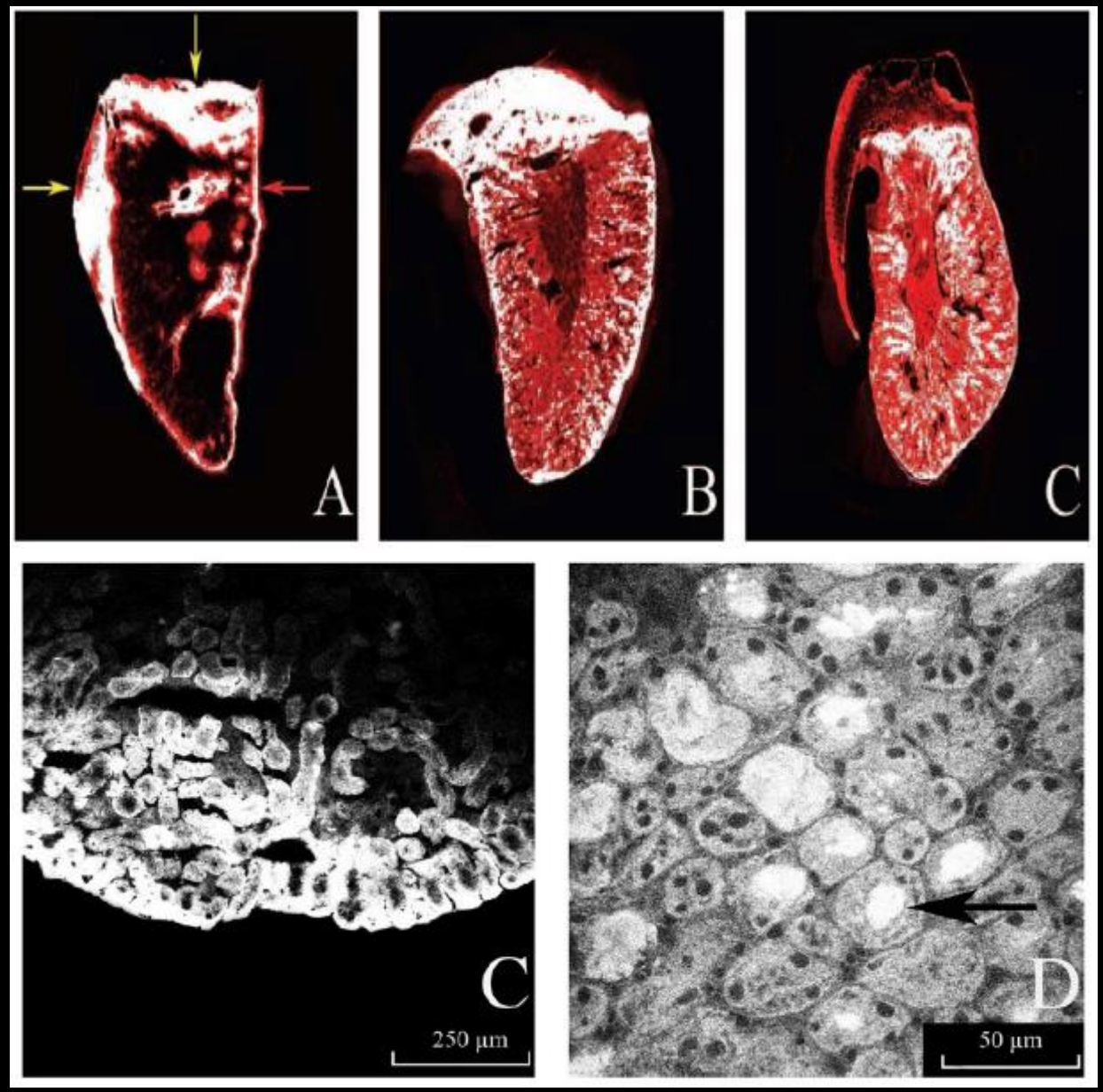

Decreasing Tissue Injury Via ICAM-1 Antisense Oligonucleotides

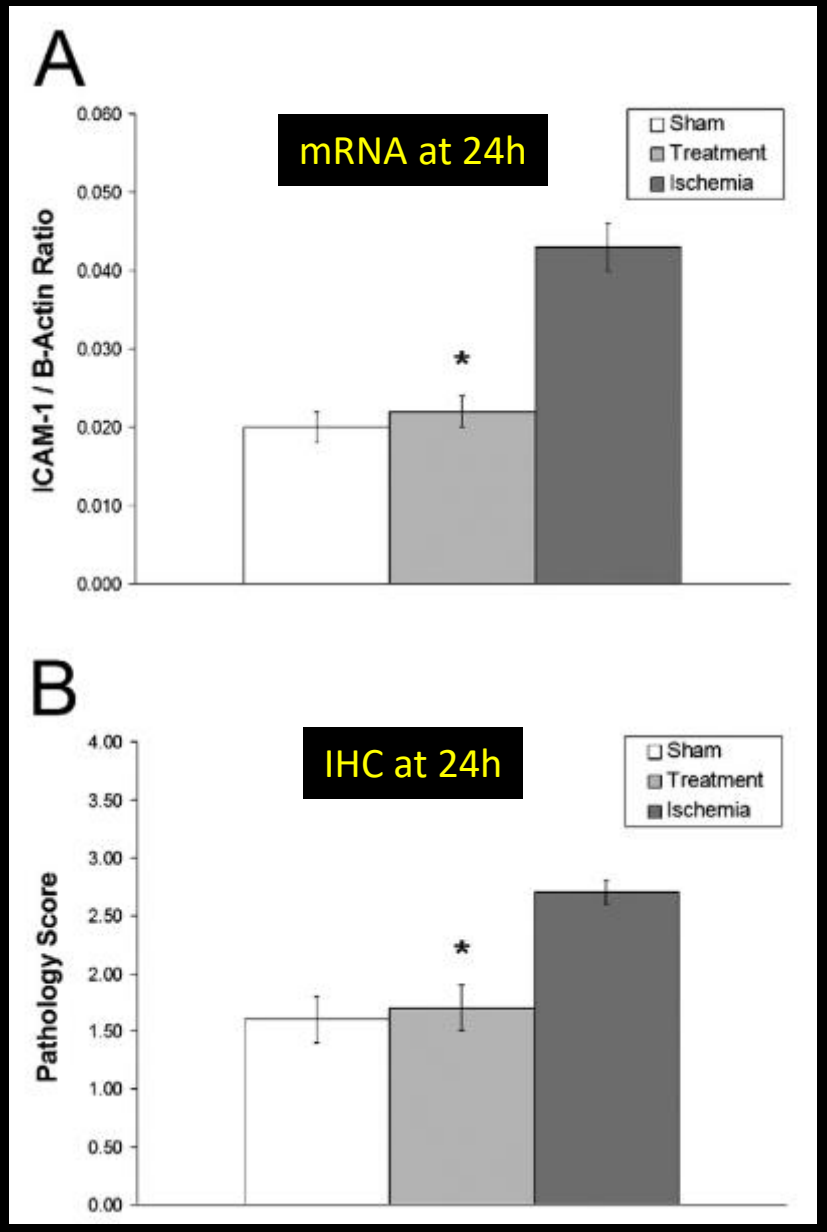

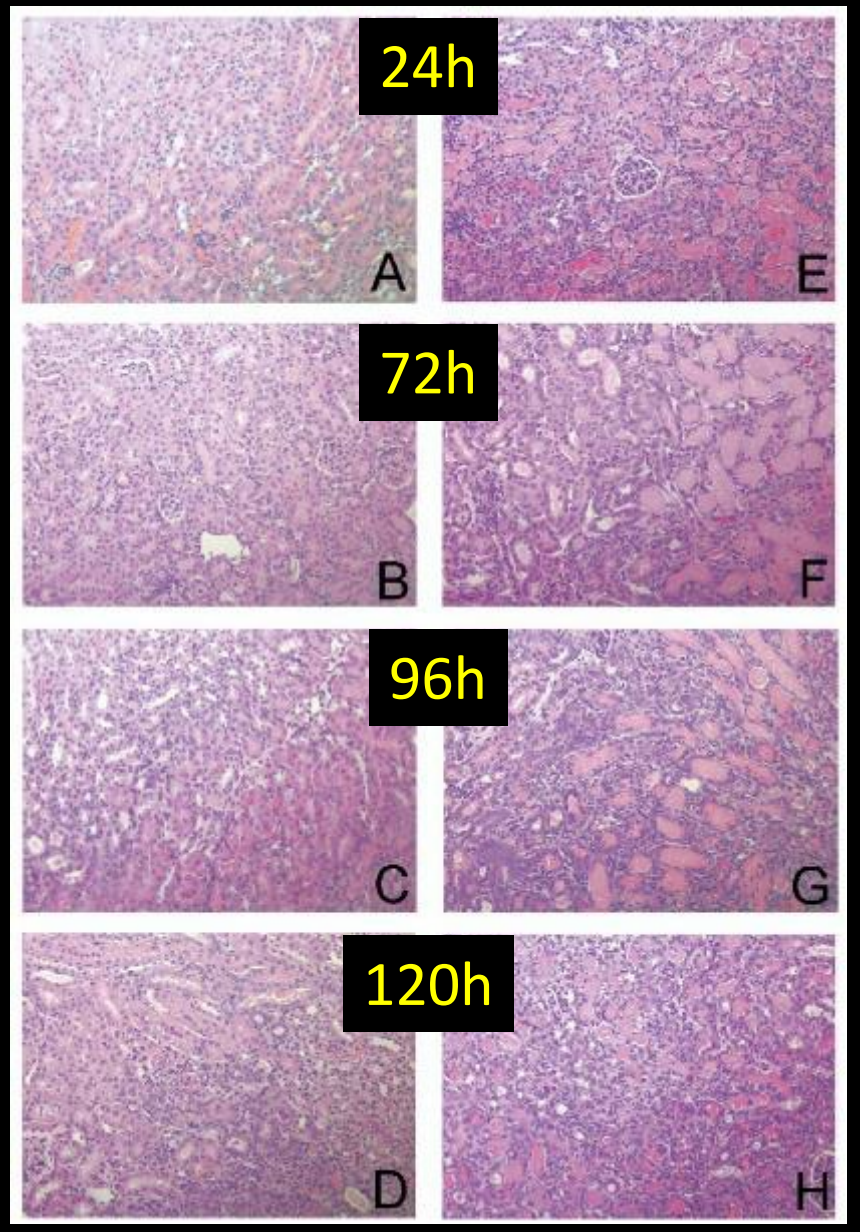

Lesson #3: Transcend Artificial Boundaries

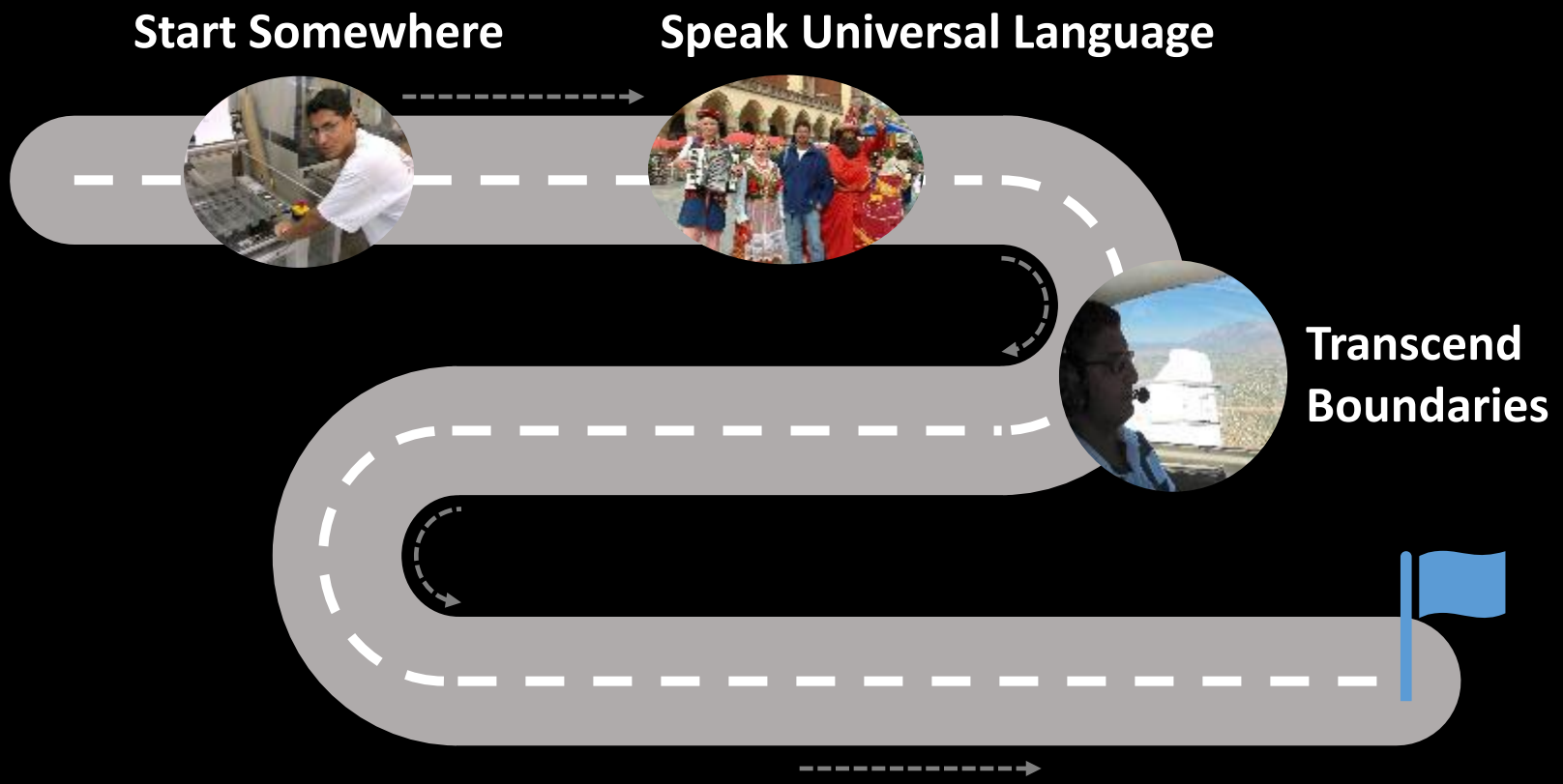

esson #4: Embrace Discomfort and Failure, the Substances of Reinventio

Cleveland Clinic: World-Class Medical Education

Cleveland Clinic
Lerner College of Medicine

CASE WESTERN RESERVE UNIVERSITY
School of Medicine

About Academics Admissions Tuition & Financial Aid Students Faculty More

/ Academics / Assessment

Assessment

Cleveland Clinic Lerner College of Medicine of Case Western Reserve University

Overview | Portfolio System | Clinical Assessment System | Physician Advisors

Overview

The philosophy of CCLCM is that assessment should enhance learning. As such, you are provided feedback on your progress in basic science, research and clinical disciplines from multiple sources. This feedback allows you to identify your own strengths and weaknesses in comparison to defined, expected standards of performance.

No grades or comprehensive exams are given. Rather, you will submit essays and supporting evidence of your achievement of the nine competency milestones to the Medical Student Promotion and Review Committee to inform promotion recommendations to the next year.

World-Class Medical Education

Well-Rounded Discomfort

Cleveland Clinic Lerner College of Medicine | CASE WESTERN RESERVE UNIVERSITY School of Medicine

About Academics Admissions Tuition & Financial Aid Students Faculty More

/ Academics / Assessment

Assessment

Overview | Portfolio System | Clinical Assessment System | Physician Advisors

Overview

The philosophy of CCLCM is that assessment should enhance learning. As such, you are provided feedback on your progress in basic science, research and clinical disciplines from multiple sources. This feedback allows you to identify your own strengths and weaknesses in comparison to defined, expected standards of performance.

No grades or comprehensive exams are given. Rather, you will submit essays and supporting evidence of your achievement of the nine competency milestones to the Medical Student Promotion and Review Committee to inform promotion recommendations to the next year.

Competencies

- Research/Scholarship
- Medical Knowledge
- Communication
- Professionalism
- Personal Development
- Patient Care
- Teamwork/Collaboration
- Systems-based Practice
- Reflective Practice

#4a: Adapt To Where Your Talents Get Heard

Increased Abdominal Pressure

↓

Increases Bladder Pressure

↓

Exceeds Urethral Resistance

↓

Urine Leakage

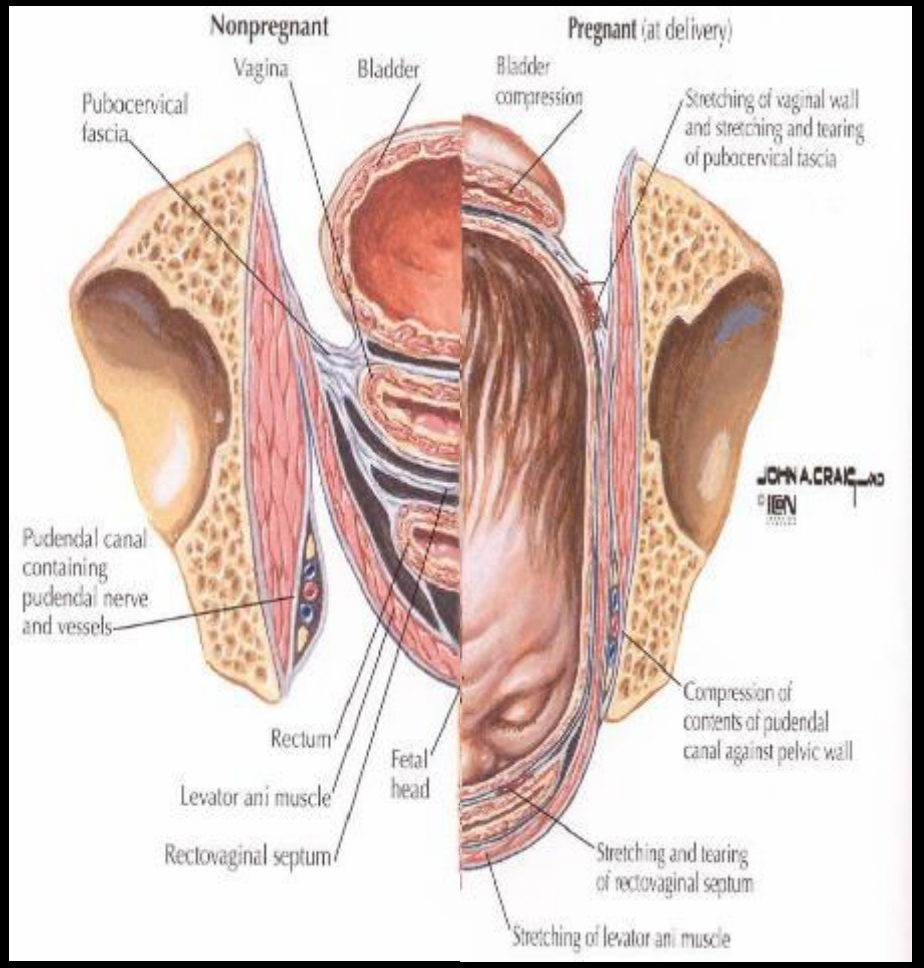

Margot Damaser

Stress Urinary Incontinence and Childbirth

Rat Model of Pelvic Injury by Childbirth

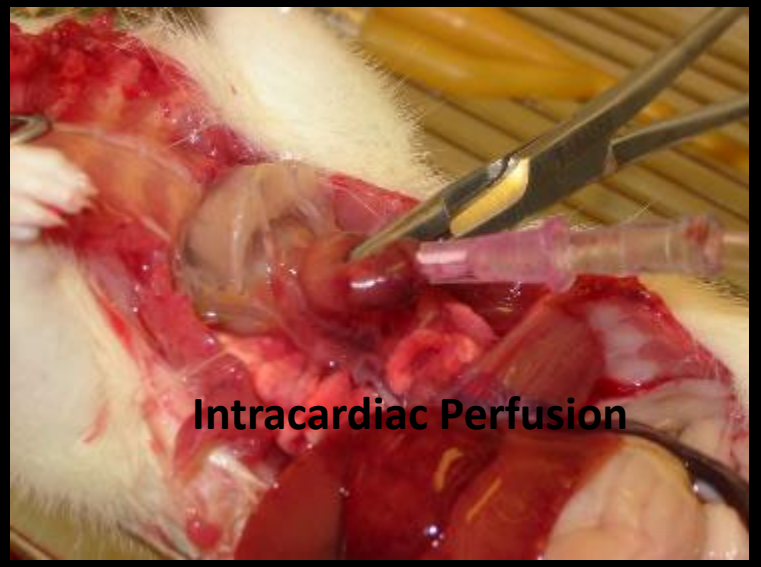

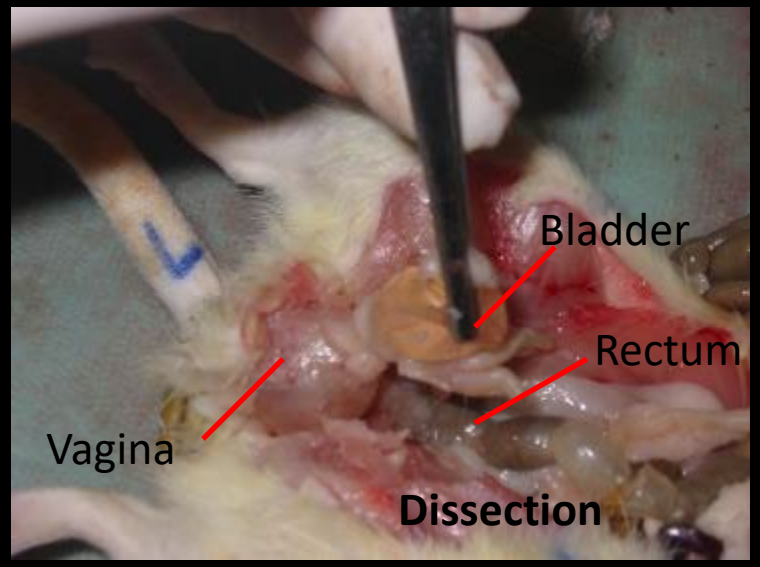

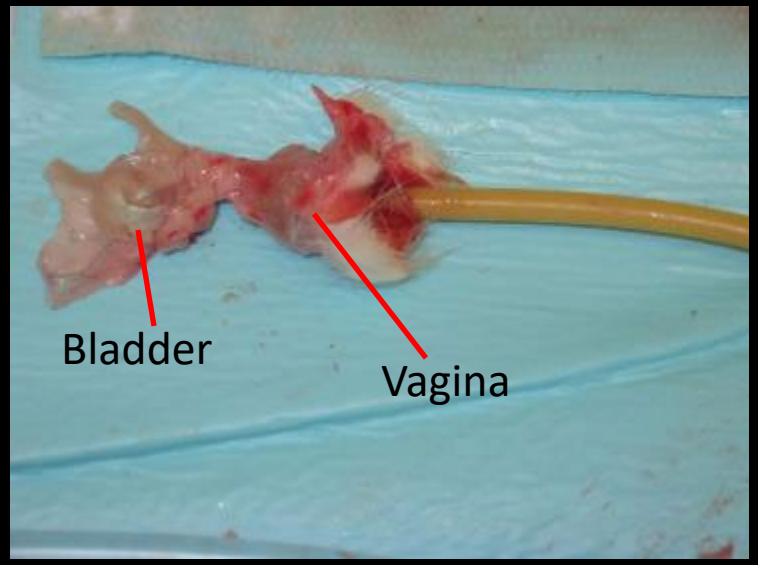

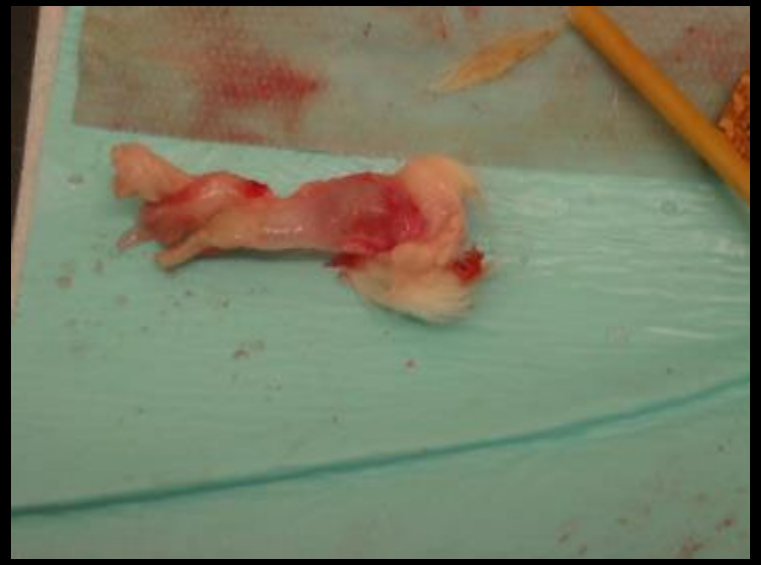

Quantifying Tissue Damage and Hypoxia

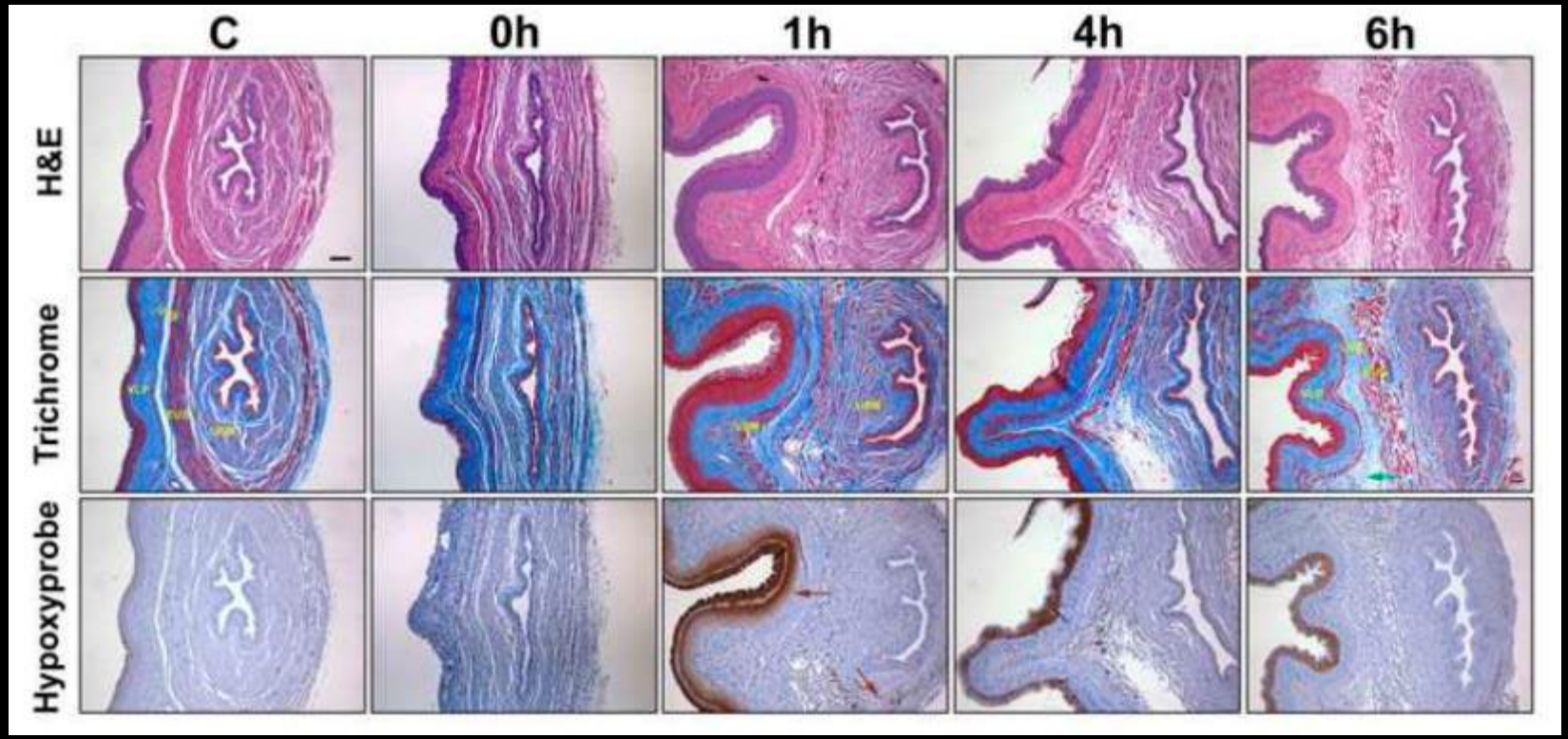

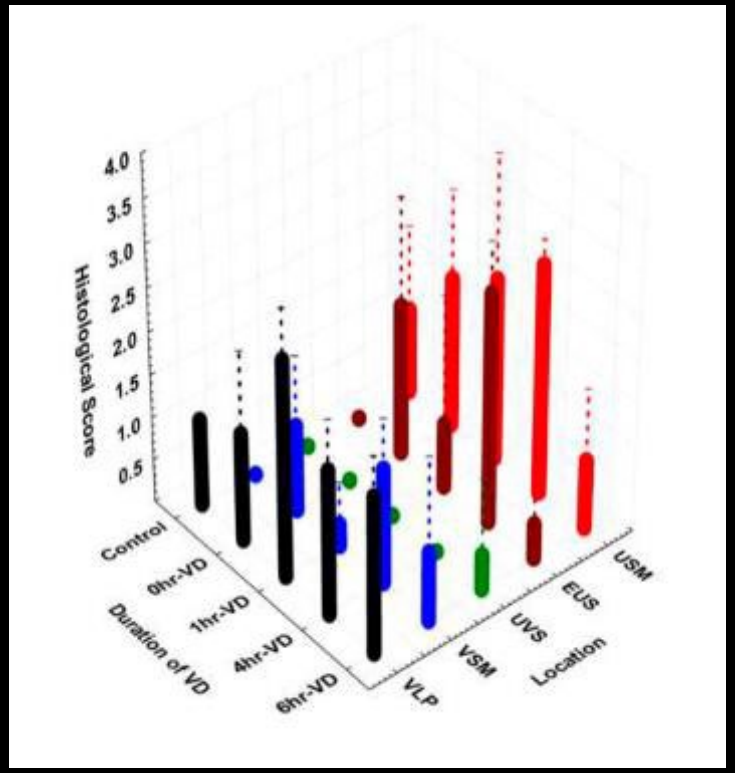

Challenges in Publication

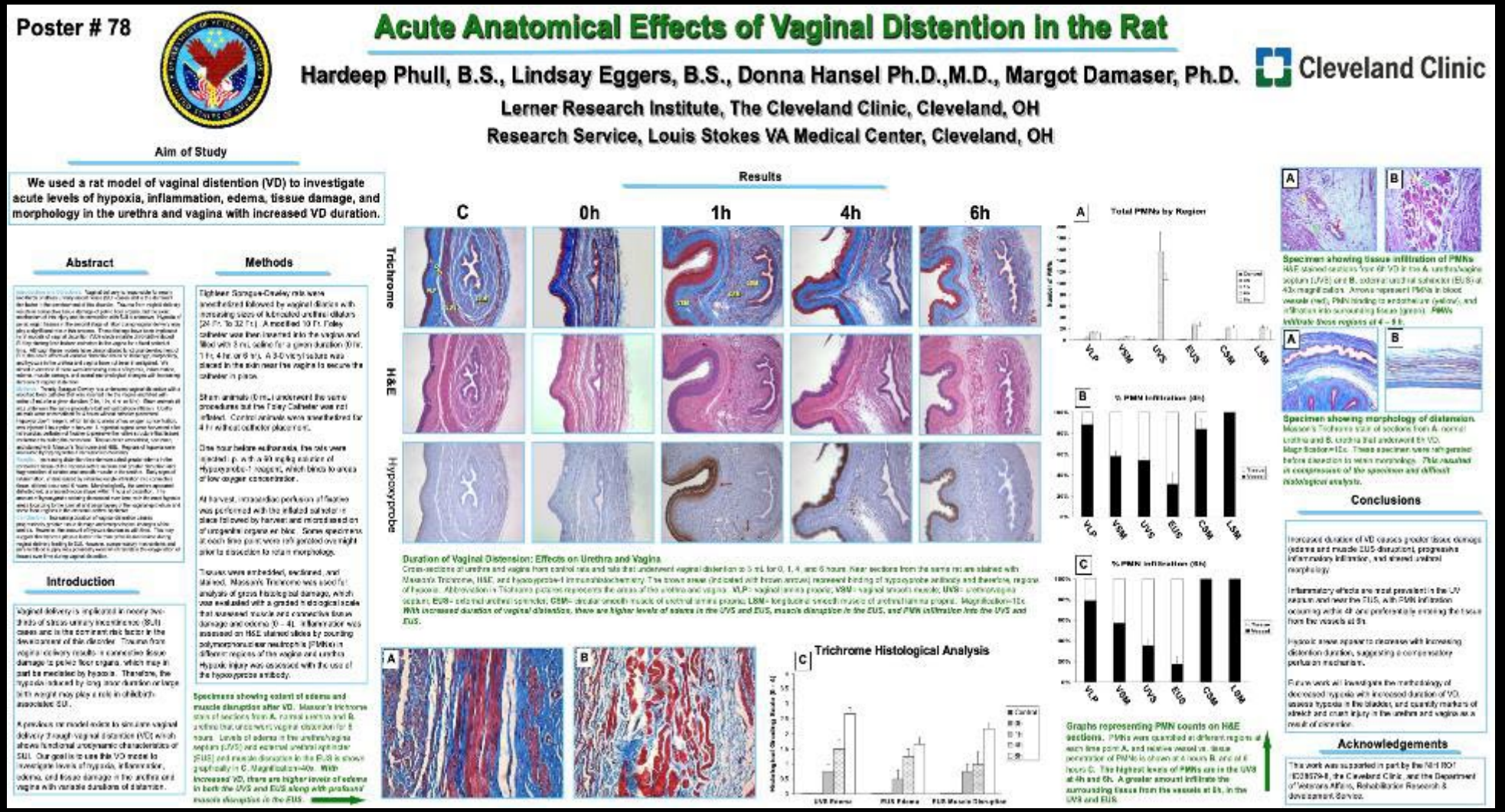

Poster # 78

Acute Anatomical Effects of Vaginal Distention in the Rat

Hardeep Phull, B.S., Lindsay Eggers, B.S., Donna Hansel Ph.D.,M.D., Margot Damaser, Ph.D.

Cleveland Clinic

Lerner Research Institute, The Cleveland Clinic, Cleveland, OH

Research Service, Louis Stokes VA Medical Center, Cleveland, OH

Aim of Study

We used a rat model of vaginal distention (VD) to investigate acute levels of hypoxia, inflammation, edema, tissue damage, and morphology in the urethra and vagina with increased VD duration.

Abstract

[illegible]

Introduction

Vaginal delivery is implicated in nearly two-thirds of stress urinary incontinence (SUI) cases and is the dominant risk factor in the development of this disorder. Trauma from vaginal delivery results in connective tissue damage to pelvic floor organs, which may in part be mediated by hypoxia. Therefore, the hypoxia induced by long labor duration or large birth weight may play a role in childbirth-associated SUI.

A previous rat model exists to simulate vaginal delivery through vaginal distention (VD) which shows functional urodynamic characteristics of SUI. Our goal is to use this VD model to investigate levels of hypoxia, inflammation, edema, and tissue damage in the urethra and vagina with variable durations of distention.

Methods

Eighteen Sprague-Dawley rats were anesthetized followed by vaginal dilation with increasing sizes of lubricated urethral dilators (24 Fr. To 32 Fr.). A modified 10 Fr. Foley catheter was then inserted into the vagina and filled with 3 mL saline for a given duration (0 hr, 1 hr, 4 hr, or 6 hr). A 3-0 Vicryl suture was placed in the skin near the vagina to secure the catheter in place.

Sham animals (0 hr.) underwent the same procedures but the Foley catheter was not inflated. Control animals were anesthetized for 4 hr without catheter placement.

One hour before euthanasia, the rats were injected i.p. with a 60 mg/kg solution of Hypoxyprobe-1 reagent, which binds to areas of low oxygen concentration.

At harvest, intravaginal perfusion of fixative was performed with the inflated catheter in place followed by harvest and micro-dissection of urogenital organs en bloc. Some specimens at each time point were left pinned overnight prior to dissection to retain morphology.

Tissues were embedded, sectioned, and stained. Masson's Trichrome was used for analysis of gross histological damage, which was evaluated with a graded histological scale that assessed muscle and connective tissue damage and edema (0 – 4). Inflammation was assessed on H&E stained slides by counting polymorphonuclear neutrophils (PMNs) in different regions of the vagina and urethra. Hypoxic injury was assessed with the use of the hypoxyprobe antibody.

Specimens showing extent of edema and muscle disruption after VD. Masson's trichrome stain of sections from A. normal control and B. urethra that underwent vaginal distention for 6 hours. Levels of edema in the urethra/vagina septum (UVS) and external urethral sphincter (EUS) and muscle disruption in the EUS is shown graphically in C. Magnification=40x. With increased VD, there are higher levels of edema in both the UVS and EUS along with profound muscle disruption in the EUS.

Results

Duration of Vaginal Distension: Effects on Urethra and Vagina

Cross-sections of urethra and vagina from control rats and rats that underwent vaginal distention at 0 hr, 1 hr, 4 hr, and 6 hours. Near sections from the same rat are stained with Masson's Trichrome, H&E, and hypoxyprobe-1 immunohistochemistry. The brown areas (indicated with brown arrows) represent binding of hypoxyprobe antibody and therefore, regions of hypoxia. Abbreviations in Trichrome pictures represent the areas of the urethra and vagina. VLP= vaginal lamina propria; VSM= vaginal smooth muscle; UVS= urethrovaginal septum; EUS= external urethral sphincter; CSM= circular smooth muscle of urethral lamina propria; LSM= longitudinal smooth muscle of urethral lamina propria. Magnification=10x. With increased duration of vaginal distention, there are higher levels of edema in the UVS and EUS, muscle disruption in the EUS, and PMN infiltration into the UVS and EUS.

Graphs representing PMN counts on H&E sections. PMNs were counted at different regions at each time point A, and relative amount vs. tissue penetration of PMNs is shown at 4 hours B, and at 6 hours C. The highest levels of PMNs are in the UVS at 4h and 6h. A greater amount infiltrate the surrounding tissue from the vessels at 6h, in the UVS and EUS.

Specimen showing tissue infiltration of PMNs

H&E stained sections from 6h VD in rat A. urethra/vagina septum (UVS) and B. external urethral sphincter (EUS) at 40x magnification. Arrows represent PMNs in blood vessels (red), PMN binding to endothelium (yellow), and infiltration into surrounding tissue (green). PMNs infiltrate these regions at 4 – 6 h.

Specimen showing morphology of distension.

Masson's Trichrome stain of sections from A. normal urethra and B. urethra that underwent 6h VD. Magnification=10x. These specimen were not pinned before dissection to retain morphology. This resulted in compression of the specimen and difficult histological analysis.

Conclusions

Increased duration of VD causes greater tissue damage (edema and muscle EUS disruption), progressive inflammatory infiltration, and altered urothelial morphology.

Inflammatory effects are most prevalent in the UV septum and near the EUS, with PMN infiltration occurring within 4h and preferentially entering the tissue from the vessels at 6h.

Hypoxic areas appear to decrease with increasing distention duration, suggesting a compensatory perfusion mechanism.

Future work will investigate the methodology of decreased hypoxia with increased duration of VD, assess hypoxia in the bladder, and quantify markers of stretch and crush injury in the urethra and vagina as a result of distention.

Acknowledgements

This work was supported in part by the NIH (R01 HD38578-8), the Cleveland Clinic, and the Department of Veterans Affairs, Rehabilitation Research & Development Service.

SUFU Society of Urodynamics, Female Pelvic Medicine & Urogenital Reconstruction

#4b: Venture outside the Comfort Zone to Try New Things

Ram Ganapathi

The use of Sorafenib as a radiosensitizing agent for the treatment of clear cell renal carcinoma

Hardeep Phull, Dale Grabowski, Adrian Grozav, Arul Mahadevan, Ram Ganapathi

Taussig Cancer Institute, The Cleveland Clinic, Cleveland, OH

Cleveland Clinic

ASCO Genitourinary Cancers Symposium

Aim and Hypothesis of Study

We wanted to determine if Sorafenib (SFB) treatment combined with ionizing radiation (IR) would have synergistic effects in overcoming the radioresistance in clear cell RCC.

We hypothesized the combination of SFB with IR would demonstrate synergistic effects in RCC cell lines and would be dependent on VHL gene status.

Abstract

Introduction

- RCC radioresistance may be due to mutation of the VHL tumor suppressor gene that is prevalent in 50% of clear cell RCC patients.
- Lack of VHL causes abnormal sensing of hypoxia, which up-regulates hypoxia inducible factor (HIF) and induces transcription of proliferative, angiogenic, and cell survival factors.
- These factors have autocrine effects, causing parallel hyperactivation of the PI3-kinase and RAF/MEK/ERK pathways which further promote the abnormal proliferative state that makes the cell radioresistant.
- SFB (BAY 43-9006), an inhibitor of tyrosine kinase and RAF kinase, has demonstrated efficacy against RCC in phase II clinical trials and may potentiate the effects of ionizing radiation (IR).

Methods

- Clear cell renal carcinoma cell lines –CAKI-1 (wild-type VHL), CAKI-2 (mutant VHL), and RC-13 (methylated VHL promoter)– were maintained in T-25 culture flasks at 37 ° C in a humidified 5% CO2/95% air atmosphere.
- The cells were grown in McCoys 5A (CAKI-1/CAKI-2 lines) or RPMI 1640 (RC-13 lines) medium supplemented with 10% fetal bovine serum and 2 mM L-glutamine.
- To further characterize the role of VHL, both of the VHL mutant lines were transfected separately with a vector expressing VHL cDNA and are referred to as CAKI2-VHL and RC13-VHL.
- Western blots were performed to assess the expression of VHL protein in the mutant lines.
- Cells were treated for 144h with either SFB at 2.5 µM, 5 µM, and 7.5 µM (suspended in 100% DMSO) for or with 200, 400, 600, or 800 rads of IR.
- In separate experiments, cells were treated with the same concentrations of SFB for 48h followed by IR with 200, 400, 600, or 800 rads, and then re-incubated in medium with drug for another 96h post-treatment.
- In all experiments, total cell count was assessed at 144h and survival data was expressed as a percentage of untreated controls. Survival fractions of independent or combined treatments were used to measure Drug-IR interactions.
- Statistical analysis to determine significant differences ($p<0.05$) between the various combinations of treatments was conducted using one-way ANOVA with post-hoc Tukey HSD tests for pair-wise comparisons between (inter-comparisons) and within (intra-comparisons) the cell lines

SFB Mechanism & Study Design

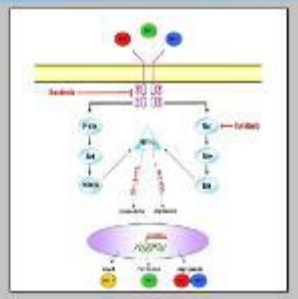

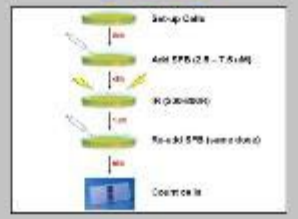

Cell Line	Wild-type	Mutant
CAKI-1	✓	
CAKI-2		✓
CAKI-2 Vector		✓
CAKI-2 VHL	✓	
RC13 Vector		✓
RC13 VHL	✓	

Survival Fraction of Drug Combination	Product of survival fractions of each drug	Drug combination Interaction
SFB at 5 µM	1.00 (1.00x)	Synergistic
IR at 400 R	1.00 (1.00x)	Additive
SFB at 5 µM + IR at 400 R	1.00 (1.00x)	Antagonistic

Results

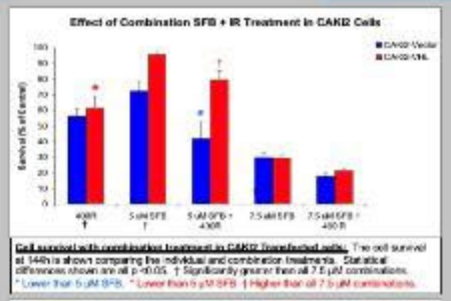

Cell survival with combination treatment in CAKI2 Transfected cells: The cell survival at 144h is shown comparing the individual and combination treatments. Statistical differences shown are all $p<0.05$. † Significantly greater than all 7.5 µM combinations.

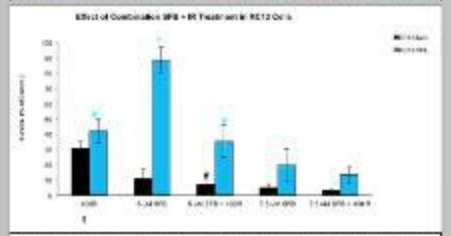

Cell survival with combination treatment in RC13 Transfected cells: The cell survival at 144h is shown comparing the individual and combination treatments. Statistical differences shown are all $p<0.05$. † Significantly greater than all 7.5 µM combinations.
* Lower than 400R.

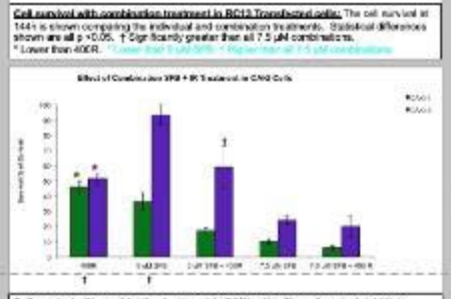

Cell survival with combination treatment in CAKI cells: The cell survival at 144h is shown comparing the individual and combination treatments. Statistical differences shown are all $p<0.05$. † Significantly greater than all 7.5 µM combinations. * Lower than 5µM SFB. † Higher than all 7.5 µM combinations.

Treatment	Survival (% of Control)	Response
400R	56 ± 7	
7.5 µM SFB 144h	ND	
2.5 µM SFB + 400R	ND	ND
5 µM SFB 144h	72 ± 11	
5 µM SFB 144h + 200R	61 ± 11	Antagonistic
7.5 µM SFB 144h	51 ± 7	
7.5 µM SFB 144h + 400R	51 ± 3	Antagonistic

Treatment	Survival (% of Control)	Response
400R	52 ± 12	
2.5 µM SFB 144h	ND	
2.5 µM SFB + 400R	ND	ND
5 µM SFB 144h	56 ± 4	
5 µM SFB 144h + 200R	70 ± 5	Antagonistic
7.5 µM SFB 144h	39 ± 3	
7.5 µM SFB 144h + 400R	31 ± 2	Antagonistic

Treatment	Survival (% of Control)	Response
400R	8 ± 7	
2.5 µM SFB 144h	31 ± 11	
2.5 µM SFB + 400R	31 ± 11	Antagonistic
5 µM SFB 144h	11 ± 3	
5 µM SFB 144h + 200R	5 ± 4	Antagonistic
7.5 µM SFB 144h	3 ± 3	
7.5 µM SFB 144h + 400R	1 ± 1	Antagonistic

Treatment	Survival (% of Control)	Response
400R	12 ± 13	
2.5 µM SFB 144h	39 ± 13	
2.5 µM SFB + 400R	39 ± 3	Antagonistic
5 µM SFB 144h	69 ± 3	
5 µM SFB 144h + 400R	33 ± 19	Synergistic
7.5 µM SFB 144h	9 ± 15	
7.5 µM SFB 144h + 400R	16 ± 7	Antagonistic

Treatment	Survival (% of Control)	Response
400R	46 ± 12	
2.5 µM SFB 144h	35 ± 3	
2.5 µM SFB + 400R	37 ± 17	Antagonistic
5 µM SFB 144h	14 ± 9	
5 µM SFB 144h + 200R	17 ± 1	Synergistic
7.5 µM SFB 144h	10 ± 2	
7.5 µM SFB 144h + 400R	6 ± 3	Additive

Treatment	Survival (% of Control)	Response
400R	31 ± 4	
2.5 µM SFB 144h	100 ± 9	
2.5 µM SFB + 400R	90 ± 14	Antagonistic
5 µM SFB 144h	94 ± 9	
5 µM SFB 144h + 400R	70 ± 19	Antagonistic
7.5 µM SFB 144h	54 ± 4	
7.5 µM SFB 144h + 400R	76 ± 9	Antagonistic

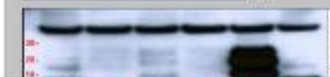

Western Blot of VHL Expression in cell lines: The expression of the VHL wild-type gene from CAKI-1 (VHD) and transfected genes in RC13-VHL and CAKI2-VHL (19 kD) are shown. The Actin control is also shown (43 kD), which does not differ among the cell lines. However, the expression of CAKI2-VHL is significantly lower compared to RC13-VHL.

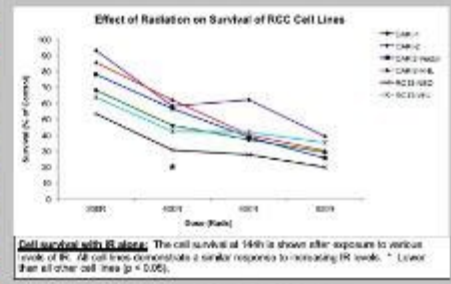

Cell survival with IR alone: The cell survival at 144h is shown after exposure to various levels of IR. All cell lines demonstrate a similar response to increasing IR levels. * Lower than all other cell lines ($p < 0.05$).

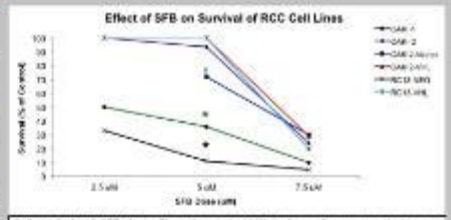

Cell survival with SFB alone: The cell survival at 144h is shown after exposure to various concentrations of SFB. Statistical differences shown are all $p<0.05$. * Lower than all other cell lines. † Lower than all other cell lines, p Lower than CAKI2-VHL

Conclusions

- Treatment with IR alone demonstrated similar cellular responses that were not dependent on VHL gene status.
- Treatment with SFB alone demonstrated that wild-type VHL expression sensitized cells to the drug.
- IR in combination with SFB at clinically achievable steady state concentrations was synergistic in clear cell renal cell carcinoma harbouring wild type VHL gene but not mutant VHL gene.
- Based on the differential results between VHL-transfected RC13 and CAKI2 cells, a threshold concentration of VHL protein expression is required to observe the synergism between SFB and IR.
- Transfection with wild-type VHL revealed that only RC13-VHL reached this threshold VHL expression, parallel to CAKI-1 wild-type VHL cells, and demonstrated synergistic effects with the combination SFB + IR treatment.
- The combination treatment of Sorafenib with ionizing radiation should be evaluated clinically in patients with wild-type VHL clear cell renal carcinoma as a novel treatment for RCC.

#4c: Fail Gracefully But Do Not Stop the Pursuit of a Silver Lining

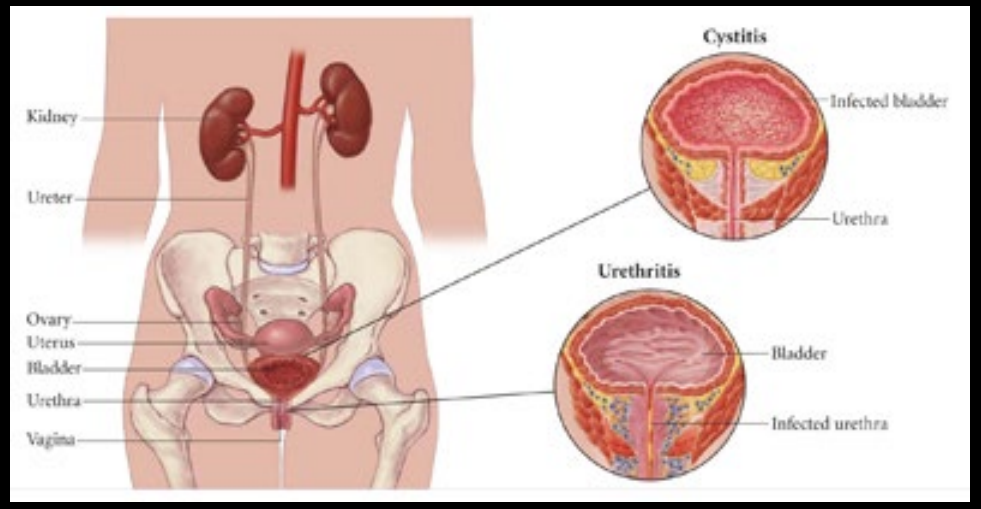

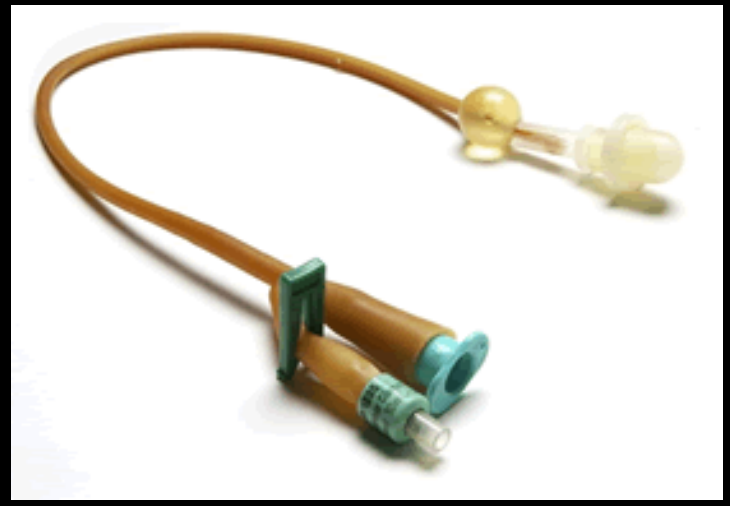

Joseph Liao

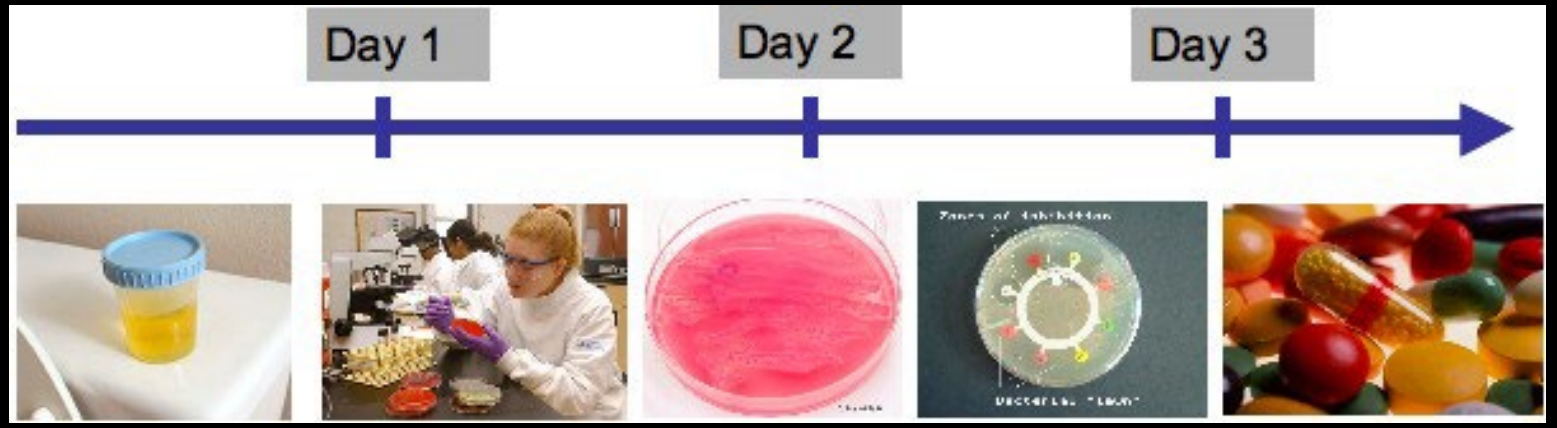

- Most common urologic disease
- Lab methods lack sensitivity & specificity
- Time/labor intensive. Not portable

- No point-of-care diagnosis
- Overuse of empiric Antibiotics
- Leads to Antibiotic resistance

Electrochemical Biosensor using16s Ribosomal RNA Probes

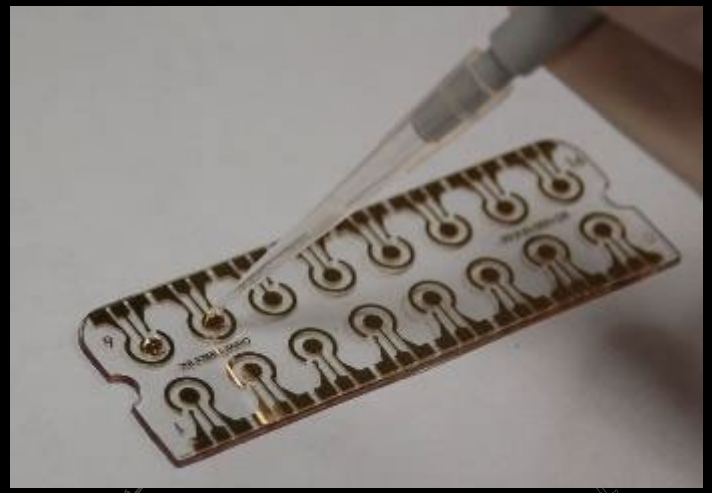

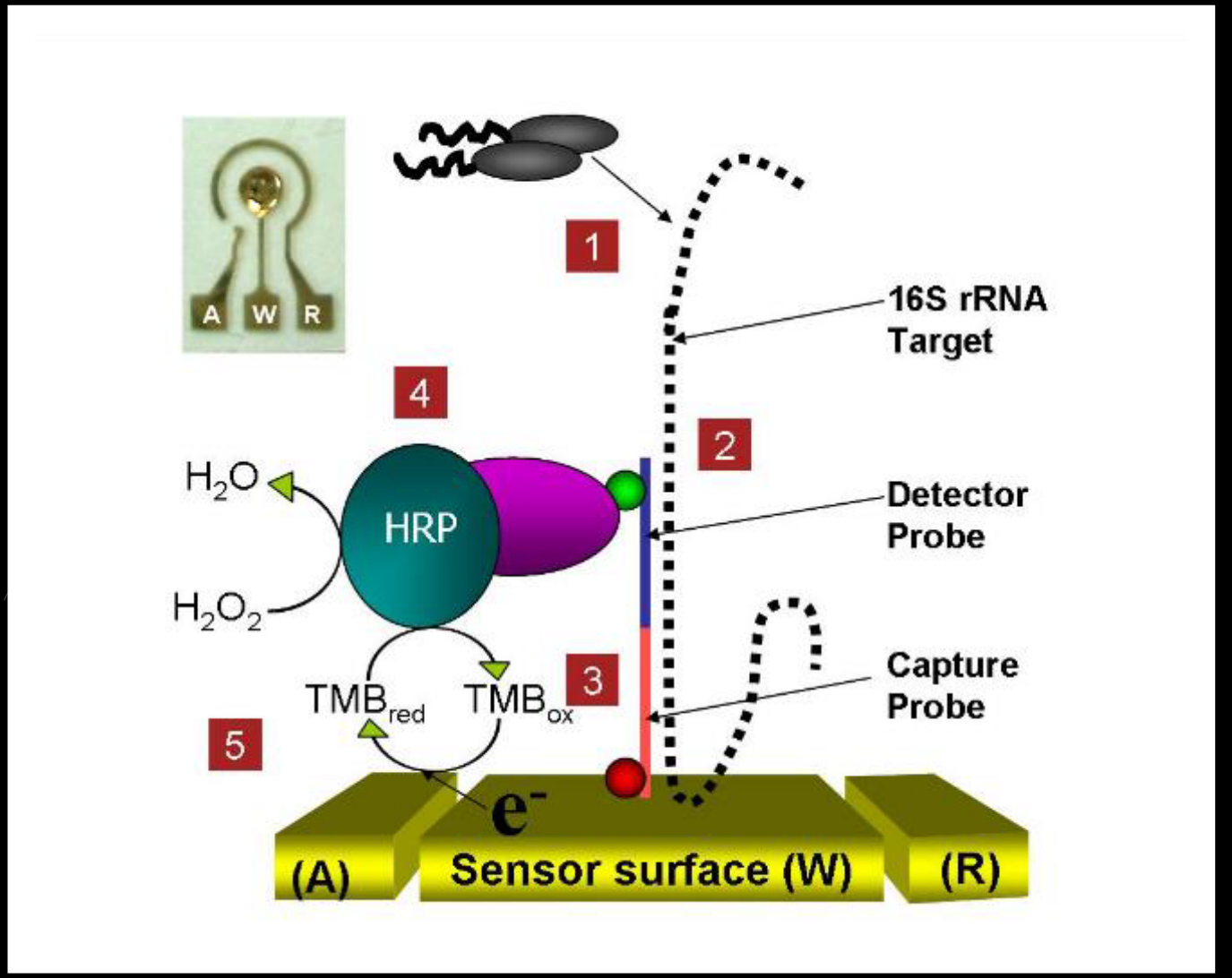

Comparing Biosensor to Existing Methods (Absorbance and Cell Counts)

Clinical Isolate

Inoculation + Abx

180m incubation

Cell counts

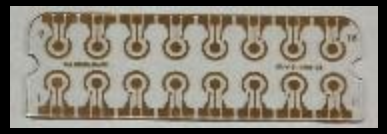

Biosensor Assay

Absorbance

Similar Growth Kinetics to Absorbance and Cell Counts

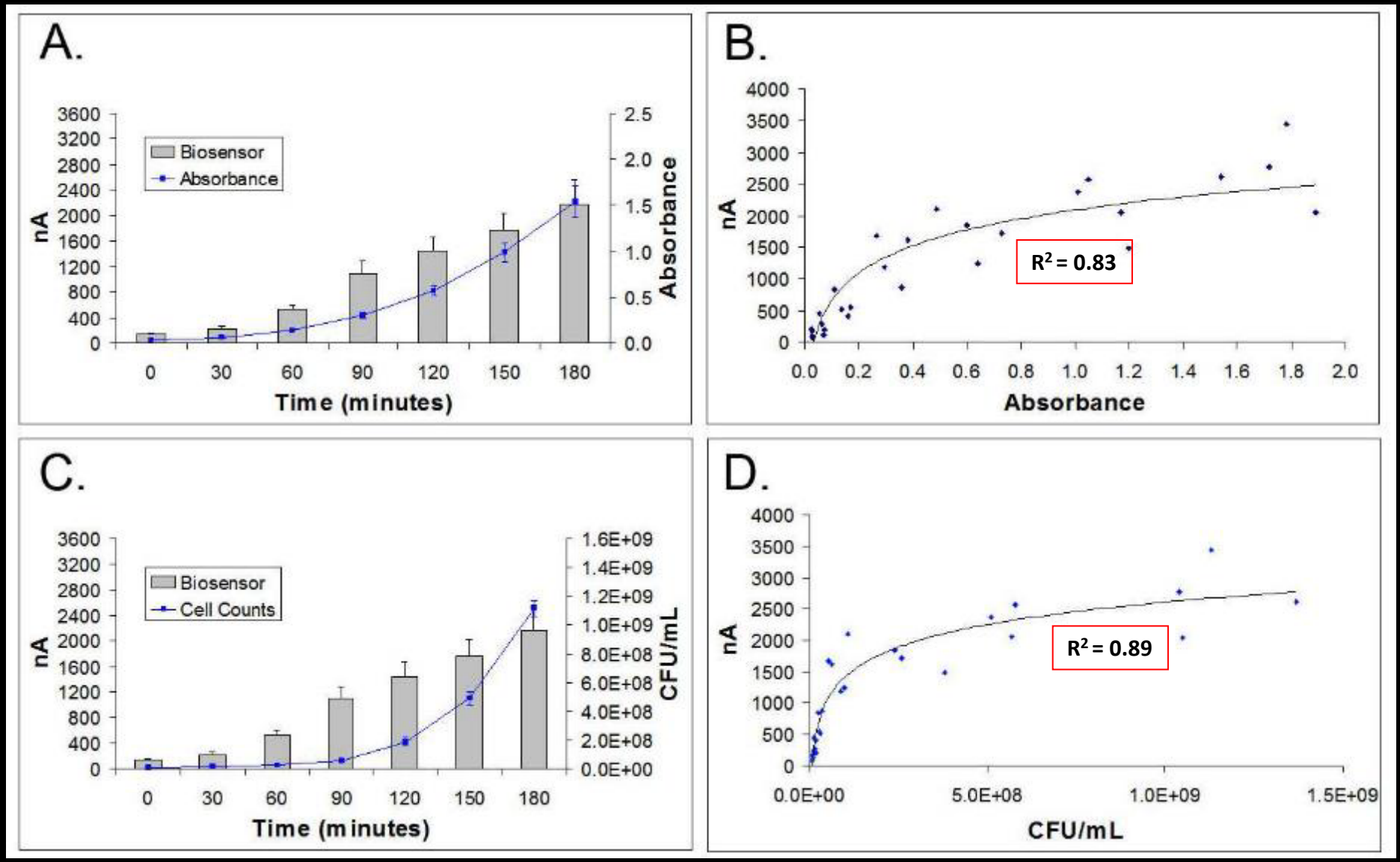

Proof of Concept in Antibiotic Resistant Strains

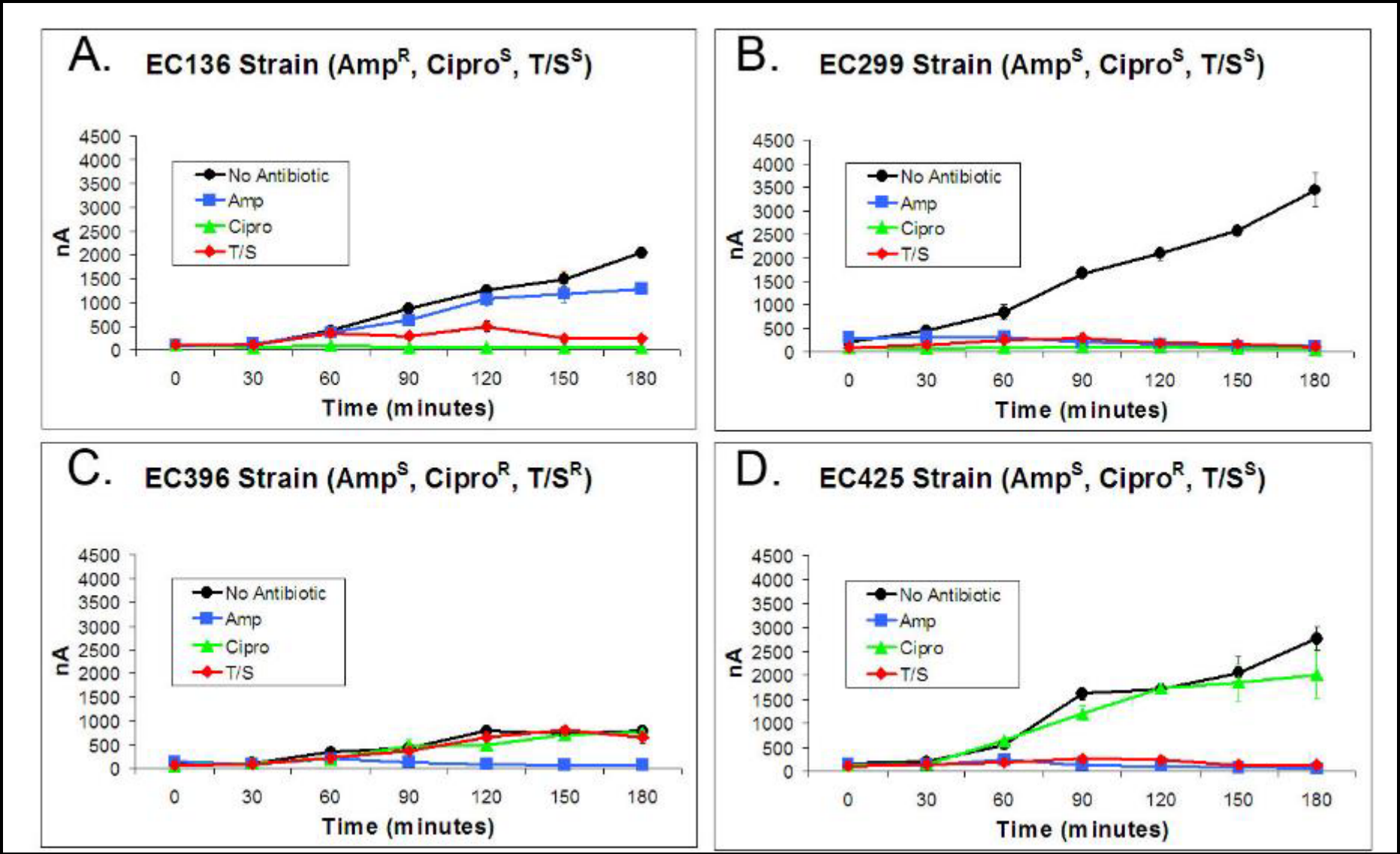

The Art of Failing Gracefully: Where is the Silver Lining?

Multiplex Pathogen Identification for Polymicrobial Urinary Tract Infections Using Biosensor Technology: A Prospective Clinical Study

THE JOURNAL of UROLOGY

Kathleen E. Mach, Christine B. Du, Hardeep Phull, David A. Haake, Mei-Chiung Shih, Ellen Jo Baron* and Joseph C. Liao†

From the Departments of Urology, Health Research and Policy and Pathology, Stanford University School of Medicine, Stanford, Veterans Affairs Palo Alto Health Care System, Palo Alto and Department of Medicine, David Geffen School of Medicine at University of California-Los Angeles and Veterans Affairs Greater Los Angeles Healthcare System, Los Angeles, California

Purpose: Rapid diagnosis of urinary tract infection would have a significant beneficial impact on clinical management, particularly in patients with structural or functional urinary tract abnormalities who are highly susceptible to recurrent polymicrobial infections. We examined the analytical validity of an electrochemical biosensor array for rapid molecular diagnosis of urinary tract infection in a prospective clinical study in patients with neurogenic bladder.

Materials and Methods: The electrochemical biosensor array was functionalized with DNA probes against 16S rRNA of the most common uropathogens. Spinal cord injured patients at a Veterans Affairs hospital were recruited into the study. Urine samples were generally tested on the biosensor within 1 to 2 hours of collection. Biosensor results were compared with those obtained using standard clinical microbiology laboratory methods.

Results: We successfully developed a 1-hour biosensor assay for multiplex identification of pathogens. From July 2007 to December 2008 we recruited 116 patients, yielding a total of 109 urine samples suitable for analysis and comparison between biosensor assay and standard urine culture. Of the samples 74% were positive, of which 42% were polymicrobial. We identified 20 organisms, of which Escherichia coli, Pseudomonas aeruginosa and Enterococcus species were the most common. Biosensor assay specificity and positive predictive value were 100%. Pathogen detection sensitivity was 89%, yielding a 76% negative predictive value.

Conclusions: To our knowledge we report the first prospective clinical study to successfully identify pathogens within a point of care time frame using an electrochemical biosensor platform. Additional efforts to improve the limit of detection and probe design are needed to further enhance assay sensitivity.

Key Words: urinary bladder, neurogenic; spinal cord injuries; urinary tract infections; biosensing techniques; RNA, ribosomal, 16S

Abbreviations and Acronyms

AB = Acinetobacter baumannii
EB = Enterobacteriaceae family
EC = Escherichia coli
EF = Enterococcus species
KE = Klebsiella-Enterobacter
NC = negative control
PA = Pseudomonas aeruginosa
PM = Proteus mirabilis
SCI = spinal cord injury
UNI = universal eubacterial
UTI = urinary tract infection
VAPAHCS = Veterans Affairs Palo Alto Health Care System

Submitted for publication March 4, 2009.

Study received approval from the Stanford University institutional review board, and VAPAHCS research and development committee.

Supported by Department of Veterans Affairs Merit Review R4872R (JCL) and National Institute of Allergy and Infectious Diseases Cooperative Agreement Award AI075565 (DAH).

* Financial interest and/or other relationship with Cepheid, OpGen, Key Scientific, AHT Medig, bioMerieux, MicroPhage and Merck.

† Correspondence: Department of Urology, 300 Pasteur Dr., S-287, Stanford University, Stanford, California 94305-5118 (e-mail: jliao@stanford.edu).

The Silver Lining : LOVE

Proposing by the Golden Gate Bridge

Our Families Meeting for the First Time

Sikh Marriage Ceremony

Bonus Silver Lining : Repurpose and Reinvent

Rapid Antibiotic Susceptibility Testing Using Electrochemical Biosensors

Hardeep Phull *, Kathleen E Mach, Christine Du, Joseph C. Liao

Department of Urology, Stanford University School of Medicine and VA Palo Alto Health Care Syste , CA

ACP American College of Physicians

1st PLACE

Introduction

- Bacterial infections remain as a major cause of morbidity and mortality worldwide
- Urinary tract infection (UTI) is the most common cause of bacterial infection, and E. coli is the most common uropathogen
- The standard culture-based diagnostic approach used in clinical microbiology labs involves a significant inherent delay in processing (1-3 days)
- This has resulted in frequent over- and misuse of antibiotics and the emergence of antibiotic-resistant pathogens
- We have previously developed a 60-minute molecular assay using sequence-specific DNA probes to bacterial 16S ribosomal RNA (rRNA) for pathogen identification on microfabricated electrochemical biosensors.
- In the current study, we report the development of a novel phenotypic approach for rapid determination of antibiotic susceptibility using electrochemical biosensors.

Methods

- Four uropathogenic clinical isolates obtained from patients with UTI were inoculated at mid-logarithmic phase into Muller-Hinton media and grown at 37° C with and without commonly used antibiotics:
  - Ampicillin (Amp, 32 μg/mL)
  - Ciprofloxacin (Cipro, 4 μg/mL)
  - Trimethoprim-sulfamethoxazole (TMP, 4 μg/mL / 76 μg/mL)
- The culture was sampled at 30-minute intervals and electrochemical detection of 16S rRNA was performed using appropriate species-specific probes on a biosensor (Genie Fluidics, Monterey Park, CA).
- The basic detection strategy, outlined in Figure 1, involves converting the hybridization between species-specific DNA probes and bacterial 16S rRNA into quantitative electrical signals via a horseradish peroxidase (HRP) reporter.
- The growth kinetics of the pathogens based on the electrochemical biosensor were compared with bacterial concentrations (CFU/mL) and absorbance measurements using a spectrophotometer (OD_{600}).
- The current output in each antibiotic growth condition was compared with the control (No antibiotics) by calculating the difference in log units between the antibiotic signal and control signal at each time interval.

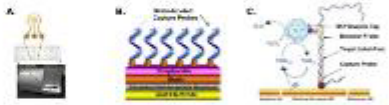

Figure 1: Overview of the Electrochemical Biosensor
(A) The electrochemical biosensor array, consisting of 16 sensors, and the multichannel potentiostat for amperometric readout is shown. Each sensor has 3 electrodes: auxiliary (A), working (W), and reference (R). (B) Activation of the alkanethiol self-assembled monolayer (SAM) allows for the tethering of organic compounds leading to the immobilization of the sequence-specific E. coli DNA 35-mer capture probes. (C) Electrochemical detection scheme of the biosensor: Sandwich hybridization of the biotin-labeled capture and fluorescein-labeled detector probes with the unlabeled target bacterial 16S rRNA. Signal amplification is achieved by binding of an enzyme tag (anti-fluorescein conjugated with HRP) to the sandwich hybrid. Amperometric signal is generated by the HRP reaction upon applying a fixed voltage between the working and the reference electrodes. Electron transfer occurs between the sensor surface and the mediator, tetramethylbenzidine (TMB).

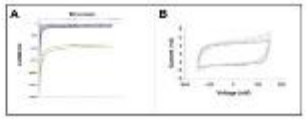

Figure 2: Electrochemical Measurements Using the Biosensor.
(A) Amperometric measurement (duplicate samples) using a biosensor with probes specific for E. coli. (B) Cyclic voltammetry of a SAM-biosensor using $K_3Fe(CN)_6$ scanning between -150 to 150 mV. Note the low peak signals (no non-specific leakage current) and overlapping curves (functional equivalency of the biosensors).

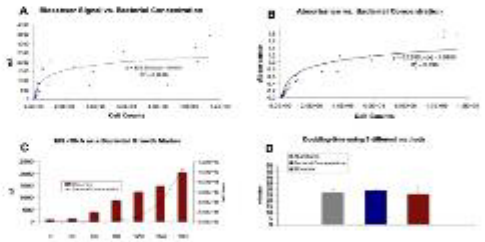

Figure 3: Bacterial Growth Kinetics
Biosensor signal shows a logarithmic correlation with both cell counts (A) and absorbance (B). Levels of 16S rRNA can serve as a surrogate marker of bacterial growth, as the relative biosensor signal based on 16S rRNA increases with measured cell counts (C). The doubling time of *E. coli* as determined by biosensor signal at 60 minutes is comparable to that achieved by the gold standard methods of absorbance and cell counts (D).

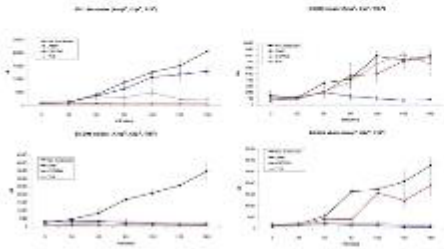

Figure 4: Antibiotic Susceptibility in *E. coli* Strains Using Biosensor Signals
In these curves showing *E. coli* strains with different antibiotic phenotypes, the control signals (no antibiotic) can be used as the reference to determine resistance or susceptibility. Antibiotic conditions which diverge remarkable from the control curve show lower signal due to fewer bacteria and subsequent 16S rRNA detected, suggesting susceptibility. By contrast, antibiotic conditions which converge with the control curve suggest resistance.

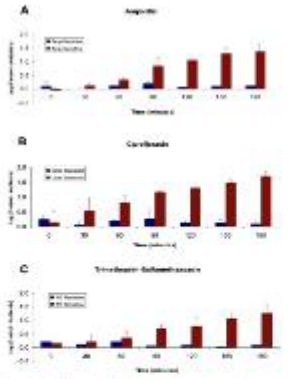

Figure 5: Differential Between Control and Susceptible/Resistant Bacteria
The graphs represent log-transformed raw biosensor signals which have been pooled by antibiotic phenotype. A larger differential suggests a greater difference from control and hence, antibiotic susceptibility. Amp and T/S show a significant differential of 0.3 within just 60 minutes of growth (A, C), whereas Cipro shows a differential value of 0.5 within only 30 minutes of growth (B).

Results

- the correlation coefficient between biosensor standard measurements of bacterial growth e and cell counts), the biosensor could be y used to monitor bacterial growth
- iosensor signal based on 16S rRNA was al to measured cell counts, suggesting RNA was a surrogate marker of bacterial
- ing the amount of 16S rRNA between growth and therefore the relative levels of surviving ells, the biosensor assay could be used to antibiotic susceptibility or resistance
- Visual comparison of antibiotic susceptibility curves demonstrated that converging and diverging signals compared to the control curve suggested resistance and susceptibility, respectively.
- In all 4 strains tested, biosensor data was in agreement with the antibiotic susceptibility phenotype of the clinical isolate
- The differential between control and susceptible bacteria grown in Amp or T/S could be ascertained within 60 minutes
- The differential between control and susceptible bacteria grown in Cipro could be ascertained within 30 minutes

Conclusions

- We describe a novel approach for determining antibiotic susceptibility using an electrochemical biosensor that is significantly faster than standard microbiology methods
- Electrochemical detection of the relative signal intensity of 16S rRNA derived from *E. coli* in different growing conditions (i.e., different antibiotics) can be used for rapid antibiotic susceptibility testing.
- Coupled with our previous reports of species-specific pathogen identification, the addition of antibiotic susceptibility testing represents a significant improvement over existing diagnostic standards for the management of UTI and other bacterial infections.
- Additional testing with different pathogens and antibiotics is underway to critically examine the growth kinetics of the different uropathogens.
- Given the compatibility of the microfabricated biosensors with microfluidics and other automation technologies and the capacity for inexpensive large-scale production, our approach is promising for point-of-care diagnostics.

Acknowledgments

This work was funded by a grant from the Department of Veteran's Affairs Merit Review. * H.P. is a medical student at Cleveland Clinic Lerner College of Medicine.

Bonus Silver Lining : Repurpose and Reinvent

Am J Physiol Renal Physiol 301: F64
First published May 25, 2011; doi:10.1152/ajprena

american physiological society

Vulnerability of continence structures to injury by simulated childbirth

Hardeep S. Phull,[1] Hui Q. Pan,[1] Robert S. Butler,[2] Donna E. Hansel,[3,4,5,6] and Margot S. Damaser[1,6,7]

[1]Department of Biomedical Engineering, Lerner Research Institute, [2]Department of Quantitative Health Sciences, [3]Pathology and Laboratory Medicine Institute, [4]Taussig Cancer Institute, [5]Genomic Medicine Institute, [6]Glickman Urological and Kidney Institute, The Cleveland Clinic, Cleveland; and [7]Research Service, Louis Stokes Cleveland Veterans Affairs Medical Center, Cleveland, Ohio

Submitted 1 March 2011; accepted in final form 24 May 2011

Phull HS, Pan HQ, Butler RS, Hansel DE, Damaser MS. Vulnerability of continence structures to injury by simulated childbirth. *Am J Physiol Renal Physiol* 301: F641–F649, 2011. First published May 25, 2011; doi:10.1152/ajprenal.00120.2011.—The goal of this study was to examine acute morphological changes, edema, muscle damage, inflammation, and hypoxia in urethral and vaginal tissues with increasing duration of vaginal distension (VD) in a rat model. Twenty-nine virgin Sprague-Dawley rats underwent VD under anesthesia with the use of a modified Foley catheter inserted into the vagina and filled with saline for 0, 1, 4, or 6 h. Control animals were anesthetized for 4 h without catheter placement. Urogenital organs were harvested after intracardiac perfusion of fixative. Tissues were embedded, sectioned, and stained with Masson's trichrome or hematoxylin and eosin stains. Regions of hypoxia were measured by hypoxyprobe-1 immunohistochemistry. Within 1 h of VD, the urethra became vertically elongated and displaced anteriorly. Edema was most prominent in the external urethral sphincter (EUS) and urethral/vaginal septum within 4 h of VD, while muscle disruption and fragmentation of the EUS occurred after 6 h. Inflammatory damage was characterized by the presence of polymorphonuclear leukocytes in vessels and tissues after 4 h of VD, with the greatest degree of infiltration occurring in the EUS. Hypoxia localized mostly to the vaginal lamina propria, urethral smooth muscle, and EUS within 4 h of VD. Increasing duration of VD caused progressively greater tissue edema, muscle damage, and morphological changes in the urethra and vagina. The EUS underwent the greatest insult, demonstrating its vulnerability to childbirth injury.

urinary stress incontinence; parturition; rat; female; histology

which simulates childbirth-induced injury by inflating a balloon catheter in the vagina, enables investigation of the injuries of childbirth in an animal model (18, 28). This model also reliably reproduces urodynamics and cystometry consistent with SUI (37). We previously determined that VD in rats causes a significant reduction in blood flow and increased levels of hypoxic injury to genitourinary organs (12). However, the acute effects of VD on edema, inflammation, and morphometry have not previously been studied.

The goal of this study was to determine the acute effects of VD duration on hypoxia, inflammation, edema, muscle damage, and morphometry of the urethra and vagina in a rat model. We hypothesized that increasing duration of VD would result in proportionally increased severity of injury and could suggest cellular mechanisms of injury during childbirth that contribute to SUI.

MATERIALS AND METHODS

All protocols were approved by the Institutional Animal Care and Use Committee of the Cleveland Clinic. Twenty-nine virgin female Sprague-Dawley rats (180–220 g body wt; 8–10 wk old) were anesthetized with 80 mg/kg ketamine and 10 mg/kg xylazine intraperitoneally. VD was performed as previously described (8). Briefly, the vagina was accommodated to a larger capacity by inserting and removing increasing sizes of urethral dilators lubricated with surgilube (E. Fougera, Melville, NY). A modified 10 Fr. Foley catheter was then inserted into the vagina and secured with a 3–0 vicryl suture. The balloon was distended with 3 ml saline, the capacity of the vagina in

esson #4: Embrace Discomfort and Failure, the Substances of Reinventio

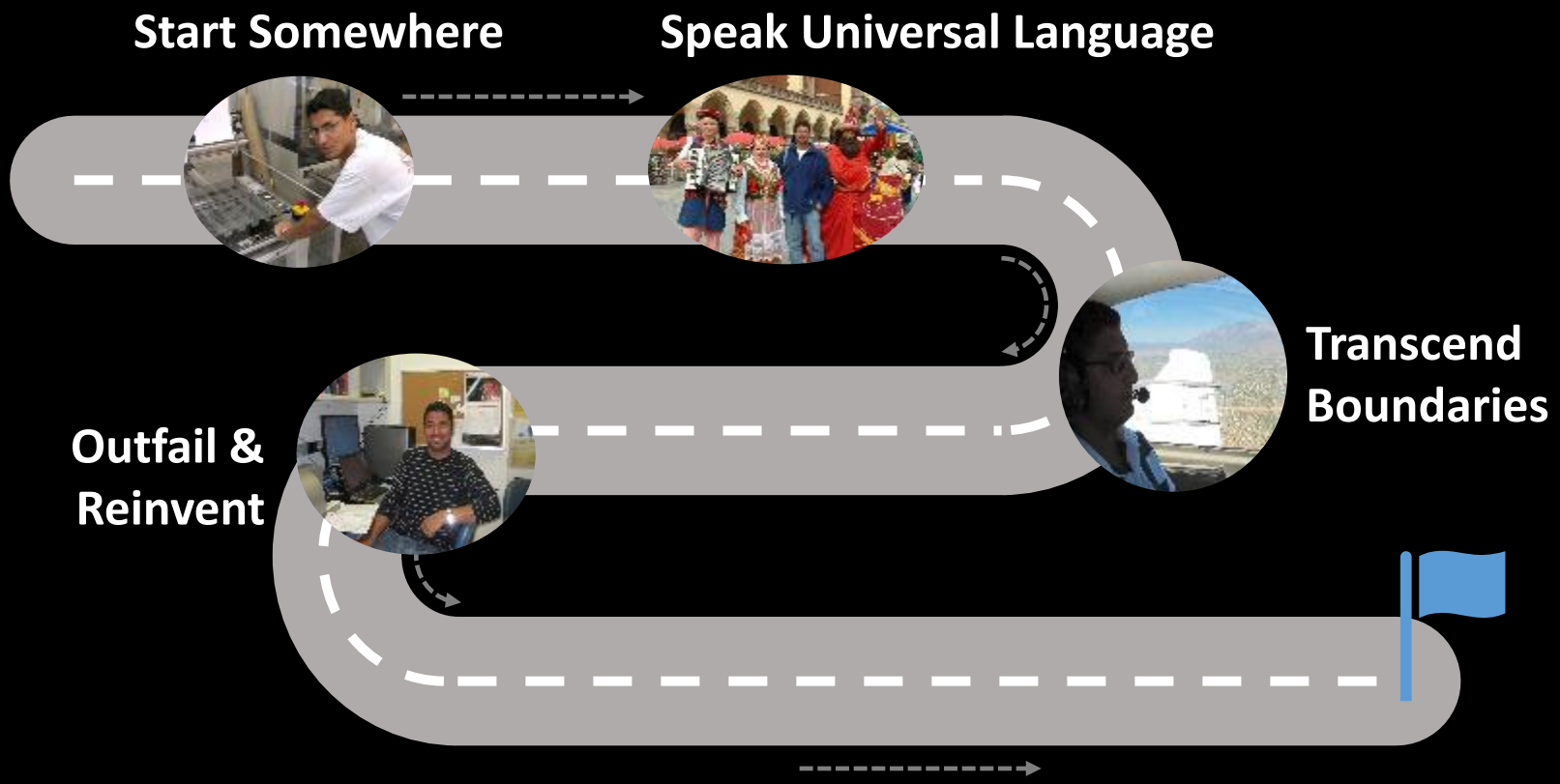

Lesson #5: Life is a Reality, not an Expectation

Lesson #5: Life is a Brief Reality, not an Expectation

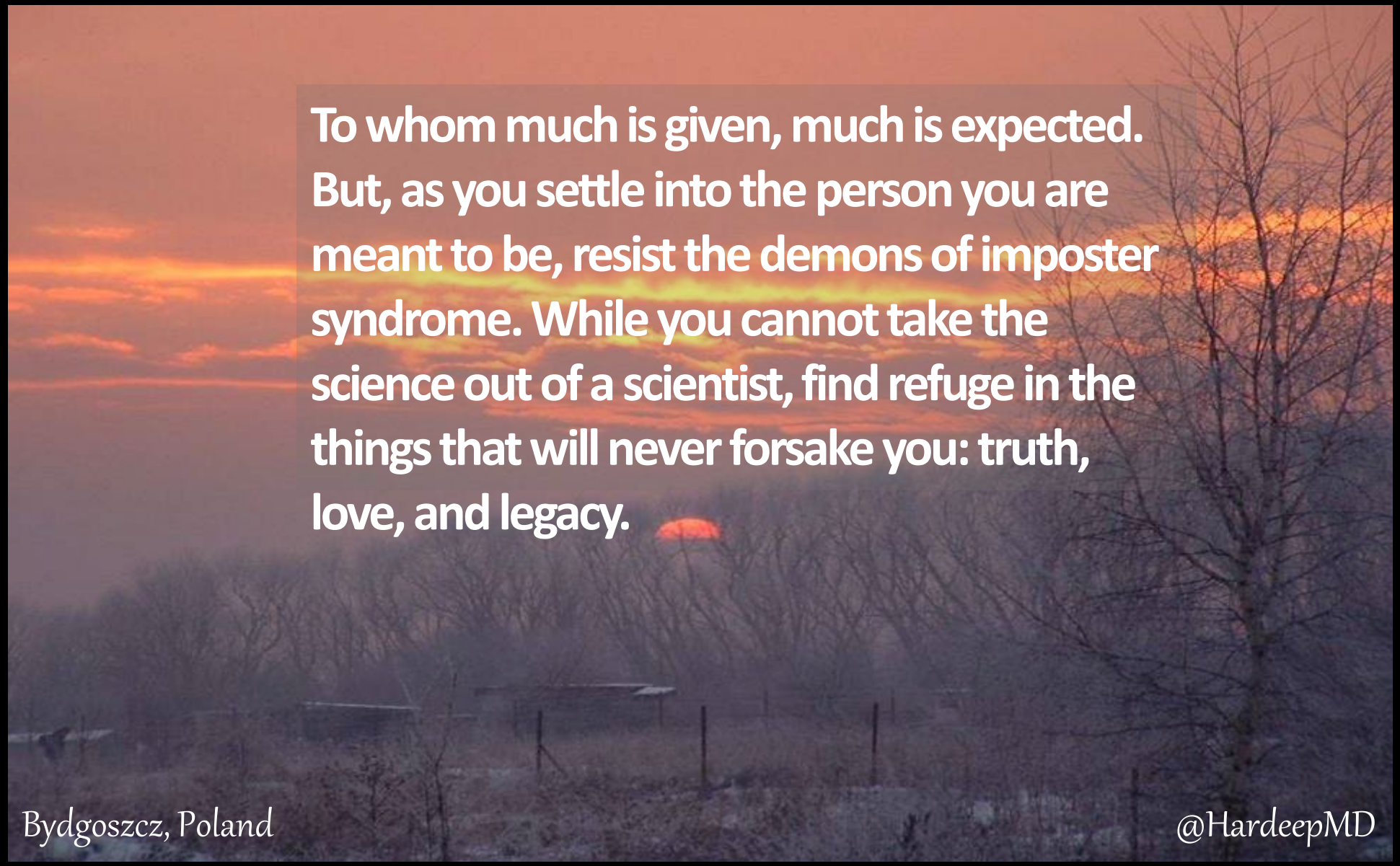

Internal Medicine Residency/KL2 Research Track

Bispecific Antibodies and CAR T-cells

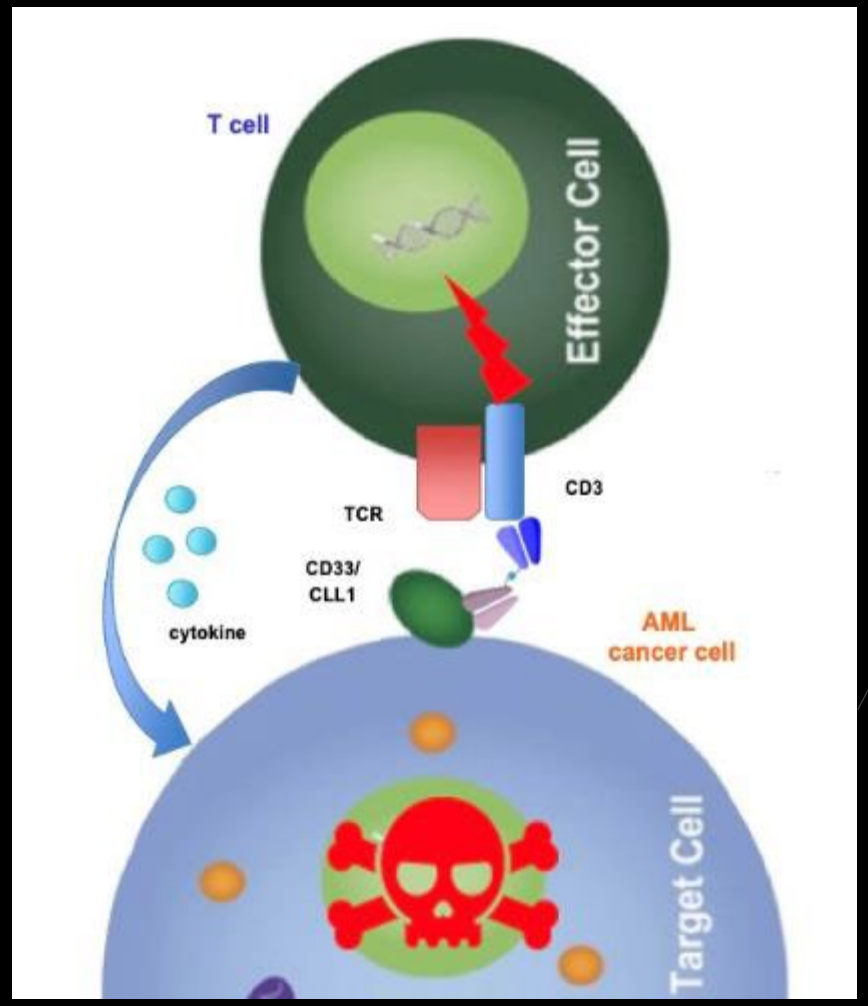

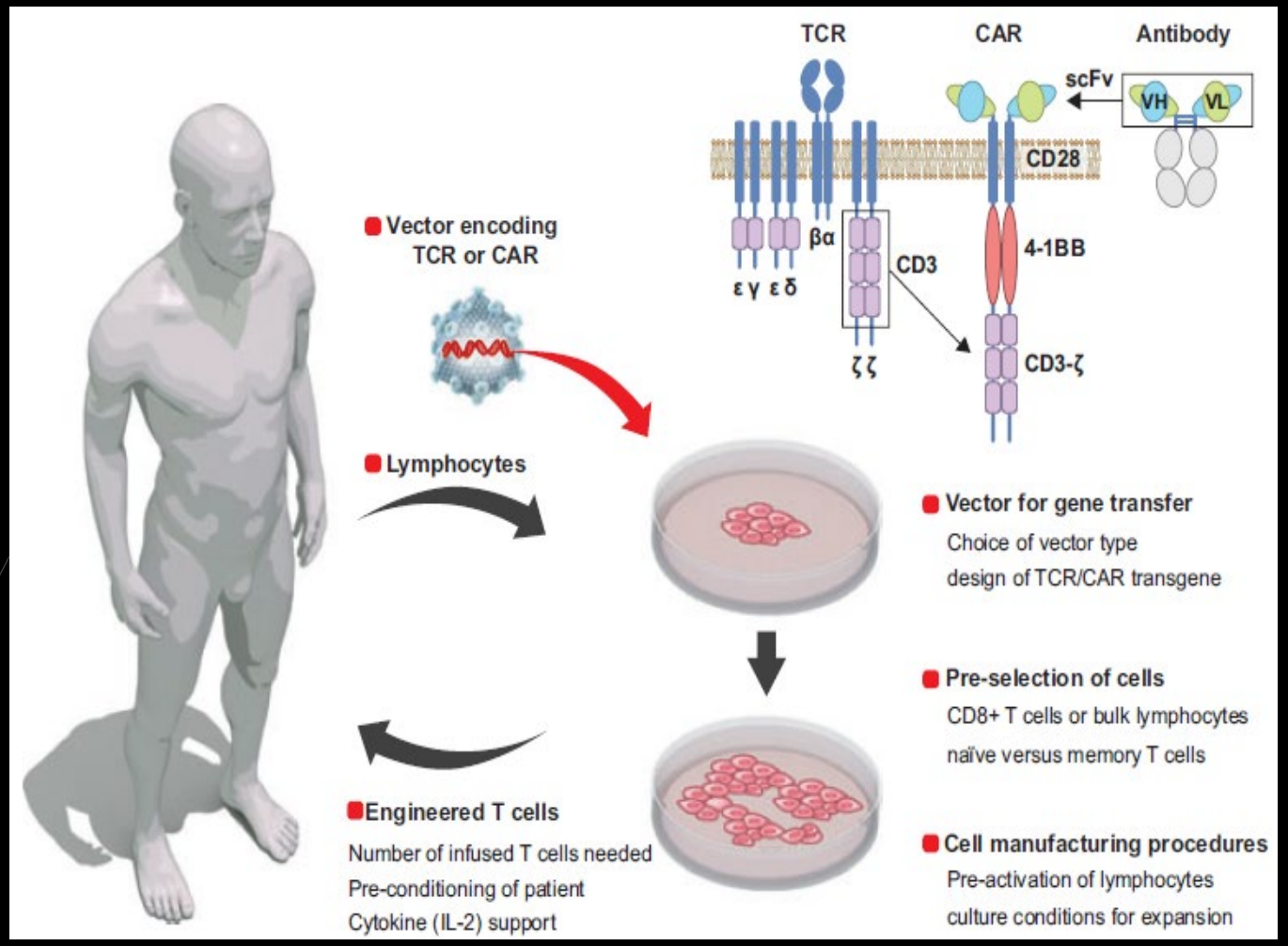

Switchable CAR T-Cells

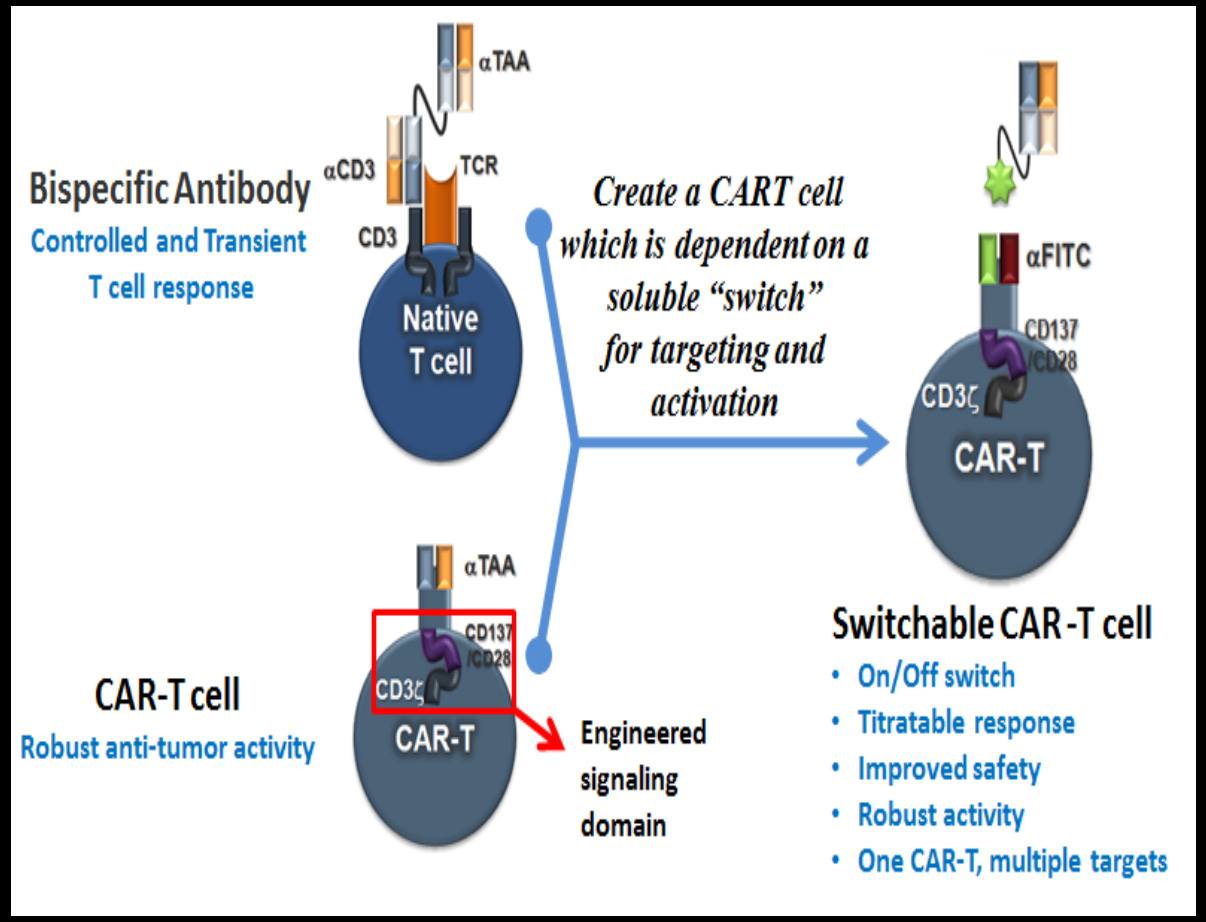

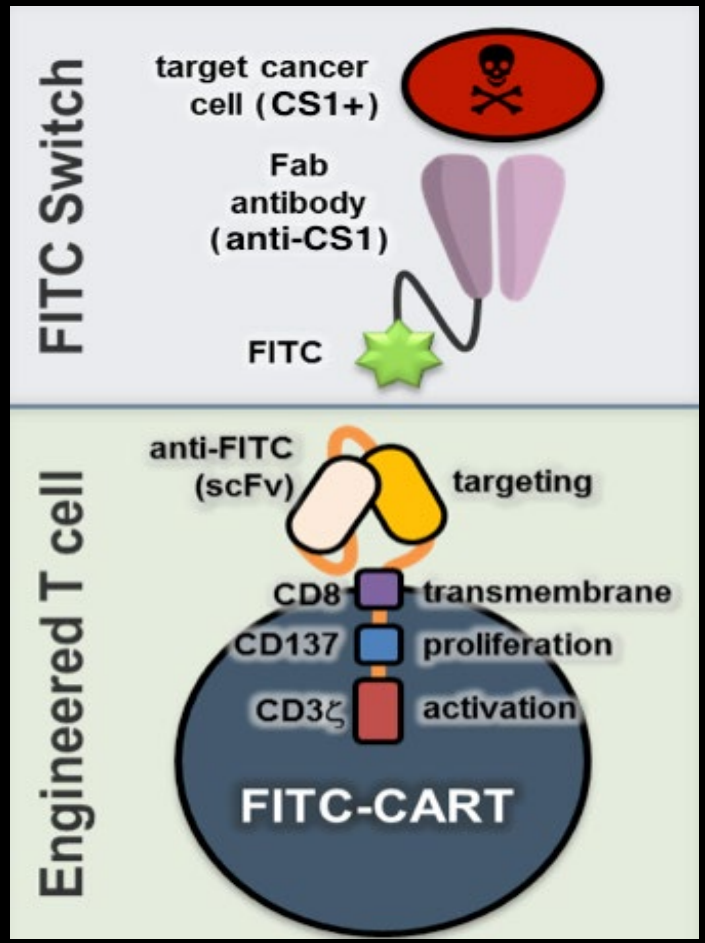

Synthesis of Bispecific Antibodies (anti-CD33 and anti-CLL1)

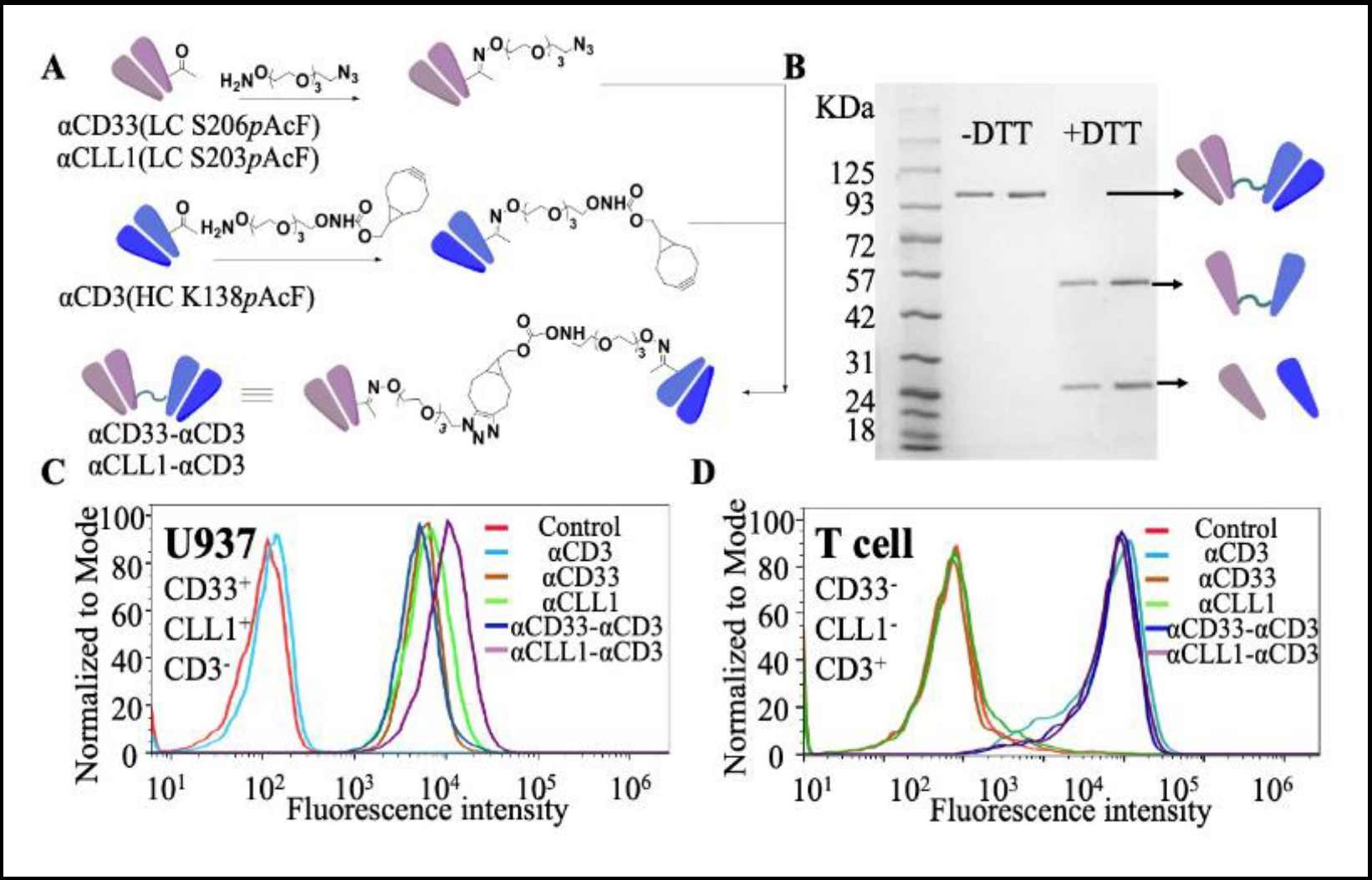

Viability in Various Cell Lines and Time points

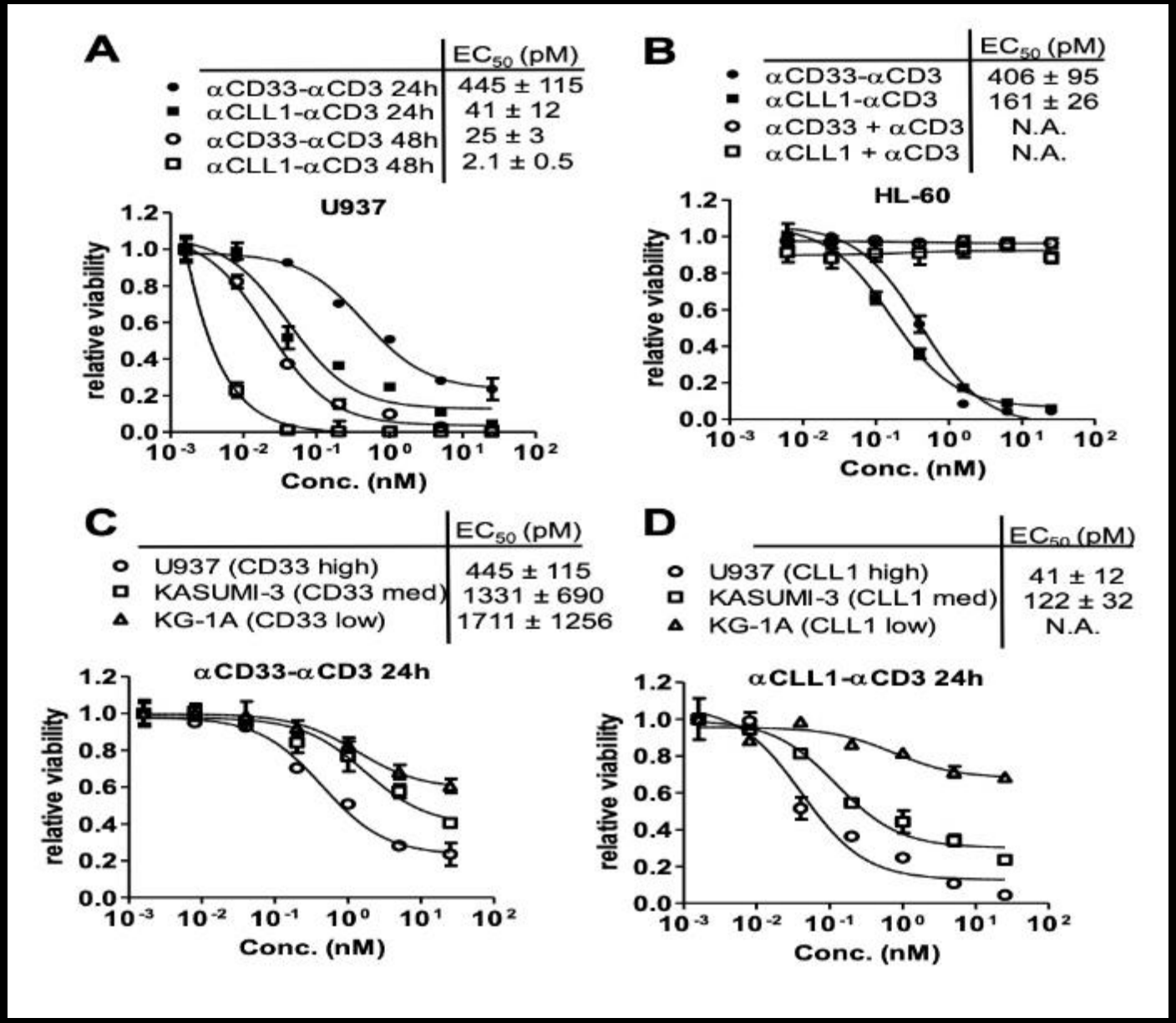

Flow Cytometry in Various Cell Lines

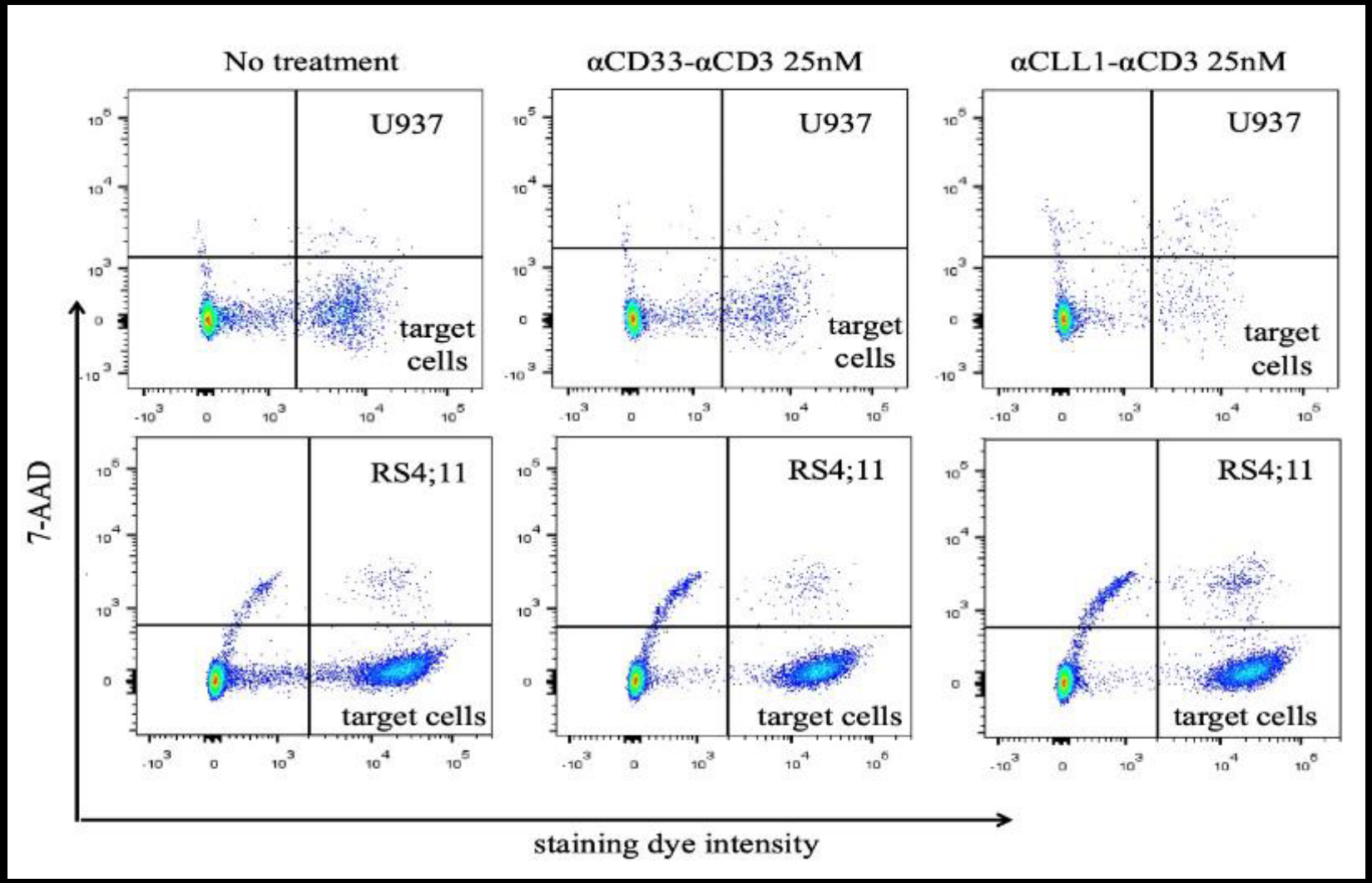

Bispecific Antibody Activity in AML Mouse Model

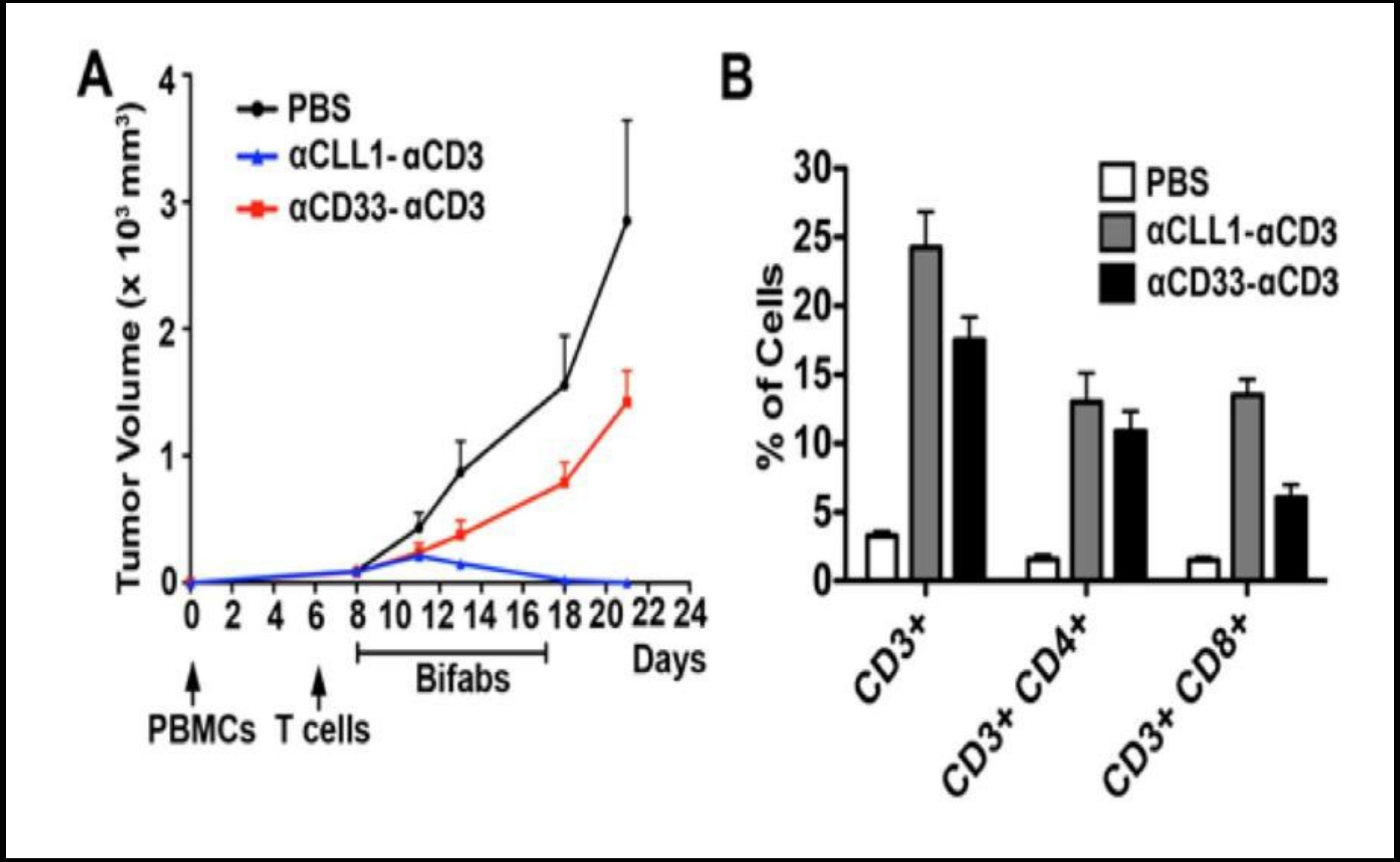

Switchable CAR T-cell in AML Mouse Model

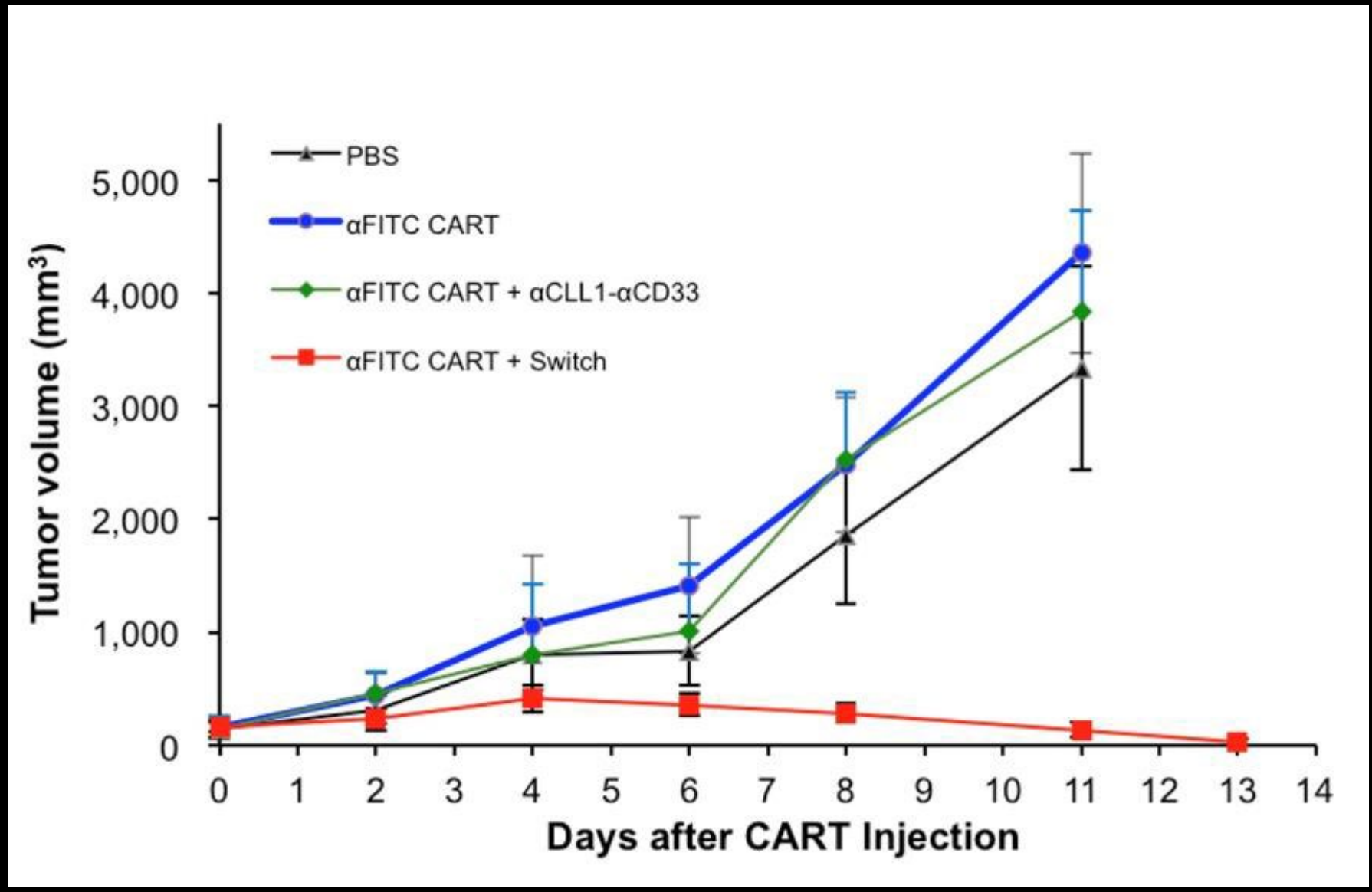

Bispecific antibodies and CAR T-cells

Bispecific Antibody Targeting of Acute Myeloid Leukemia

Hardeep Phull MD *, Chan Hyuk Kim PhD, James Mason MD, Peter Schultz PhD
Scripps Green Hospital and The Scripps Research Institute, La Jolla, CA

The Scripps Research Institute

American College of Physicians

Introduction

- Acute myeloid leukemia (AML) is a rapidly progressive malignancy associated with high relapse rates
- Two common AML cell surface markers, CD 33 and C type lectin like molecule 1 (CLL-1), have been used as potential drug targets
- Current antibody drug conjugates against AML are limited by drug toxicity, variable cell surface antigen expression, and the existence of drug pump leading to drug resistance
- A new class of therapy, bispecific antibodies (bi-ab), simultaneously target two separate antigens
- In this study, we elaborate on a novel biFab approach of concurrently targeting specific antigens on AML cells and host T cells, to mediate an immunogenic cytotoxic response
- We hypothesize that a synthetic biFab against CD-33 and CLL-1 will result in specific cell-mediated cytotoxicity in AML patient derived cell lines and blood samples

Methods

- Genes encoding the heavy and light chains of anti-CD 33 and CLL 1 were engineered as monoclonal fragments via recombinant E. coli technology
- To generate the biFab, bifunctional polyethylene glycol linkers were synthesized via Click chemistry
- The biFab construct was confirmed by western blot, while affinity, specificity, and cytotoxicity were confirmed with flow cytometric analysis
- In vitro efficacy of the biFab was evaluated in CLL 1 and CD 33 positive human leukemia (HL-60) cell lines
  - Various concentrations of biFab were incubated for 24 hours with HL-60 cells
  - An equal volume of purified human peripheral blood mononuclear cells (PBMC) was added containing lymphocytes of which 85% were CD3+ T cells
  - Flow cytometry was used to evaluate cytotoxicity in the AML cell populations
- Through an IRB approved protocol, a separate in vitro analysis was also performed on primary clinical samples obtained from AML patients at Scripps Green Hospital, co-cultured with CK and PBMCs

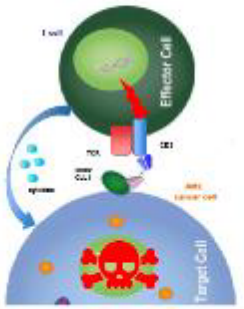

Figure 1: Bispecific Antibody Targeting Strategy
The synthesized biFab simultaneously binds the target cell antigen of interest (in this case CD 33 or CLL 1 on AML cells) along with CD 3 on host cytotoxic T cells. This results in a host-mediated cytokine response and cytotoxicity of the target cancer cell.

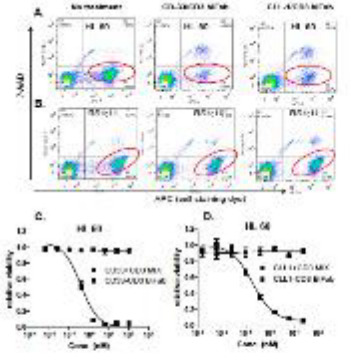

Figure 3: In vitro Cytotoxicity in HL-60 Cell Lines
(A) In an HL-60 cell line (CD33+/CLL-1+), incubation with the anti-CD-33/CD3 and anti-CLL-1/CD3 biFab results in specific depletion of the AML tumor cells, compared to no treatment. (B) In the negative control REC-1 cell line (CD 33 /CLL-1), similar incubation as above does not result in any cytotoxicity as expected. Dose response curves in HL-60 cells shows that both the anti-CD-33/CD3 (C) and anti-CLL-1/CD3 (D) biFab have an EC_{50} of 100-200 picomolar

Figure 2: Synthesis of biFab
(A) A light chain p-azidophenylalanine (pAF) mutant Fab from a full-length CD 33 and CLL 1 is selectively conjugated to a heavy chain pAF mutant Fab of an anti-CD3 antibody via a bifunctional crosslinker. (B) The resulting biFab is a homogeneous antibody of the expected molecular weight, as characterized on Western blot and SDS PAGE. (C) Flow cytometry confirms that the site specific conjugation method does not compromise either antibody's affinity or specificity to its appropriate antigen

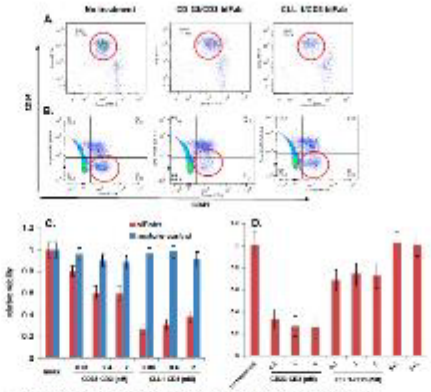

Figure 4: In vitro Cytotoxicity in Primary AML Patient Blood Samples
Flow cytometry data (A & B) and the corresponding graphical data (C &D) are shown. Prior to the assay, patient #1 (A & C) was determined to have 20% endogenous CD 3 T cells, low CD 33 expression, and medium CLL 1 expression. Patient #2 (B & D) had 0.6% endogenous CD-3 T cells, high CD-33 expression, and low CLL 1 expression. In the assay above, the blood sample of patient # 2 was combined with an equal volume of healthy donor T-cells. Incubation with the anti-CD-33/CD3 and anti-CLL-1/CD3 bi-ab in patient #1 resulted in greater cytotoxicity with the anti-CLL-1/CD3 biFab. On the contrary, in patient #2 the inverse scenario was observed with higher cytotoxicity using the anti-CD-33/CD3 bi-ab

- Synthesized anti- were shown to bi- molecular weight
- Our site-specific unlike antibody's
- Incubation with b combination resu cells in an HL-60
- An EC_{50} of 100-3 biFab in HL-60 ce
- In the blood samp CD-33 expressio cytotoxicity was o
- In AML patient #2, expression and l were observed wit
- Though AML patie counts, exogenou donor resulted in a robust cytotoxic response

1st PLACE

Conclusions

- We demonstrate the successful development and efficacy of an innovative approach using biFab that simultaneously bind cell specific targets while recruiting host T cells, to mediate cytotoxicity in AML cell lines and patient samples
- The synthesized biFabs in this study have favorable attributes including stability, potency, and long half life
- In primary AML patient blood samples, we are able to tailor therapy based on cell-surface expression level and demonstrate the ability to effectively overcome immunocompromised status by introducing exogenous T-cells into the system
- Our approach of selectively directing the host immune system against tumor-associated antigens offers potential advantages to conventional treatments including the ability to bypass drug resistance mechanisms, overcome variable expression levels of cell markers, and modulate treatment response

References

1. Kim CH, et al. (2012) Synthesis of bispecific antibodies using genetically encoded unnatural amino acids. J Am Chem Soc 134(24):9918-9921.
2. Hoffmann C (2012) Site-specific labeling, bispecific antibodies, the beginnings, and 50 years on. Cancer Immunity 12:12
3. Beck A, et al. (2010) Trends and perspectives of antibody-drug conjugates for cancer therapy. Expert Rev Mol Med 12:e28.
4. Baeuerle PA & Reinhardt C (2009) Bispecific T-cell engaging antibodies for cancer therapy. Cancer research 69(12):4941-4944

IMDb Featured Review

3

Evolving Roles and Priorities with Parenthood

Hematology/Oncology Fellowship: Risking Authenticity

UC San Diego
MOORES CANCER CENTER

Eric Roeland

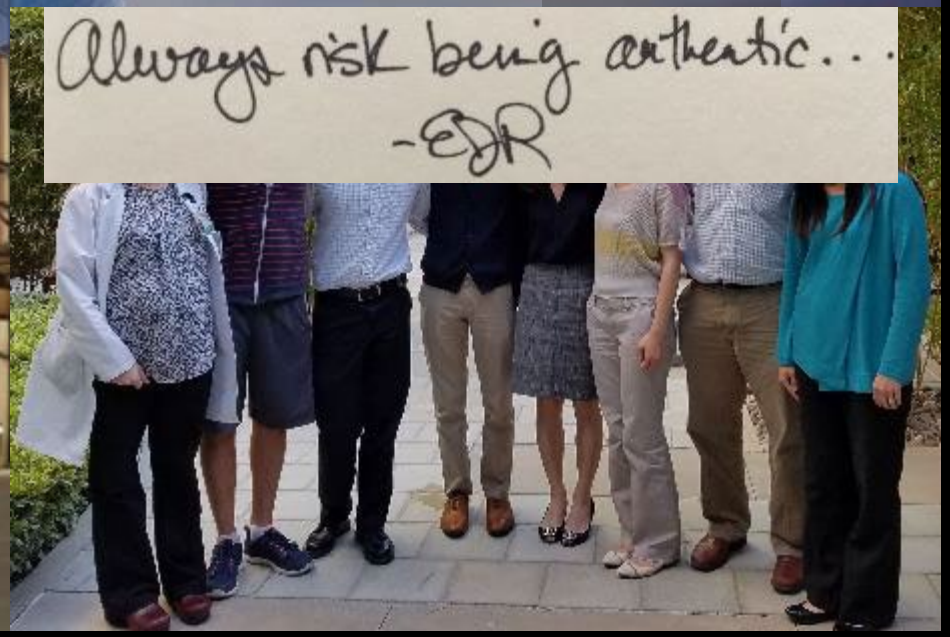

Body Composition in Cancer Patients on Immunotherapy

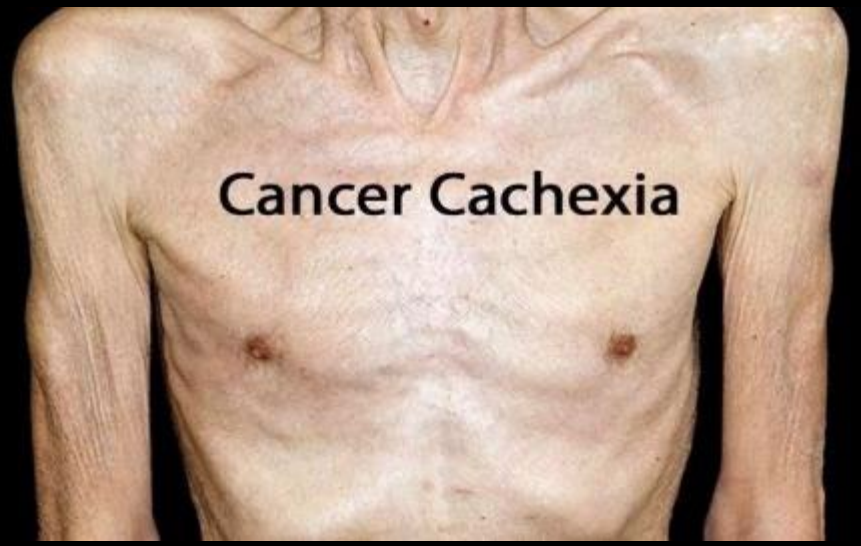

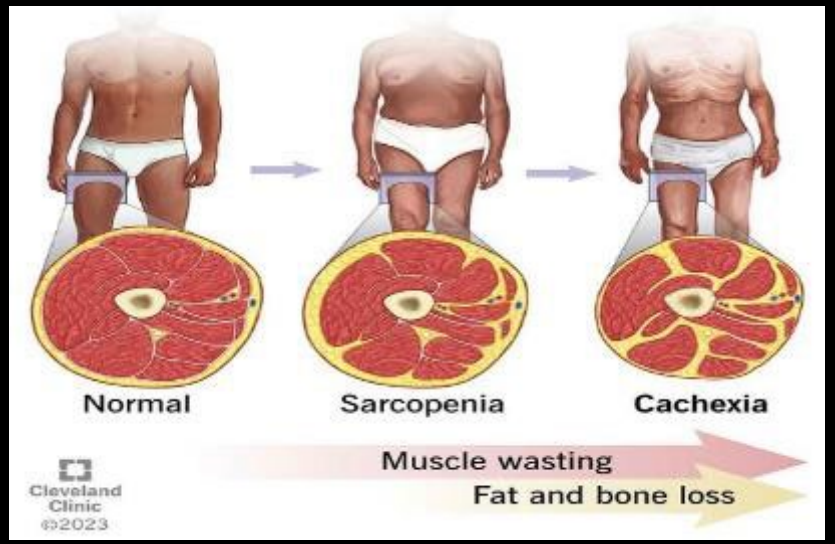

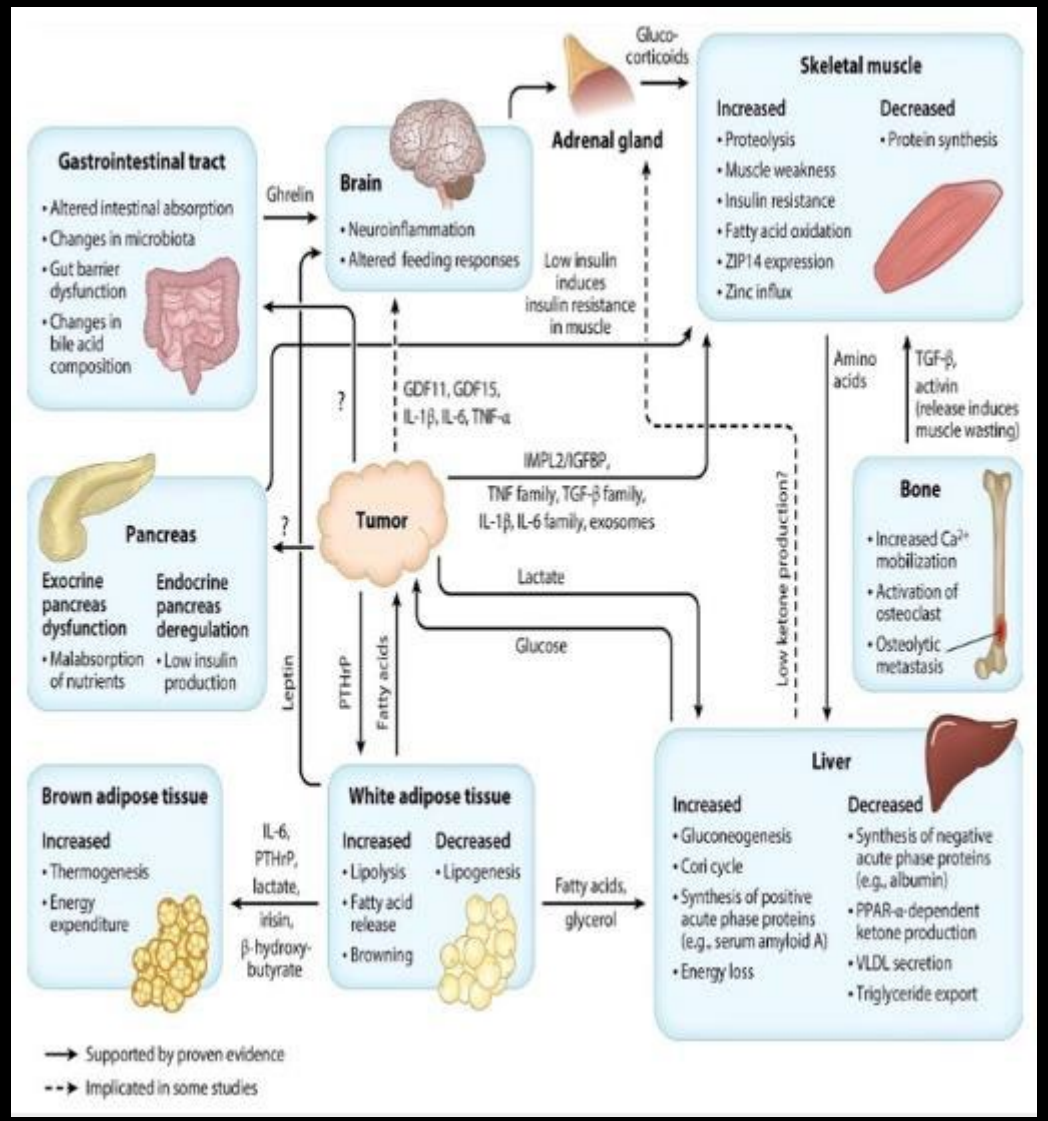

CACHEXIO: Evaluation of body composition changes and immunotherapy in patients with metastatic cancer.

Authors: Eric Roeland, Areej El-Jawahri, Nora Honick, Sandahl H Nelson, Andrea Gallivan, Ryan David Nipp, Yael Cohen-Arazi, Sarah Friedman, Chris Sera, Joseph Ma, Vickie E Baracos, Sandip Pravin Patel, and Hardeep Phull SHOW FEWER AUTHORS INFO & AFFILIATIONS

Publication: Journal of Clinical Oncology • Volume 36, Number 34_suppl • https://doi.org/10.1200/JCO.2018.36.34_suppl.209

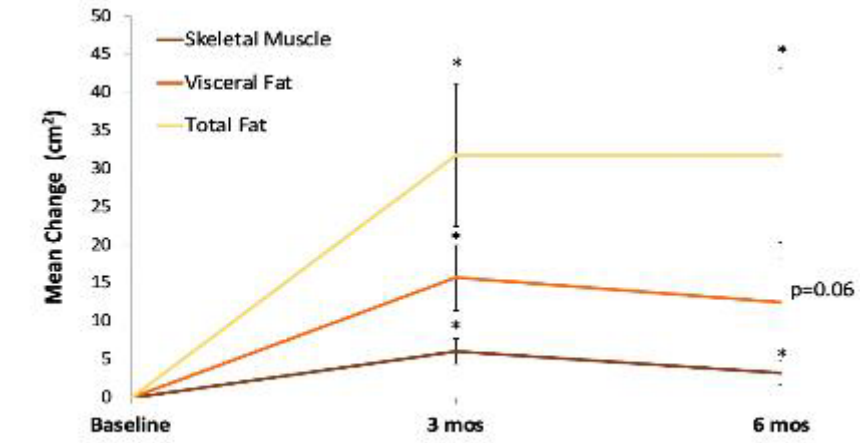

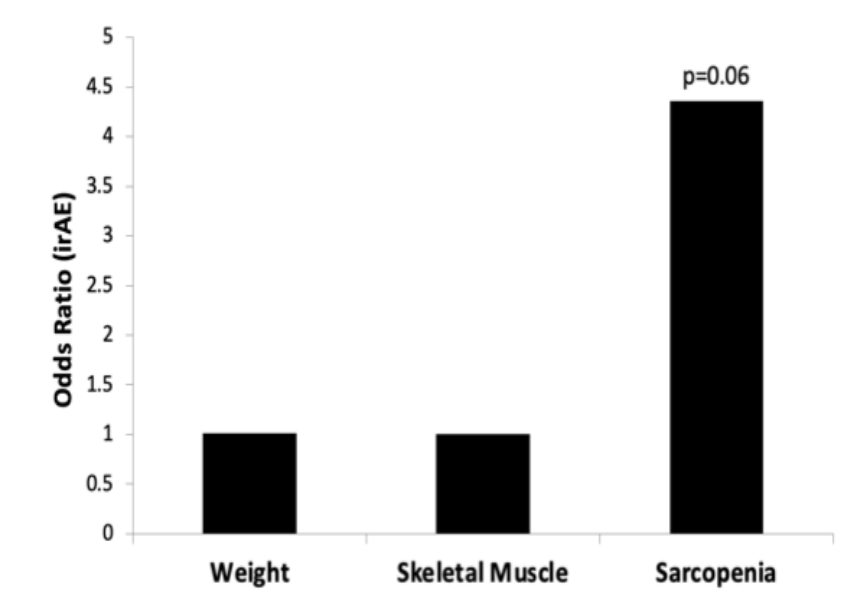

Supportive Care in Cancer
https://doi.org/10.1007/s00520-020-05730-4

ORIGINAL ARTICLE

FIT: Functional and imaging testing for patients with metastatic cancer

Eric J. Roeland[1,2] · H. Phull[2] · C. Hagmann[2] · C. Sera[2] · A. D. Dullea[2] · A. El-Jawahri[1] · S. Nelson[2] · A. Gallivan[3] · J. D. Ma[2] · R. D. Nipp[1] · V. E. Baracos[3]

Received: 8 June 2020 / Accepted: 28 August 2020

Abstract

Background Selecting study endpoints in prospective cancer cachexia trials remains poorly defined. The aim of this study was to further evaluate associations in changes in weight, body composition, functional outcomes, and patient-reported outcomes (PROs) in patients with metastatic cancer.

Methods We completed a 2-year (2016–2018) observational study in patients with metastatic solid cancer and ECOG performance status 0 to 2 while receiving chemotherapy and/or immunotherapy. We completed assessments at study enrollment and 3 months from enrollment. We analyzed longitudinal changes in weight and body composition using validated methods. Functional assessments included the 6-Min Walk Test, Timed Up and Go Test, and Short Physical Performance Battery. PROs included the Functional Assessment of Anorexia/Cachexia Therapy and Functional Assessment of Cancer Therapy Fatigue. We analyzed changes in body composition and functional assessment using paired *t* tests. Additionally, we utilized linear regression models to assess relationships between changes in body composition and function outcomes and PROs, adjusting for age and sex.

Results A total of 57 patients completed baseline assessments, but 19 patients did not complete 3-month assessments (5 died, 1 hospice, 13 withdrew). Of the 38 patients with complete data, the mean age was 61.8 years and 47% were female. Metastatic cancer types included 71% gastrointestinal, 13% lung, and 8% gynecologic. Half received chemotherapy, 16% immunotherapy, and 34% a combination. From enrollment to 3 months, we did not observe a change in weight or skeletal muscle but did find an increase in total adipose tissue (16.9 ± 52.4 cm^2, 95% CI − 33.79–0.63; $p = 0.059$; ~ 1.5 pounds). We did not observe any association with changes in weight with any functional outcomes or PROs. However, greater losses in skeletal muscle were associated with greater declines in physical function (6-Min Walk Test [$B = 0.04$, $p = 0.01$], Short Physical Performance Battery [$B = 2.44$, $p < 0.01$]).

Conclusions Patients with metastatic cancer receiving cancer-directed therapy may not experience a change in body weight. However, we found an association between losses in skeletal muscle and greater declines in physical function. Therefore, when selecting study endpoints, prospective cancer cachexia studies may consider selecting changes in body composition over weight.

A Novel Therapeutic Antibody for Cachexia Based on Our Work

The NEW ENGLAND JOURNAL of MEDICINE

Ponsegromab for Cancer Cachexia

A PLAIN LANGUAGE SUMMARY

Based on the NEJM publication: Ponsegromab for the Treatment of Cancer Cachexia
by J.D. Groarke et al. (published September 14, 2024)

In this trial, researchers examined the safety and efficacy of the monoclonal antibody ponsegromab for treating cancer cachexia.

Cachexia — also known as wasting syndrome — occurs commonly in patients with cancer and can lead to weight loss, muscle wasting, functional impairment, and reduced survival.

WHY WAS THE TRIAL DONE?

Pharmacologic treatment options for cancer cachexia are limited. Ponsegromab is a humanized monoclonal antibody that binds to growth differentiation factor 15 (GDF-15), a stress-induced cytokine implicated in the development of cachexia. In a small phase 1b study of ponsegromab, patients with cancer cachexia and an elevated circulating GDF-15 level had improved outcomes and few adverse events.

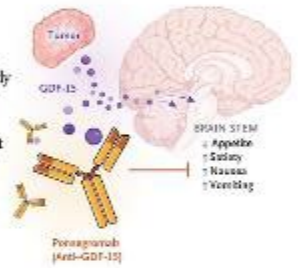

HOW WAS THE TRIAL CONDUCTED?

Adults with cancer cachexia and elevated serum GDF-15 levels were assigned to receive ponsegromab (100 mg, 200 mg, or 400 mg) or placebo, administered subcutaneously every 4 weeks for three doses. The primary end point was the change in body weight at 12 weeks.

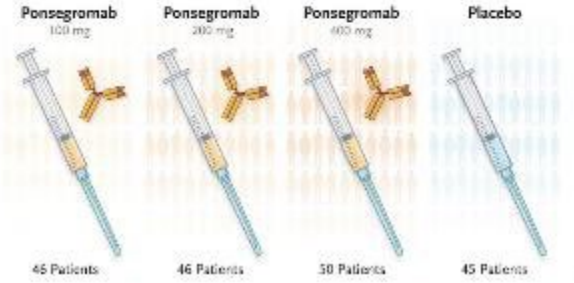

PATIENTS

WHO

187 adults

Median age, 67 years

Men: 63%; Women: 37%

CLINICAL STATUS

Cachexia (involuntary weight loss of >5% within the previous 6 months or >2% with BMI <20)

Serum GDF-15 level of at least 1500 pg per milliliter

ECOG performance-status score of 3 or less (scale, 0 to 5, with higher numbers reflecting greater disability)

Life expectancy of at least 4 months

TRIAL DESIGN

- PHASE 3
- RANDOMIZED
- DOUBLE-BLIND
- PLACEBO-CONTROLLED
- DOSE-RANGING
- DURATION: 22 WEEKS
- LOCATIONS: 74 SITES IN 11 COUNTRIES

If I could have ONE wish, what would it be?

Make Cancer a Chronic Dise

My Ongoing Journey as a Physician-Scientist

Educator & Mentor

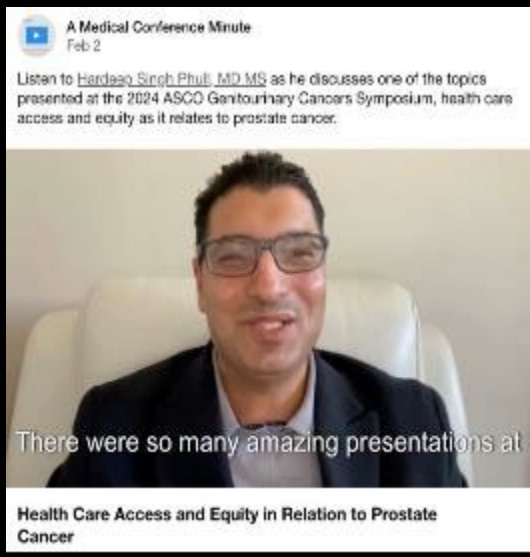

My Ongoing Journey as a Physician-Scientist

Writer & Consultant

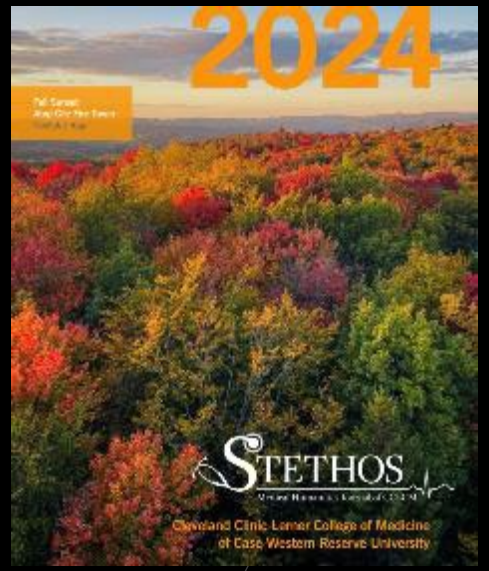

My Ongoing Journey as a Physician-Scientist

Empowering Patient Advocate

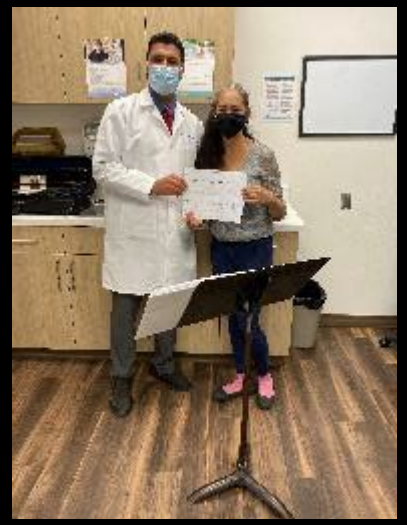

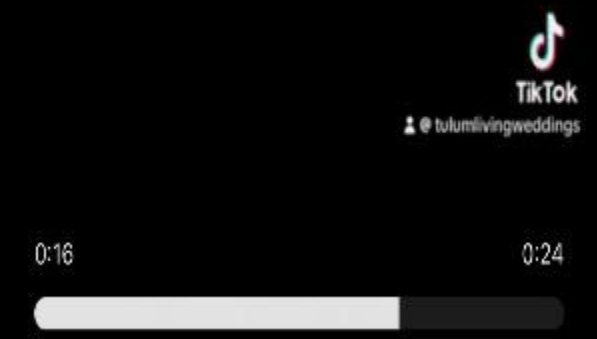

My Ongoing Journey as a Physician-Scientist

Media Personality & Podcaster

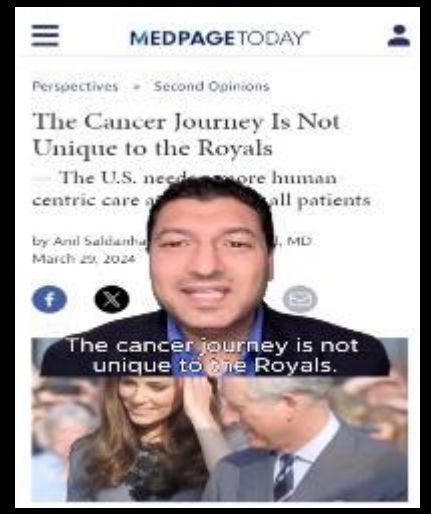

My Ongoing Journey as a Physician-Scientist

Girl Dad & Husband

Lesson #5: Life is a Brief Reality, not an Expectation

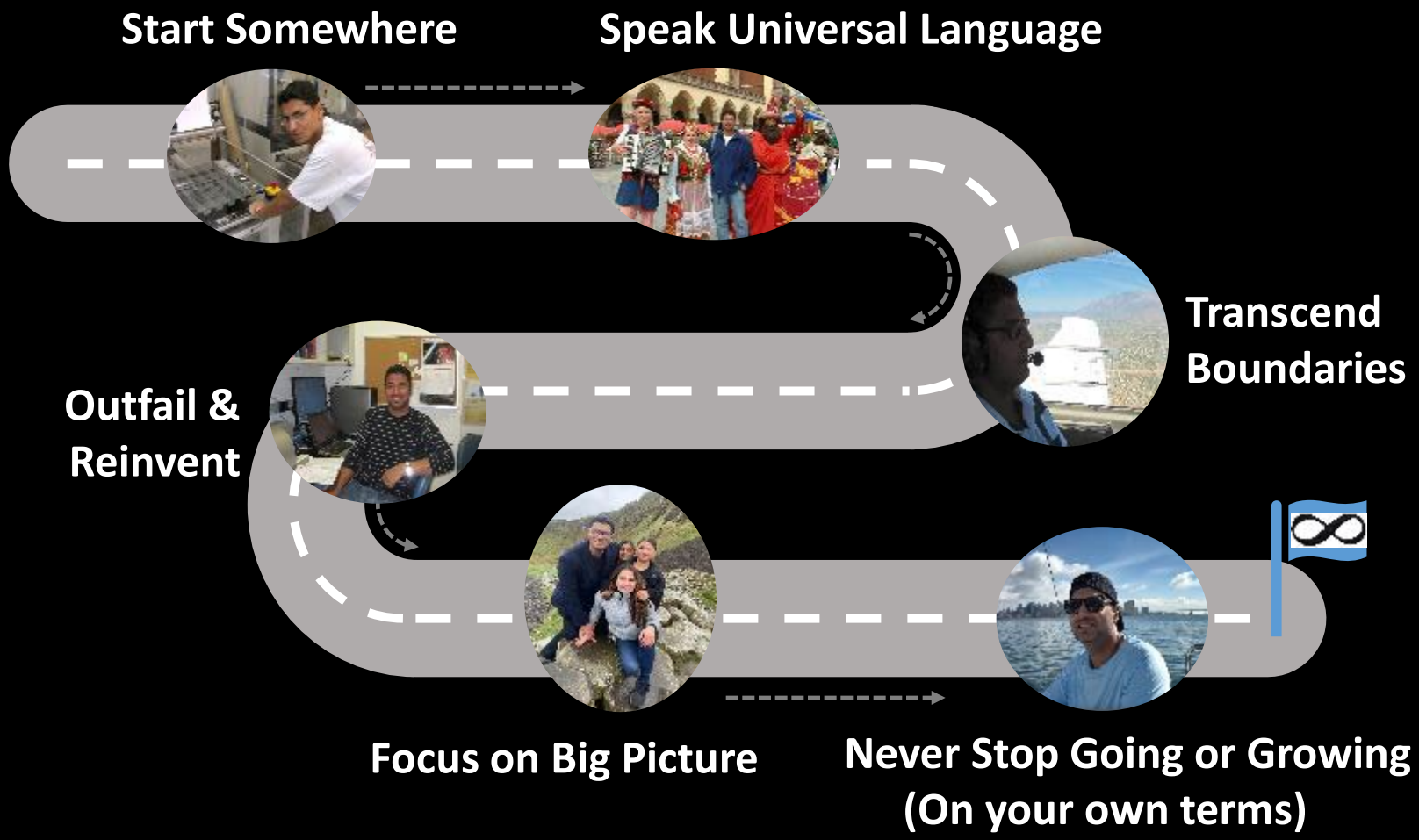

The Winding Path Builds Character

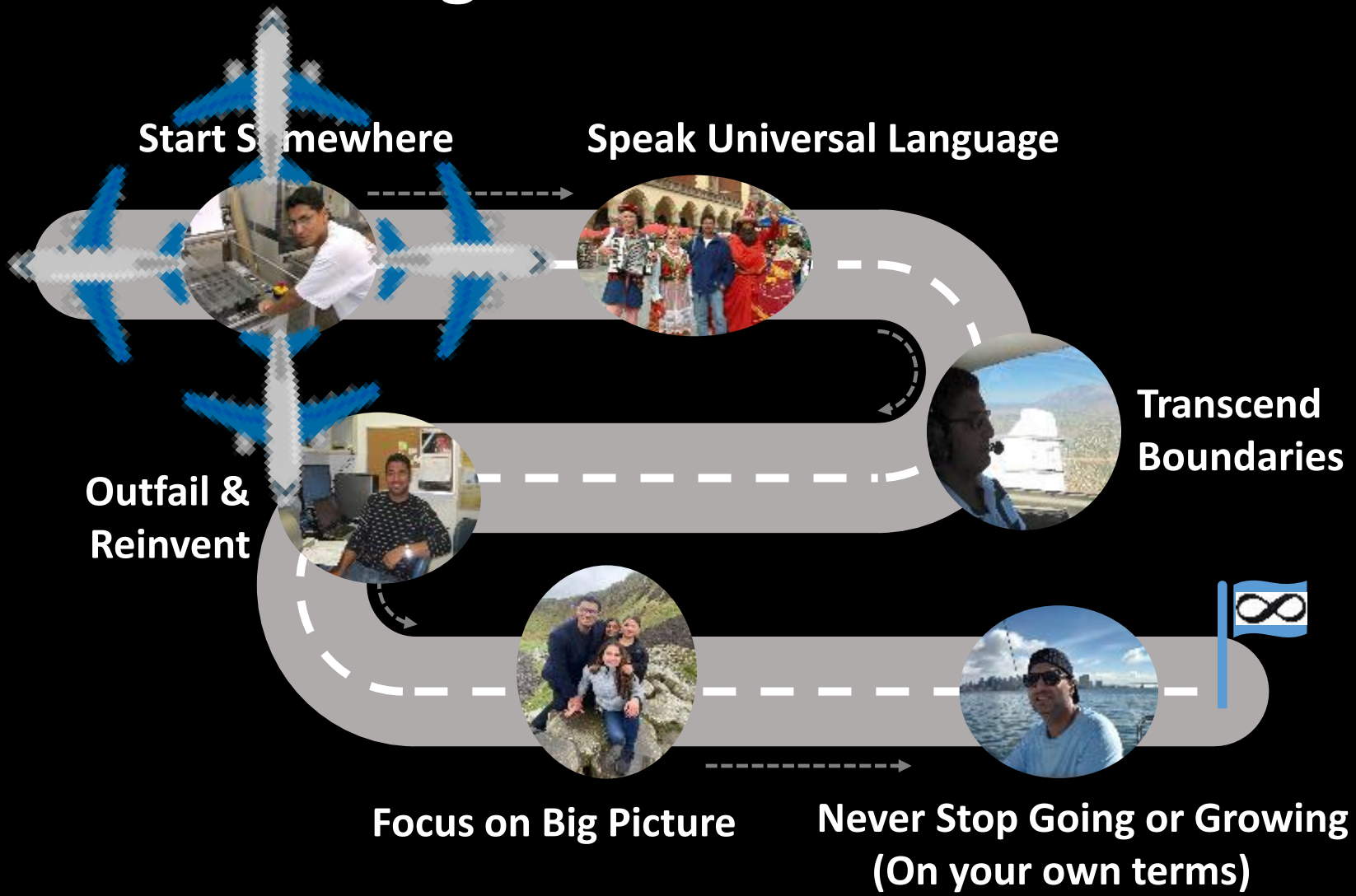

The Shortcut is Straight

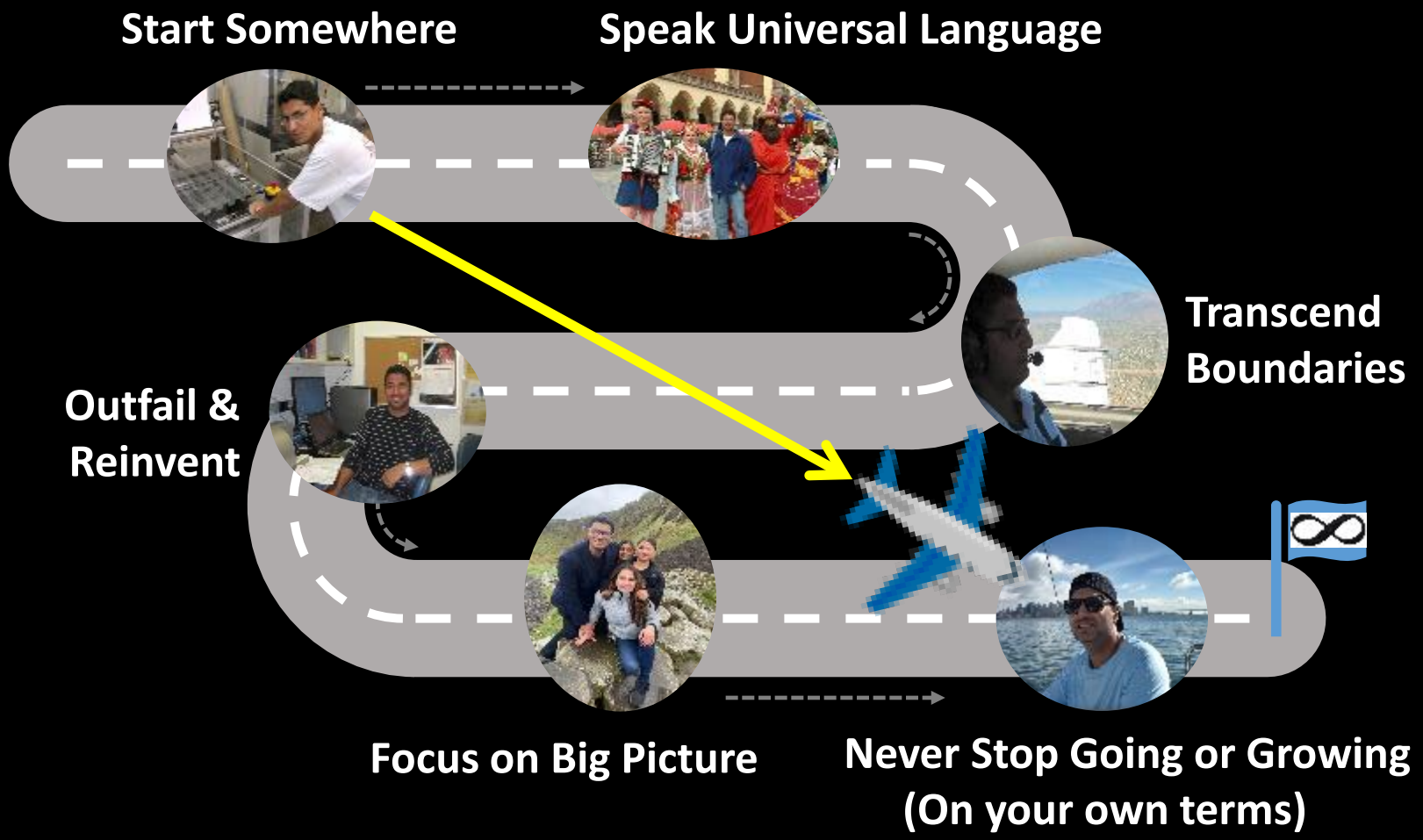

The Shortcut is Straight and boring & unfulfilling

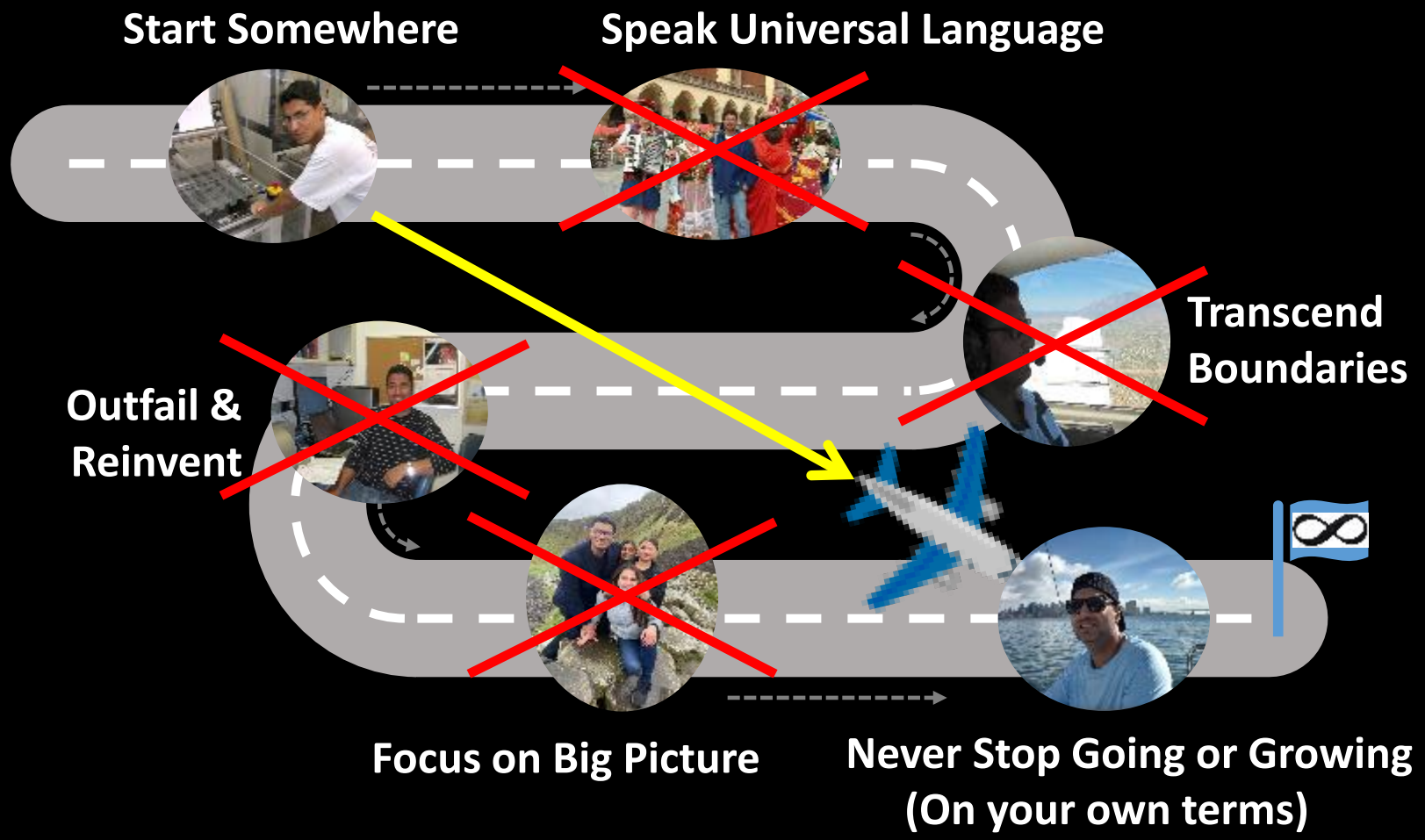

The Winding Path Builds Gratitude

Dr. Michael Deyholos
Dr. David Galbraith
Georgina Lambert
Carol Bender
Jennifer Cubeta
Dr. Elwira Sliwinska
Dr. Iwona Jedrzecyk
Harish Rekapally
Dr. Hakan Ozkan
Dr. Arik Harel
Dr. Rangaswamy Elumalai
Dr. Sanjay Ramakumar
Dr. Craig Comiter
Dr. Margot Damaser
Dr. Richard Prayson
Dr. Joseph Liao
Dr. Steve Campbell
Dr. Laura Nicholson
Dr. William Miller
Dr. Peter Schultz
Dr. Eric Topol
Dr. Eric Roeland